

EXHIBIT D

Polymer Science and Materials Chemistry

Exponent[®]

**Wave 1 Supplemental Report
Dr. Steven MacLean**

**United States District Court
For The Southern District Of
West Virginia
Charleston Division**

**This document relates to:
Ethicon Inc.,
Pelvic Repair System
Products Liability Litigation**



**Wave 1 Supplemental Report
Dr. Steven MacLean**

**UNITED STATES DISTRICT COURT
FOR THE SOUTHERN DISTRICT OF
WEST VIRGINIA
CHARLESTON DIVISION**

Prepared for

Chad R. Hutchinson
Butler Snow LLP
Renaissance at Colony Park
Suite 1400
1020 Highland Colony Parkway
Ridgeland, MS 39158-6010

Prepared by

Exponent
17000 Science Drive
Suite 200
Bowie, MD 20715

March 22, 2016

© Exponent, Inc.

Contents

	<u>Page</u>
List of Figures	iv
List of Tables	vii
Limitations	viii
Steven MacLean, Ph.D., P.E. Biography	1
Introduction	4
Motivation	4
PROLENE Mesh and Sutures	4
PROLENE Composition	5
Hematoxylin and Eosin (H&E) Stain	5
Experimental Investigation of the Capacity of PROLENE and Oxidized PROLENE to Accept H&E Stain	8
Sample Preparation Prior to Sectioning	9
Exemplar PROLENE Samples	9
Chemically Oxidized PROLENE Samples	9
QUV-Oxidized PROLENE Samples	10
Fetal Bovine Serum (FBS) Coated PROLENE Samples	10
Histology Sample Preparation	12
Results	12
Scanning Electron Microscopy of PROLENE and Polypropylene Samples	12
Fourier Transform Infrared Spectroscopy (FTIR) Analysis of Intentionally Oxidized Samples	22
Intentionally Oxidized PROLENE TVT and Hernia Mesh Devices, Sutures, and Polypropylene Pellets Were Not Stained by the Hematoxylin & Eosin Dyes	23
Imaging Artifacts	28
Thickness Variation and Stain Pooling	29
Polarizing Artifact	31
Mechanical Behavior of PROLENE Fibers	32
Conclusion and Opinions	33

Appendix A: Histology Protocols	35
Paraffin-embedded samples	35
Resin-embedded samples	37
Appendix B: Steven MacLean, Ph.D., P.E. CV	38
Professional Profile	38
Academic Credentials and Professional Honors	39
Licenses and Certifications	39
Publications	39
Presentations	40
Prior Experience	41
Professional Affiliations	41
Appendix C: Testimony of Steven MacLean, Ph.D., P.E.	42
Appendix D: List of Documents Reviewed	43
Literature	43
Production Materials	56
Bellew Case Materials	63
Expert Reports	63
Depositions	64
Trial	64
Miscellaneous	64
Huskey Case Materials	64
Depositions	64
Expert Reports	65
Appendix E: Compensation	70
Appendix F: Study Images	71

List of Figures

	<u>Page</u>
Figure 1. Amino acids that contain a net positive or negative charge.	7
Figure 2. SEM images of pristine untreated samples. Left column: samples intended for paraffin mounting, sectioning, and staining as part of following Dr. Iakovlev's protocol. Right column: samples intended for resin mounting, sectioning, and staining.	13
Figure 3. SEM image of a representative pristine TVT mesh sample prior to being subjected to Dr. Iakovlev's histological processing protocol.	14
Figure 4. SEM images of chemically treated samples. Left column: samples intended for paraffin mounting, sectioning, and staining per Dr. Iakovlev's protocol. Right column: samples intended for resin mounting followed by staining with H&E.	15
Figure 5. SEM images of an area of a TVT device after exposure to chemical treatment.	16
Figure 6. SEM images with corresponding EDS analysis areas performed on TVT Device 3859228 #1 after chemical treatment." (a) SEM image of mesh, (b) 500× magnification of mesh fiber, (c) EDS elemental profile of mesh fiber surface, (d) EDS elemental profile of light-colored crystals.	17
Figure 7. SEM images of QUV-oxidized TVT Device 3859228 #1 resin sample. Left: representative overall image at 30× magnification. Right: representative images at 100× magnification.	18
Figure 8. SEM images of representative areas of QUV-oxidized samples. Left column: samples intended for paraffin mounting, sectioning, and staining according to Dr. Iakovlev's protocol. Right column: samples intended for resin mounting. Longitudinal and radial cracks are observed over the entire surface.	19
Figure 9. SEM images of serum-coated samples. Left column: samples intended for paraffin mounting, cross-sectioning, and staining according to Dr. Iakovlev's protocol. Right column: samples intended for resin embedding. Green arrows indicate examples of proteinaceous coating and cracks within the coating.	20
Figure 10. SEM images of polypropylene pellets intended for paraffin mounting. (a) Pristine sample, (b) chemically oxidized sample, and (c) serum-coated sample.	21

- Figure 11. SEM images of polypropylene pellets intended for resin mounting. (a) Pristine sample, (b) chemically oxidized sample, and (c) serum-coated sample. Samples intended in for resin mounting. 21
- Figure 12. FTIR spectra of a pristine (untreated control) TVT mesh sample, QUV-treated sample, and chemically treated sample. Bands consistent with -OH groups ($\sim 3000\text{ cm}^{-1} - 3500\text{ cm}^{-1}$) and $\text{C}=\text{O}$ groups ($1600\text{ cm}^{-1} - 1760\text{ cm}^{-1}$) are observed in the treated samples but not in the pristine samples. 22
- Figure 13. Processed and sectioned tissue that has been subjected to the staining protocol and is modified by the H&E stain. Representative images of rabbit tissue embedded in paraffin (left) and resin (right) are shown. 23
- Figure 14. Serum-coated PROLENE fibers. (a) Paraffin embedded and (b) resin embedded are from TVT devices. (c) Resin embedded is from a hernia device. All samples were subjected to the staining protocol. 24
- Figure 15. Blue granules from a PROLENE fiber are visible within the protein-rich serum coating, giving the illusion of stained PROLENE. 25
- Figure 16. Pristine mesh fiber embedded in paraffin and subjected to Dr. Iakovlev's protocol (left). Pristine mesh fiber embedded in Technovit resin and subjected to staining (right). Both samples show an absence of H&E dye being absorbed. 25
- Figure 17. Cobalt-based crystallites adhered to the fiber surface are observed to be pink prior to being exposed to stain and after being stained. 27
- Figure 18. Cobalt-based crystallites are lodged between fibers. A bright field image is shown (left) as well as an image of the same fibers under cross-polarized light (right). 27
- Figure 19. QUV-oxidized PROLENE fibers with several cracks embedded in paraffin. No staining is evident. Mesh fibers are shown under bright field light (a) and (b) and illuminated under cross-polarized light (c). 28
- Figure 20. Same micrograph image of pristine PROLENE shown on two different computer monitors. A photograph of the image on the screen of monitor 2 was taken to preserve the observed pink coloring artifact. 29
- Figure 21. Potential formation mechanism of pooling artifact. A mesh fiber (A) can encounter the microtome blade at an angle (B), forming a section with an angled ledge (C), under which stain can pool (D) and give the appearance of true staining (E). 30
- Figure 22. Example of stain pooling is shown. A fiber cross section from a pristine TVT mesh, not expected to stain, is shown with different planes of focus. For image (a), the plane nearest the reader is in focus. For image (b), the stain pooled underneath the fiber is in focus. 30

Figure 23. Pristine, nonoxidized PROLENE mesh after staining with H&E. Image (a) was obtained without polarized light. Images (b) and (c) were acquired with polarized light.

31

List of Tables

	<u>Page</u>
Table 1. PROLENE Samples for Sectioning	11

Limitations

At the request of Butler Snow LLP, Exponent reviewed relevant scientific literature, historic documented studies and expert reports for the pending litigation. Exponent investigated specific issues relevant to this report as requested by the client. The scope of services performed during this investigation may not adequately address the needs of other users of this report, and any reuse of this report or its findings, conclusions, or recommendations is at the sole risk of the user. The opinions and comments formulated during this investigation are based on observations and information available at the time of the investigation.

The findings presented herein are made to a reasonable degree of scientific and engineering certainty. We have endeavored to be accurate and complete in our assignment. If new data become available or there are perceived omissions or misstatements in this report, we ask that they are brought to our attention as soon as possible so we have the opportunity to address them.

Steven MacLean, Ph.D., P.E. Biography

I am a Senior Managing Engineer in the Polymer Science and Materials Chemistry Practice at Exponent Failure Analysis Associates, Inc. (“Exponent”). My expertise and experience includes the chemical and physical behavior of polymeric materials in end-use applications, specifically in the evaluation of polymeric components in product safety assessments and product failure analysis. I have a B.S. and M.E. in Mechanical Engineering from Rensselaer Polytechnic Institute, and an M.S. in Material Science and Engineering from Rochester Institute of Technology. I also obtained a Ph.D. in Material Science from the University of Rochester in 2007. I am a registered Professional Engineer in New York and Maryland, a Senior Member of the Society of Plastics Engineers (SPE), and a board member of SPE’s Failure Analysis and Prevention Special Interest Group.

During the pursuit of my advanced degrees in materials science, my chosen field of study was polymer science and engineering. Graduate courses taken during my academic career that specifically focused on polymers included, but were not limited to, polymer science, organic polymer chemistry, polymer physics, polymer rheology, polymer processing, bulk physical properties of polymers, adhesion theory, and analytical techniques for polymeric materials. Supplemental course work included mechanics of materials, fracture mechanics, thermodynamics of materials and electron microscopy practicum. At the master’s degree level, my polymer research included characterizing the changes in chemical and physical properties of polycarbonate due to multiple heat histories from processing. At the doctoral level, my polymer research was focused on developing and investigating novel formulations of rubber-toughened polyphenylene ether polymers for use in pressurized, potable water systems. The primary emphasis of my dissertation included quantifying changes in select mechanical properties, including fracture toughness and tensile properties, due to the degrading effects from persistent exposure to chlorinated water at elevated temperatures.

In addition to my academic education and training, I have also been actively practicing in the field of polymer science and engineering for the past 20 years. Throughout that time, I have routinely utilized numerous polymer characterization techniques including, but not limited to, infrared spectroscopy, chromatography, mass spectrometry, calorimetry as well as optical,

scanning electron and transmission electron microscopy. In particular, I have used these microscopic techniques to examine the topography and morphology of fracture surfaces created as a result of polymer cracking. I have also employed these techniques to characterize modes of polymer failure such as creep, fatigue, stress overload, and environmentally assisted stress cracking. In many instances, I have published the use of these analytical techniques to investigate polymer failures in commercialized products in peer-reviewed journal articles and scientific conference proceedings.

Prior to joining Exponent in 2011, I worked for more than 15 years at General Electric Plastics (GE) and SABIC Innovative Plastics (SABIC) in a variety of technical roles of increasing responsibilities. Throughout my tenure, I was routinely involved in material selection, performance, and testing for, among other things, high-demand applications, product safety assessments, and product failure analysis. As a result, I have significant expertise and experience with industry standards and applicable regulations that prescribe the technical performance of polymeric materials in end-use applications, including those in the medical device industry.

At GE Plastics, I was trained extensively in the Six Sigma quality process, and became certified as a Six Sigma Black Belt. As a Certified Six Sigma Black Belt, my responsibilities included improving business processes by employing a variety of well-established statistical methods as well as mentoring and training Six Sigma Green Belts throughout the company.

Throughout my career, I have evaluated the suitability and performance of polymeric materials in end-use applications, including specifically, for the medical device industry. While at GE and SABIC, I worked with numerous medical device companies on material development, material specification, design and manufacturing for a wide variety of medical device applications. These efforts included, inter alia, developing and implementing tests related to the bulk physical properties of polymeric materials specified in said devices as well as material formulation development to meet unique device requirements that could not be met with off-the-shelf grades of resin. Formulation development often included the selection and refinement of base polymers or alloys, molecular weight, additives, stabilizers, processing aides, lubricants, colorants and inorganic fibers and fillers. In addition to proactive design and material selection assistance, I

have worked on hundreds of product safety assessments and failure analyses involving polymeric materials, many of which were performed on medical devices and components.

In my prior role as Director of Global Agency Relations and Product Safety at GE/SABIC, part of my leadership responsibilities included being an active member of the business' Healthcare Resins Advisory Board. The board developed internal processes and standards for the specification, use and sale of GE/SABIC resins in medical device applications. These efforts included ensuring that commercial resin grades within the GE/SABIC healthcare portfolio were assessed for biocompatibility using industry accepted test protocols such as United States Pharmacopeia (USP) Class VI, Tripartite Biocompatibility Guidance or ISO 10993 Biological Evaluation of Medical Devices standards. For the past several decades, the latter two standards have been supported by the Food and Drug Administration (FDA) and commonly employed to assess the potential for cytotoxicity, hemolysis, pyrogenicity, sensitization issues, among other biological effects, when the human body is exposed to foreign materials. In addition, the board also ensured that "good manufacturing processes" were globally implemented to maximize the purity levels of all compounded materials within the healthcare resin portfolio.

In addition to my relevant training, education and industry experience, I have also reviewed and synthesized the available public literature pertaining to *in vivo* and *in vitro* studies of polymeric mesh devices, long-term implantation of polymeric medical devices, foreign body response to implantable materials, as well as select plaintiff reports which allege *in vivo* PROLENE mesh degradation.

Introduction

Motivation

Plaintiff's expert, Dr. Vladimir Iakovlev, opines that Ethicon's PROLENE mesh degrades *in vivo* based on a cracked layer observed on the outer surface of mesh after explantation. While this assertion has been made by other plaintiff's experts,^{1,2} Dr. Iakovlev claims that the outer degradation layer is oxidized and "differs from the non-degraded core by its ability to trap histological dyes in the nanocavities produced in polypropylene due to degradation."³

Dr. Iakovlev bases his conclusions on flawed experiments in which he purports to show that oxidized, degraded PROLENE is stained using histological dyes such as Hematoxylin and Eosin (H&E). In previously conducted experiments, we demonstrated that purposefully oxidized PROLENE mesh samples—oxidized using two different methods—do not stain with the histological dyes H&E, contrary to Dr. Iakovlev's assertions. The purpose of this report is to show that our initial work is highly repeatable, because it holds true across five different PROLENE devices including three separate TVT devices (from two different lots), one hernia mesh device, and one suture. Polypropylene pellets were included as controls. Furthermore, as part of our experimental design and protocols, we also coated PROLENE devices with fetal bovine serum (FBS) as a positive control. FBS forms a protein-rich coating on the outside of PROLENE fibers that is stained by H&E whereas the underlying PROLENE fibers do not absorb stain, as expected. In this report, we further address the scientific deficiencies of Dr. Iakovlev's experiments and conclusions from a polymer science perspective. This report does not address issues related to histology⁴ or Dr. Iakovlev's histological analysis.

PROLENE Mesh and Sutures

Ethicon's antioxidant-stabilized polypropylene-based resin is known by its trademarked name PROLENE. The resin was determined to be "safe and effective for use" in nonabsorbable

¹ Expert report of Dr. Howard Jordi dated 8-24-15, p. 13.

² Expert report of Dr. Scott Guelcher dated 8-24-15, p. 2.

³ Expert report of Dr. Vladimir Iakovlev dated January 29, 2016, p. 18.

⁴ Histology relates to the microscopic study of tissue. Here, I focus on the microscopic study of PROLENE polymer fibers, although the chemistry of histological staining is discussed from a background perspective.

surgical sutures by the FDA in 1969 and has been used ever since.⁵ PROLENE sutures are manufactured by a melt spinning process.⁶ In addition to sutures, Ethicon knits PROLENE filaments into mesh materials used in hernia repair and to treat pelvic organ prolapse and stress urinary incontinence.

PROLENE Composition

As with many commercially available resin compounds, Ethicon's PROLENE resin is composed of several raw material ingredients in addition to the base isotactic polypropylene. The additional formulation ingredients and corresponding loading level ranges are:⁷

- Calcium stearate (0.25–0.35%) lubricant to help reduce tissue drag and promote tissue passage
- Santonox R (0.10–0.30%), a primary hindered phenol antioxidant
- Dilaurelthiodipropionate (DLTDP, 0.40–0.60%), a secondary thioester antioxidant
- Procol LA-10 (0.25–0.35%) lubricant to help reduce tissue drag and promote tissue passage
- Copper phthalocyanate (CPC) pigment (0.55% max) colorant to enhance visibility (in blue filaments only)

A summary of the full resin history including information on compounding, manufacturing, and formulation changes can be found in John Karl's memo entitled "PROLENE Resin Manufacturing Specifications."⁸

Hematoxylin and Eosin (H&E) Stain

Hematoxylin and Eosin, also referred to as H&E, are common stains used for illuminating components of cells and tissue, many of which are long molecules (polymers). The hematoxylin dye solution itself is a mixture of hematoxylin, hematein, aluminum ions, and solvent. It is used in combination with a "mordant" compound that helps link it to the tissue. This mordant is

⁵ NDA—4.16.1969 PROLENE FDA Approval (ETH.MESH.09625731-09625737).

⁶ FDA—Reclassification.pdf (ETH.MESH.10665538—1065565).

⁷ John Karl's January 23, 2003. Memo titled PROLENE Resin Manufacturing Specifications (Eth. Mesh.02268619–02268621).

⁸ Ibid.

typically a metal cation, such as aluminum. This complex is cationic (positively charged) and can react with negatively charged, basophilic cell components, such as nucleic acids in the nucleus, rough endoplasmic reticulum, ribosomes, and acidic mucin. Eosin, used in combination with hematoxylin, is negatively charged and attracts positively charged molecules. It stains structures with positive charges, such as cellular membranes, cytoplasm, connective tissue, and extracellular matrix tissue.

Ionic bonding is the most important type of bonding that occurs during histological staining.⁹ The mechanism for H&E “staining” of tissue is simple ionic bonding between two charges: charge on the H&E staining molecules and charges on the molecules that comprise the tissue. As an example, amino acids are the molecular building blocks of proteins (which are also polymeric), and some of these amino acids contain a charge, as shown in Figure 1.¹⁰ These charged compounds will bind ionically¹¹ (charge to charge) with H&E molecules and appear stained. In summary, the published mechanism for how H&E stains is chemical, not physical, in nature. In other words, physical voids, cracks, or crevices in PROLENE (as posited by Dr. Iakovlev)¹² or other materials do not “trap” or hold H&E stain, especially once adequate washing and rinsing are performed.

Polypropylene or PROLENE molecules are not ionically charged and are therefore not expected to stain with H&E. Furthermore, as shown in my expert report, which discusses the pathways of polypropylene oxidation, oxidized polypropylene does not possess a distinct ionically charged region. Therefore, in accordance with not only first principles of polymer science, but also the accepted methodology and assessment routinely reported in the literature, oxidized polypropylene is also not expected to stain with H&E.

⁹ Veuthey, T., Herrera, G., & Doderio, V. I. (2014). Dyes and stains: from molecular structure to histological application. *Frontiers in bioscience* (Landmark edition), 19, 91.

¹⁰ Adapted from Dan Cojocari, University of Toronto, 2011, pKa Data, *CRC Handbook of Chemistry*, 2010.

¹¹ A common, familiar ionically bonded material is sodium chloride, or table salt, in which Na^+ and Cl^- are bound together by ionic attraction.

¹² Expert report of Dr. Vladimir Iakovlev dated January 29, 2016, p. 18, 92, 93.

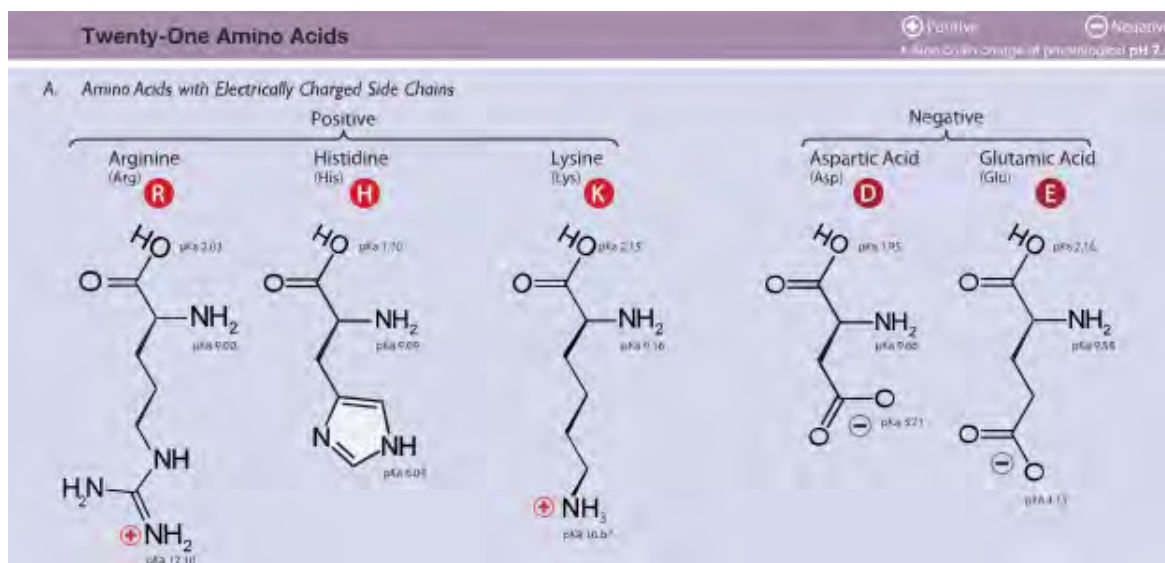


Figure 1. Amino acids that contain a net positive or negative charge.¹⁰

Experimental Investigation of the Capacity of PROLENE and Oxidized PROLENE to Accept H&E Stain

I sought to investigate the capability of PROLENE and oxidized PROLENE to accept H&E stain since my review of the literature and first principles of polymer science did not explain the phenomenon observed and reported by Dr. Iakovlev. In my previous report, I demonstrated that intentionally oxidized PROLENE does not stain with H&E. In addition to my reliance on the literature and first principles of polymer science, I conducted a set of laboratory experiments to further validate my previous work that demonstrated that H&E does not stain PROLENE or oxidized PROLENE.

In the experiments reported herein, pristine (i.e., out-of-the-box, never implanted in the body), serum-coated, and purposefully oxidized PROLENE-based mesh and suture products were processed and subjected to histological dyes (Hematoxylin & Eosin) in accordance with protocols previously provided by plaintiff's expert Dr. Iakovlev. In expanding on experiments I have already carried out, multiple PROLENE devices were evaluated in these experiments. Specifically, to ensure repeatability, the following devices were examined:

- Ethicon PROLENE GYNECARE TVT™ Trans-Vaginal Tape Mesh Devices from two different lots
- Ethicon PHSE PROLENE Hernia System Extended Mesh Device
- Ethicon PROLENE 6-0 Blue Monofilament Suture

Rabbit tissue was included as a positive control for histological staining and polypropylene pellets that do not contain the same additive package (e.g., antioxidants, processing aids, or lubricants) as PROLENE in our analysis.

The above PROLENE devices and polypropylene pellets were subjected to the following preconditioning treatments prior to treating them with Dr. Iakovlev's staining protocol:

1. Photo-oxidation treatment by UV light¹³

¹³ QUV conditions employed here are the same UV conditions used in my microscopy report dated September 10, 2015.

2. Chemical oxidation solution treatment that reportedly degrades polypropylene¹⁴
3. Fetal bovine serum treatment as a protein-rich matrix

Pristine mesh was also included as a control. Preconditioning treatments are described in greater detail in later sections of this report. It is important to note that none of the materials included and examined here have been implanted in the body.

Sample Preparation Prior to Sectioning

Exemplar PROLENE Samples

Pristine PROLENE TVT mesh (Ethicon TVT Devices—Ref. No. 810041B, two devices from Lot Number 3859228 and one device from Lot Number 3832826), PHSE hernia mesh (Lot No. 27770-20), suture 6-0, and polypropylene resin pellets were received and kept in their original packaging until use. A clean razor blade was used to cut ~ 1 cm long sections of each sample for laboratory analysis (Table 1). Polypropylene pellets (Sigma-Aldrich, isotactic, average M_w ~340,000, average M_n ~97,000) were used as received.

Chemically Oxidized PROLENE Samples

Sections of PROLENE TVT meshes, PHSE hernia mesh, 6-0 suture, and polypropylene resin pellets were oxidized according to the protocol published by Guelcher and Dunn (Exponent protocol “Chemical Oxidation Protocol per Guelcher,” 1504469.000-5191).¹⁵ Samples were incubated at 37°C for 5 weeks in oxidative media composed of 0.1 M CoCl_2 in 20 wt% H_2O_2 . This solution purportedly simulates the oxidative environment created by macrophages in response to a foreign object.¹⁶ The oxidative solution was changed every two to three days. Prior to processing, the samples were rinsed copiously in deionized water, then immersed in an ultrasonic bath (Exponent protocol “Rinsing Samples After Chemical Oxidation,” 1504469.000-7542). Samples were subsequently air-dried and assessed for visual appearance using optical microscopy and morphological changes using scanning electron microscopy (SEM).

¹⁴ Guelcher, S. A., & Dunn, R. F. (2015, June). Oxidative degradation of polypropylene pelvic mesh in vitro. *International. Urogynecology Journal*. 26 (Suppl 1): S55–S56.

¹⁵ Ibid.

¹⁶ Ibid.

QUV-Oxidized PROLENE Samples

Sections of PROLENE TVT meshes, PHSE hernia mesh, and suture 6-0 were placed inside a Q-Lab QUV Accelerated Weathering Tester and irradiated with $0.98 \left(\frac{W}{m^2}\right)$ UV light at 60°C (Exponent protocol “QUV Oxidation Protocol for PROLENE,” 1504469.000-4837). Samples were imaged by SEM periodically and QUV exposure was stopped after extensive cracking was observed over the entire UV-exposed surface of the samples (5–12 days). Prior to being sent to a third-party lab for histological processing, the samples were assessed for morphological changes using SEM and optical microscopy.

Fetal Bovine Serum (FBS) Coated PROLENE Samples

Sections of PROLENE TVT meshes, PHSE hernia mesh, suture 6-0, and polypropylene resin pellets were incubated in solutions of fetal bovine serum (FBS) at 37 °C for six days (Exponent protocol “Serum Coated PROLENE Protocol,” 1504469.000-1151). After six days, the samples were removed from the serum, air-dried, assessed with optical microscopy and SEM, and immersed in a 10% formalin buffer solution for storage. Prior to being sent to a third-party lab for histological processing, samples were removed from formalin, air-dried, visually inspected for appearance using optical microscopy, and assessed for morphological changes using SEM.

Table 1. PROLENE Samples for Sectioning

	QUV Oxidized (Paraffin) ¹⁷	QUV Oxidized (Resin)	Chemically Treated (Paraffin)	Chemically Treated (Resin)	Serum-coated (Paraffin)	Serum-coated (Resin)	Pristine (Out-of-the-box) Control (Paraffin)	Pristine (Out-of-the-box) Control (Resin)
PROLENE TVT mesh Lot 3859228 #1	ID: 157162 TVT Device Lot 3859228 #1 QUV-P	ID: 157163 TVT Device Lot 3859228 #1 QUV-R	ID: 157164 TVT Device Lot 3859228 #1 ChemOx-P	ID: 157165 TVT Device Lot 3859228 #1 ChemOx-R	ID: 157166 TVT Device Lot 3859228 #1 Serum-P	ID: 157167 TVT Device Lot 3859228 #1 Serum-R	ID: 157880 TVT Device Lot 3859228 #1 Control-P	ID: 157169 TVT Device Lot 3859228 #1 Control-R
PROLENE TVT mesh Lot 3859228 #2	ID: 157170 TVT Device Lot 3859228 #2 QUV-P	ID: 157171 TVT Device Lot 3859228 #2 QUV-R	ID: 157172 TVT Device Lot 3859228 #2 ChemOx-P	ID: 157173 TVT Device Lot 3859228 #2 ChemOx-R	ID: 157174 TVT Device Lot 3859228 #2 Serum-P	ID: 157175 TVT Device Lot 3859228 #2 Serum-R	ID: 157884 TVT Device Lot 3859228 #2 Control-P	ID: 157177 TVT Device Lot 3859228 #2 Control-R
PROLENE TVT mesh Lot 3832826	ID: 157178 TVT Device Lot 3832826 QUV-P	ID: 157179 TVT Device Lot 3832826 QUV-R	ID: 157180 TVT Device Lot 3832826 ChemOx-P	ID: 157181 TVT Device Lot 3832826 ChemOx-R	ID: 157182 TVT Device Lot 3832826 Serum-P	ID: 157183 TVT Device Lot 3832826 Serum-R	ID: 157895 TVT Device Lot 3832826 Control-P	ID: 157185 TVT Device Lot 3832826 Control-R
PROLENE hernia mesh	ID: 157186 Hernia Mesh Lot 27770-20 QUV-P	ID: 157187 Hernia Mesh Lot 27770-20 QUV-R	ID: 157188 Hernia Mesh Lot 27770-20 ChemOx-P	ID: 157189 Hernia Mesh Lot 27770-20 ChemOx-R	ID: 157190 Hernia Mesh Lot 27770-20 Serum-P	ID: 157191 Hernia Mesh Lot 27770-20 Serum-R	ID: 157899 Hernia Mesh Lot 27770-20 Control-P	ID: 157193 Hernia Mesh Lot 27770-20 Control-R
PROLENE 6-0 suture	ID: 157194 PROLENE 6-0 Suture QUV-P	ID: 157195 PROLENE 6-0 Suture QUV-R	ID: 159703 PROLENE 6-0 Suture ChemOx-P	ID: 159704 PROLENE 6-0 Suture ChemOx-R	ID: 157198 PROLENE 6-0 Suture Serum-P	ID: 157199 PROLENE 6-0 Suture Serum-R	ID: 157903 PROLENE 6-0 Suture Control-P	ID: 157201 PROLENE 6-0 Suture Control-R
Polypropylene Pellet	--	--	ID: 157232 Polypropylene pellet Sample #1	ID: 157233 Polypropylene pellet Sample #2	ID: 157234 Polypropylene pellet Sample #3	ID: 157235 Polypropylene pellet Sample #4	ID: 157236 Polypropylene pellet Sample #5	ID: 157237 Polypropylene pellet Sample #6

¹⁷ The embedding material is listed parenthetically.

Histology Sample Preparation

Exemplar, oxidized, and serum-coated mesh samples were embedded in both paraffin and resin (Technovit), sectioned, and stained with H&E. All processing was performed by an independent GLP-compliant¹⁸ histology lab with more than 25 years of experience in histological processing of samples. Detailed embedding and staining protocols can be found in Appendix A.

Paraffin-embedded samples were prepared by following the protocol submitted by Dr. Iakovlev. Briefly, samples were sequentially dehydrated in reagent alcohol and xylene substitute using an automated tissue processor, and then embedded in Leica EM400 paraffin wax. Sections of the paraffin blocks (4–6 µm thick) were obtained using a microtome, briefly floated in a 40–45°C water bath, and mounted onto slides. Sections were air-dried for 30 minutes, then baked in a 45–50°C oven overnight.

Resin-embedded samples were sequentially dehydrated in reagent alcohol using an automated tissue processor and embedded in Technovit 7200. The polymerized resin block was trimmed. Then sections were cut and ground to a thickness of 10–61 µm with a mean thickness of approximately 30 µm.

Paraffin and resin-embedded samples were subjected to staining with H&E. All slides were imaged by Exponent personnel using a microscope equipped with polarizing filters.

Results

Scanning Electron Microscopy of PROLENE and Polypropylene Samples

All samples listed in Table 1 were imaged with SEM prior to histological processing and microscopy evaluation (Figure 2). To observe surface features clearly, images of mesh samples were obtained at 100× magnification. Representative images of 6-0 suture samples were obtained at 200× magnification (Figure 3).

¹⁸ Per 21 CFR Part 58 – Good Laboratory Practice for Nonclinical Laboratory Studies.

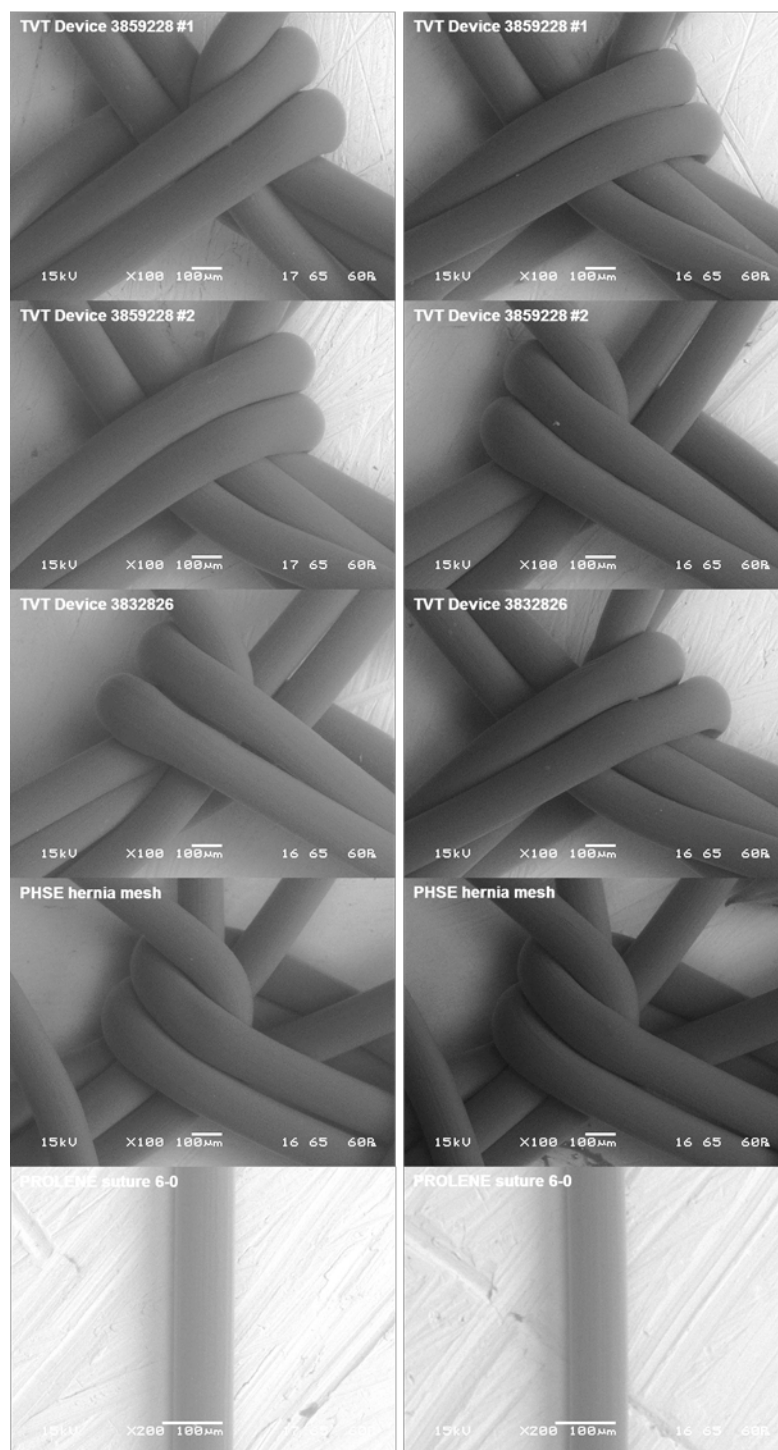


Figure 2. SEM images of pristine untreated samples. Left column: samples intended for paraffin mounting, sectioning, and staining as part of following Dr. Iakovlev's protocol. Right column: samples intended for resin mounting, sectioning, and staining.¹⁹

¹⁹ The images were brightened during post-processing to enhance contrast.

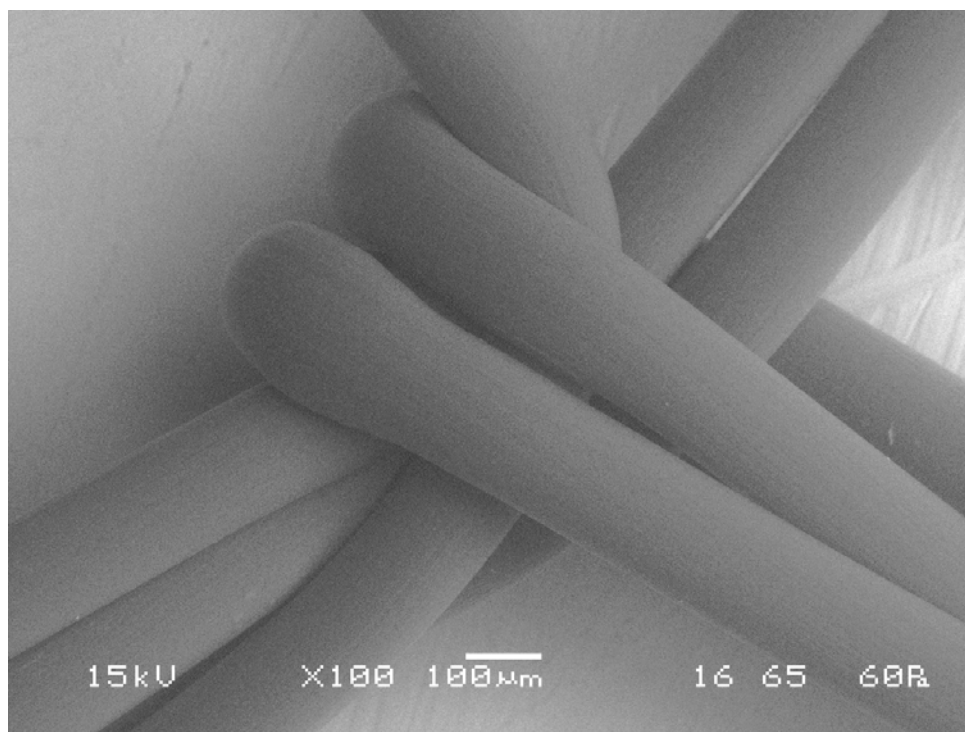


Figure 3. SEM image of a representative pristine TVT mesh sample prior to being subjected to Dr. Iakovlev's histological processing protocol.²⁰

As expected, the sample surfaces of pristine untreated PROLENE TVT devices, PHSE hernia mesh, and 6-0 suture appeared smooth and uniform, with no apparent defects or cracking. The surface of the polypropylene pellet, as imaged by SEM, was similarly smooth and uniform, with no apparent defects (Figure 10A).

The surfaces of chemically oxidized samples were similarly smooth and uncracked (Figure 4). However, several crystals, likely inorganic, cobalt-based crystals, were observed to be well-adhered to the surface of the PROLENE samples after exposure to the chemical treatment protocol as shown in Figure 5.

²⁰ Ibid.

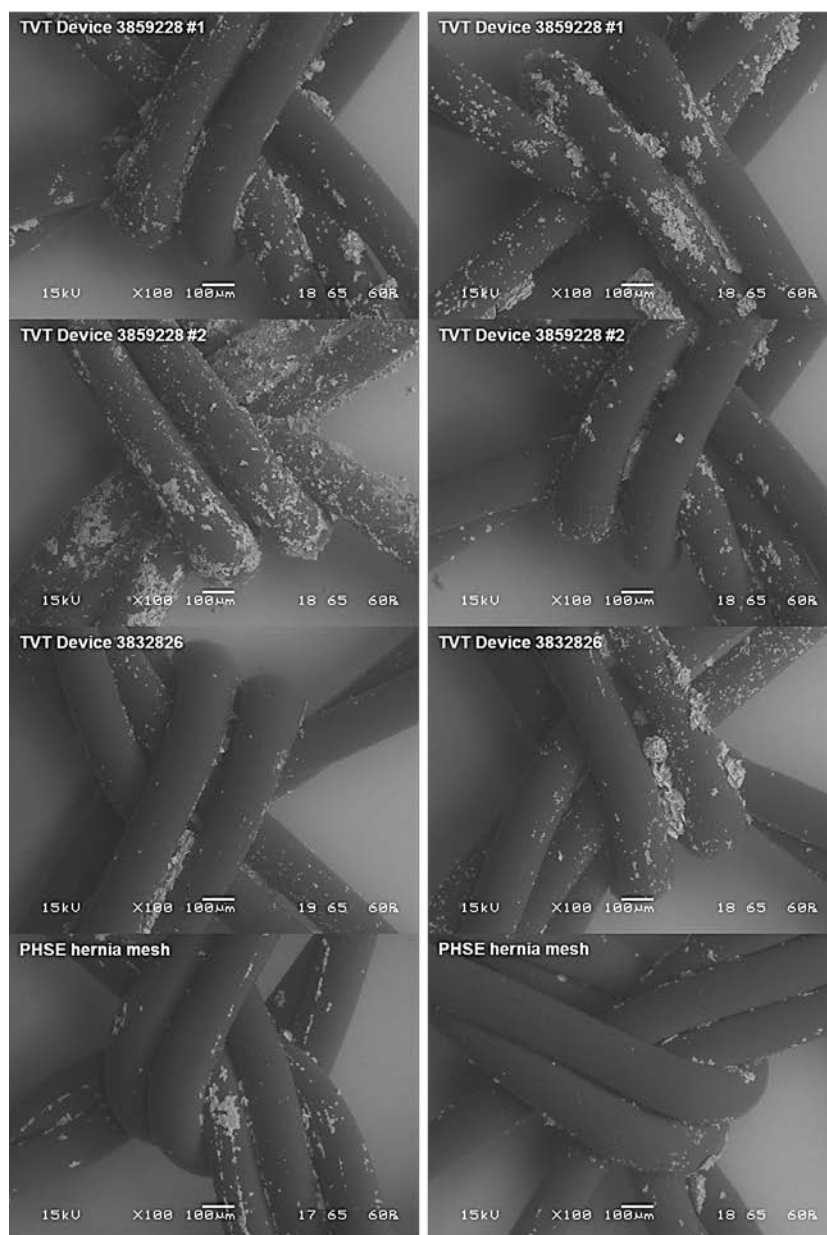


Figure 4. SEM images of chemically treated samples. Left column: samples intended for paraffin mounting, sectioning, and staining per Dr. Iakovlev's protocol. Right column: samples intended for resin mounting followed by staining with H&E.

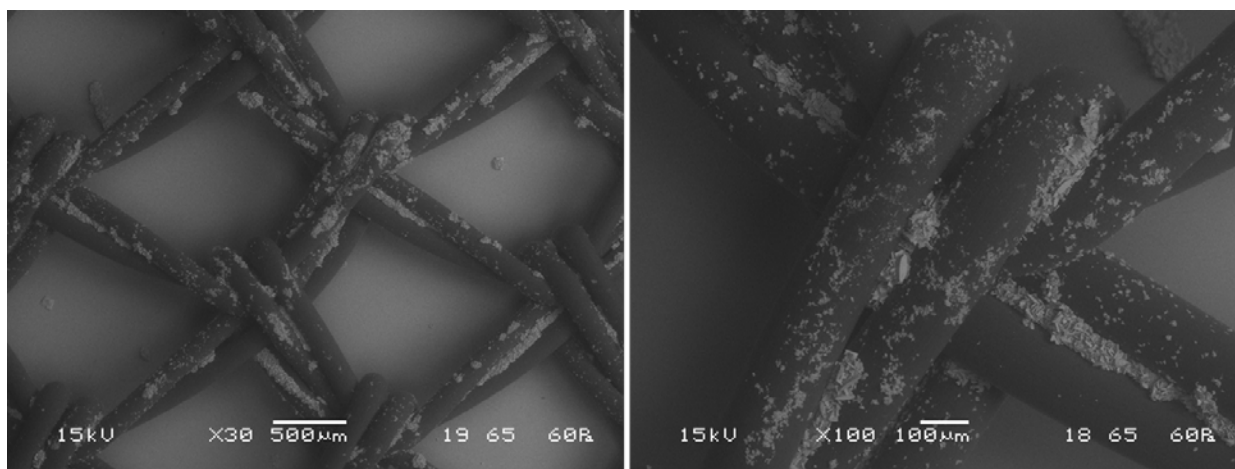


Figure 5. SEM images of an area of a TVT device after exposure to chemical treatment.

These observations differ from the results published by Guelcher and Dunn, who reported “pitting” and “flaking” in polypropylene meshes subjected to the same treatment conditions.¹⁴ The light-colored crystallite material not removed during the rinsing procedure (Exponent protocol “Rinsing Samples After Chemical Oxidation,” 1504469.000-7542) and observed on the surface of the samples is consistent with cobalt-based crystallite deposits according to energy dispersive X-ray spectroscopy (EDS) analysis. EDS was performed on two areas of a representative mesh sample (TVT Device 3859228 #1) after chemical oxidation treatment. EDS measurements revealed that the PROLENE surface was composed predominantly of carbon, and that the light-colored crystals were predominantly composed of cobalt (Figure 6).

In contrast to the pristine (untreated control) and chemically treated samples, QUV-oxidized samples exhibited extensive cracking covering most of the mesh and suture surfaces. A representative image illustrating the extensive cracking observed over most of the surface is shown in Figure 7. Longitudinal cracks with length scales of several hundreds of microns were observed traversing the length of the mesh fibers. Accompanying radial cracks, with length scales on the order of 100 microns or less, were observed perpendicularly to the longitudinal cracks. The extent of cracking was uniform across the five different PROLENE devices examined (Figure 8).

Prior to embedding, cross-sectioning, and staining per Dr. Iakovlev’s protocol, the serum-coated samples were also imaged with SEM. The proteinaceous coating deposited on the surface of PROLENE mesh samples treated with FBS can be seen clearly with SEM (Figure 9). The

coating had a sheet-like appearance that concentrated predominantly in the areas between the mesh fibers. However, the PROLENE surfaces themselves were uncracked and smooth, and similar to pristine untreated samples. A thin layer of the proteinaceous coating was also observed on the surface of 6-0 suture samples and polypropylene pellet samples (Figure 10c and Figure 11c).

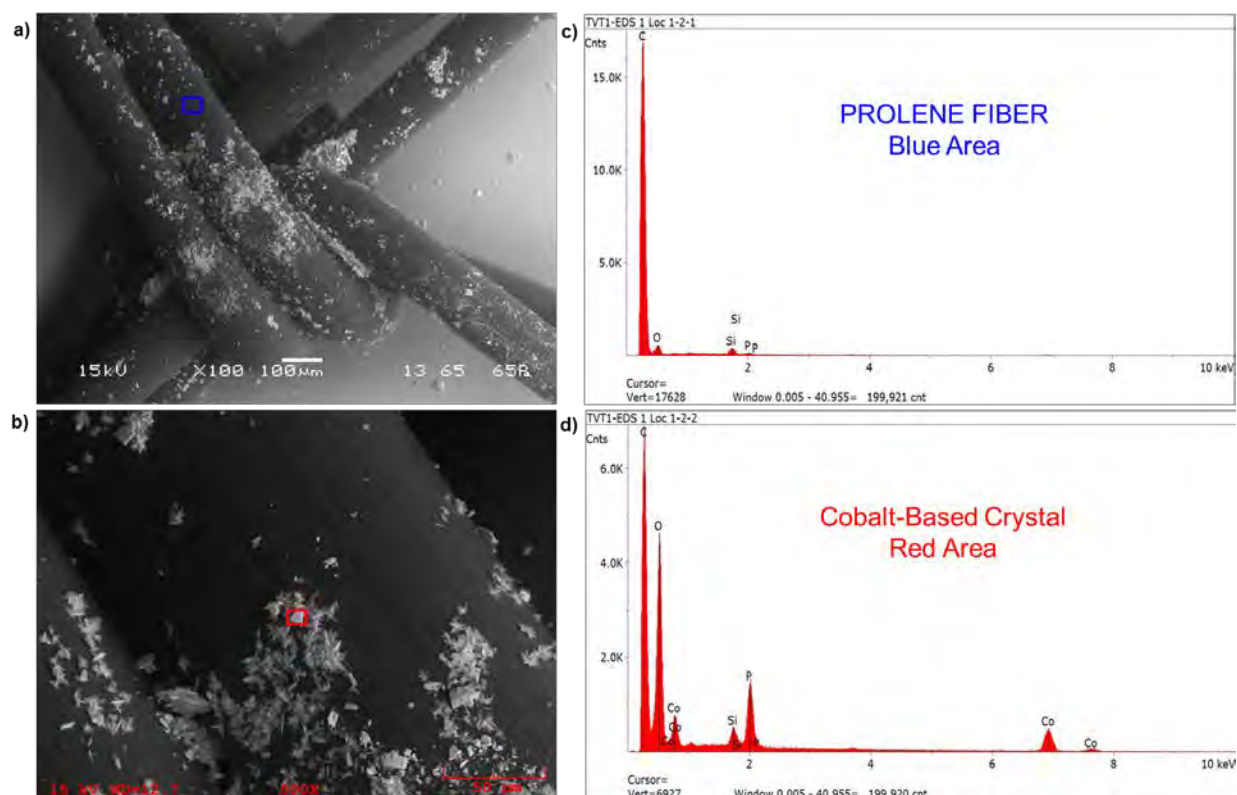


Figure 6. SEM images with corresponding EDS analysis areas performed on TVT Device 3859228 #1 after chemical treatment.^{21,22,23} (a) SEM image of mesh, (b) 500x magnification of mesh fiber, (c) EDS elemental profile of mesh fiber surface, (d) EDS elemental profile of light-colored crystals.

²¹ Guelcher, S. A., & Dunn, R. F. (2015 June). Oxidative degradation of polypropylene pelvic mesh in vitro. *International Urogynecology Journal* 26 (Suppl 1): S55-S56.

²² Exponent protocol "Chemical Oxidation Protocol per Guelcher," 1504469.000-5191.

²³ Exponent protocol "Rinsing Samples After Chemical Oxidation," 1504469.000-7542.

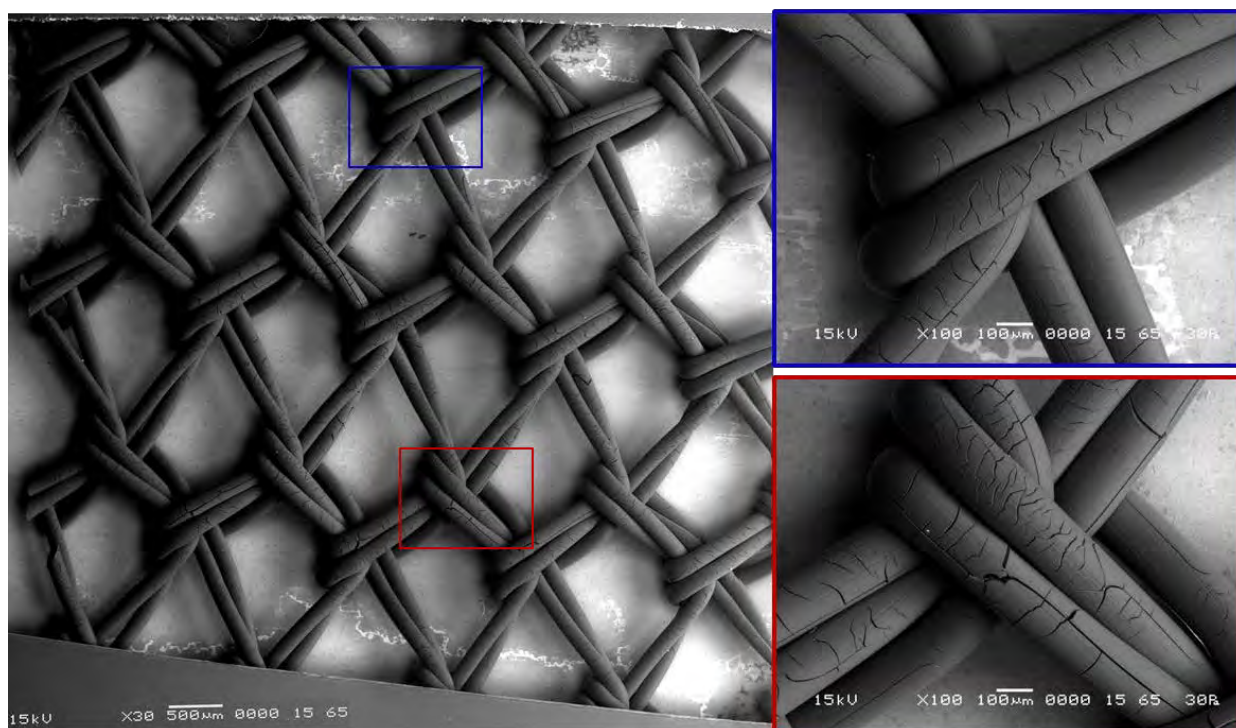


Figure 7. SEM images of QUV-oxidized TVT Device 3859228 #1 resin sample. Left: representative overall image at 30x magnification. Right: representative images at 100x magnification.

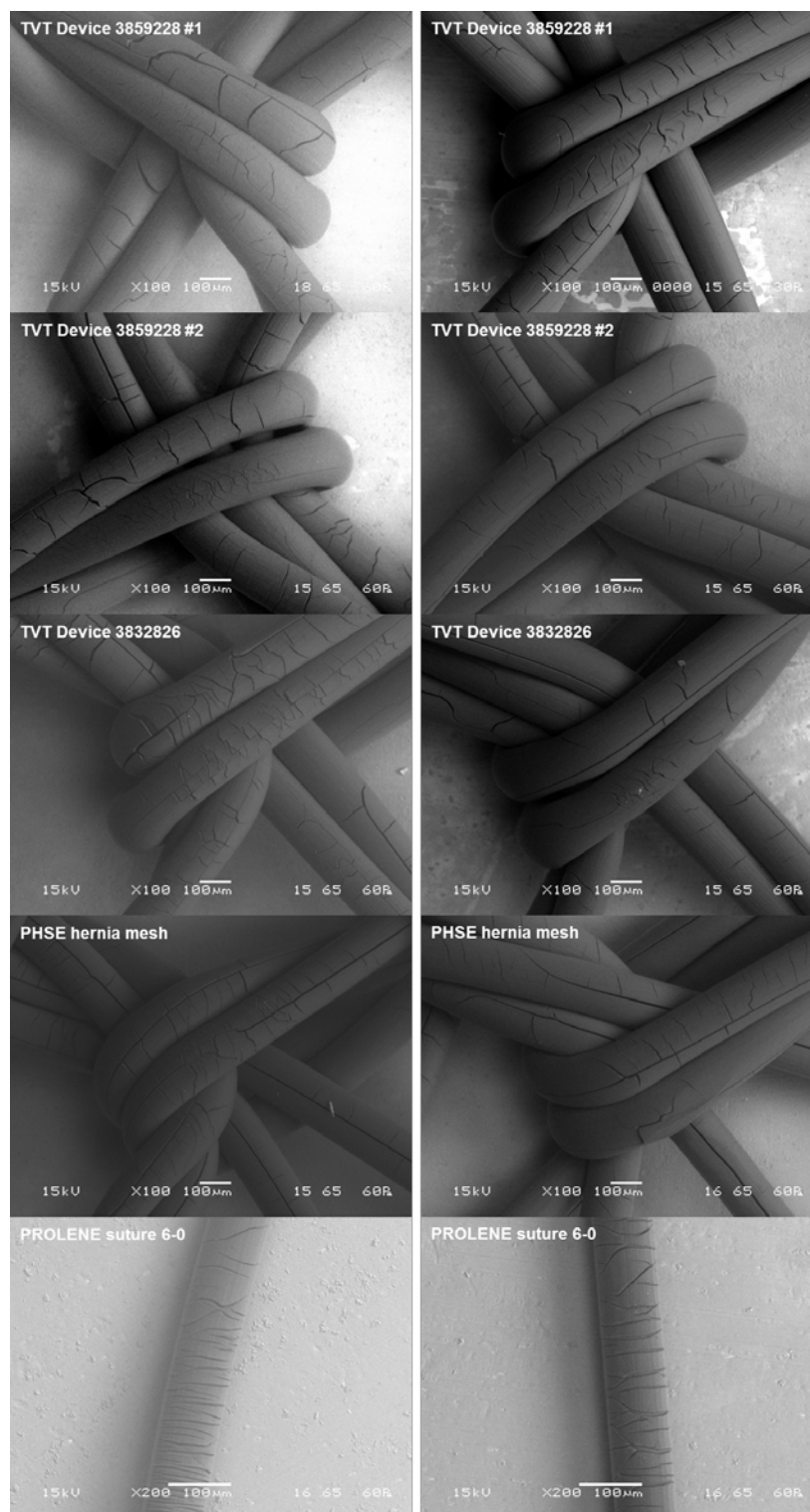


Figure 8. SEM images of representative areas of QUV-oxidized samples. Left column: samples intended for paraffin mounting, sectioning, and staining according to Dr. Iakovlev's protocol. Right column: samples intended for resin mounting. Longitudinal and radial cracks are observed over the entire surface.

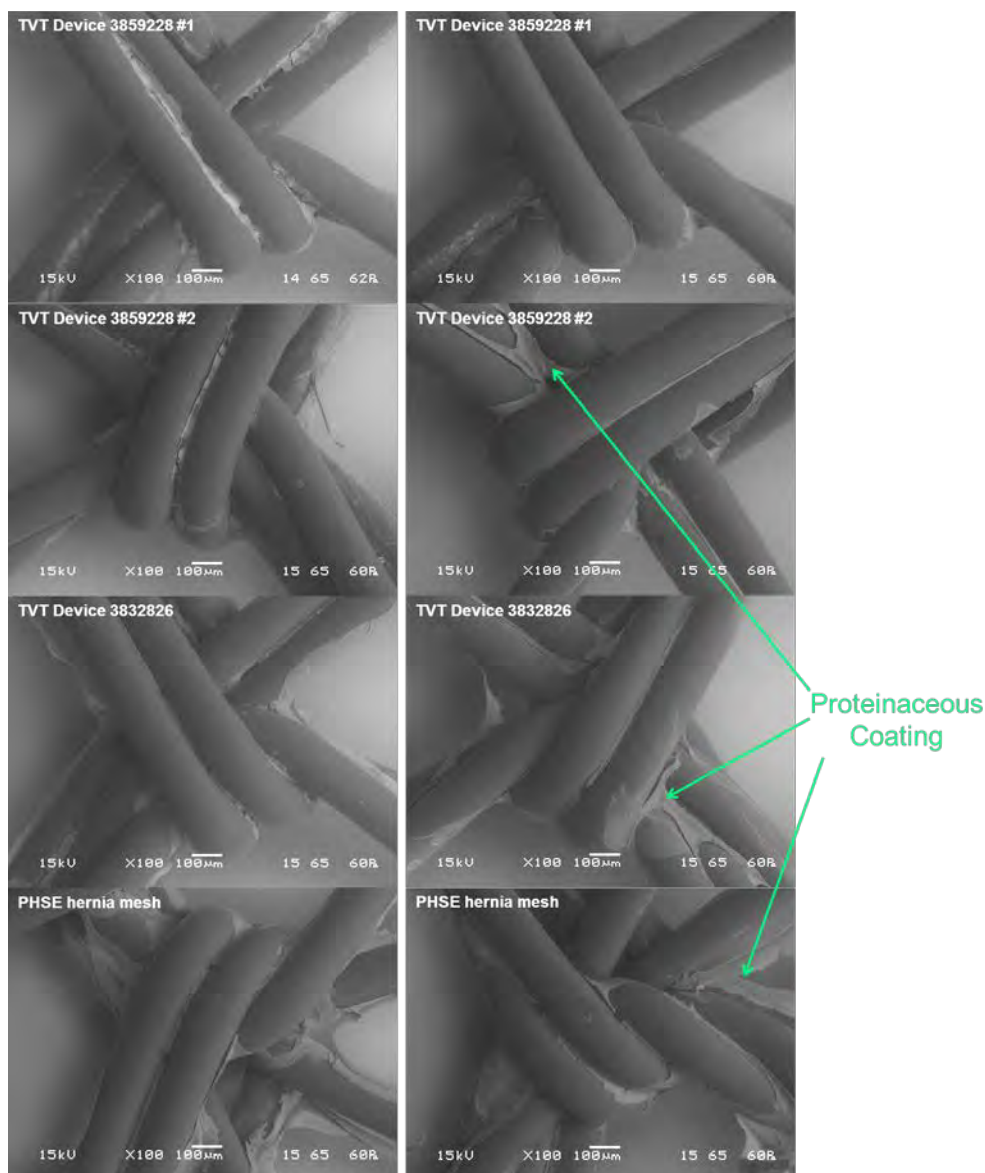


Figure 9. SEM images of serum-coated samples. Left column: samples intended for paraffin mounting, cross-sectioning, and staining according to Dr. Iakovlev's protocol. Right column: samples intended for resin embedding. Green arrows indicate examples of proteinaceous coating and cracks within the coating.²⁴

²⁴ The images were brightened during post-processing to enhance contrast.

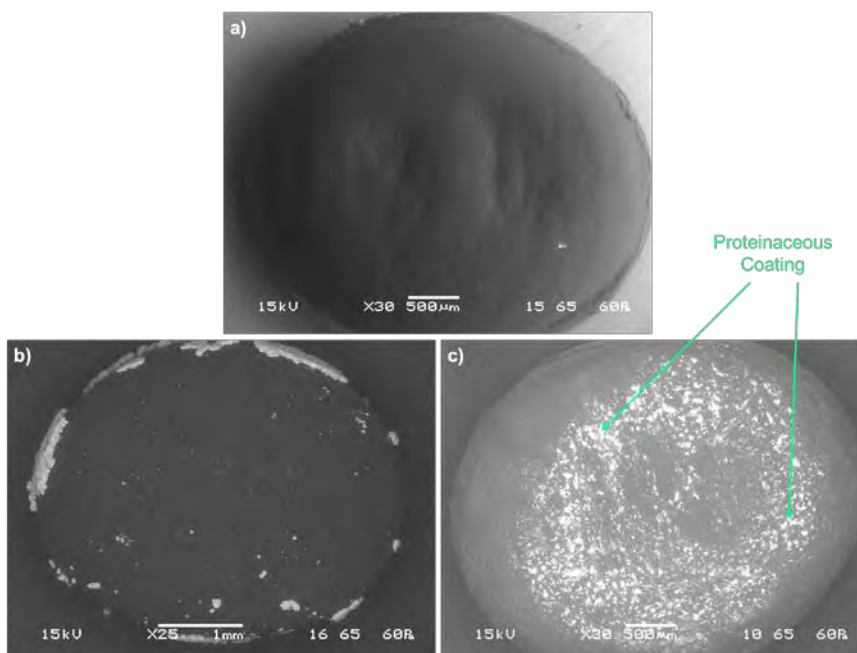


Figure 10. SEM images of polypropylene pellets intended for paraffin mounting. (a) Pristine sample, (b) chemically oxidized sample, and (c) serum-coated sample.²⁵

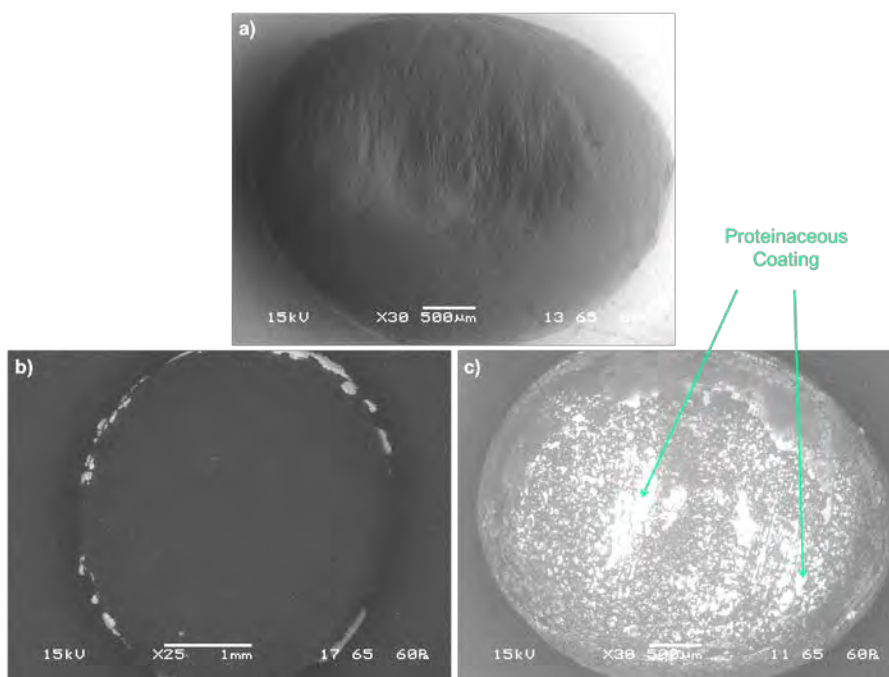


Figure 11. SEM images of polypropylene pellets intended for resin mounting. (a) Pristine sample, (b) chemically oxidized sample, and (c) serum-coated sample. Samples intended in for resin mounting.

²⁵ The images were brightened during post-processing to enhance contrast.

Fourier Transform Infrared Spectroscopy (FTIR) Analysis of Intentionally Oxidized Samples

Small segments of the chemically treated and UV-oxidized samples listed in Table 1 were analyzed by Fourier transform infrared spectroscopy (FTIR) to potentially identify functional groups consistent with oxidation. FTIR spectra were acquired on a pristine PROLENE sample for comparison. In the UV-treated and chemically treated samples, we observed bands consistent with hydroxyl (OH) bands and carbonyl (C=O) bands that can be indicative of oxidation. These bands were not observed in the pristine samples. Representative spectra are shown in Figure 12.

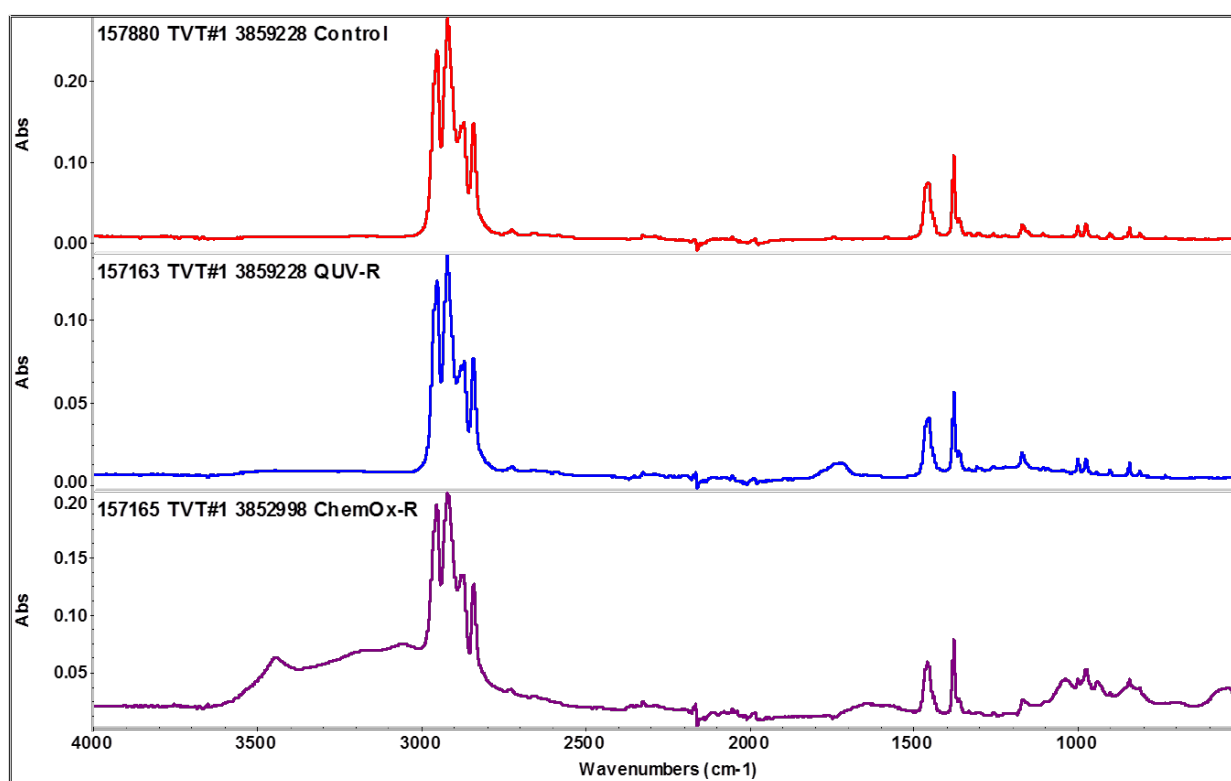


Figure 12. FTIR spectra of a pristine (untreated control) TVT mesh sample, QUV-treated sample, and chemically treated sample. Bands consistent with -OH groups ($\sim 3000\text{ cm}^{-1} - 3500\text{ cm}^{-1}$) and $\text{C}=\text{O}$ groups ($1600\text{ cm}^{-1} - 1760\text{ cm}^{-1}$) are observed in the treated samples but not in the pristine samples.

Intentionally Oxidized PROLENE TVT and Hernia Mesh Devices, Sutures, and Polypropylene Pellets Were Not Stained by the Hematoxylin & Eosin Dyes

Positive Control: Rabbit Skin Tissue

A positive control (rabbit skin tissue) was processed to demonstrate the effectiveness of the processing and staining protocol. PROLENE meshes and sutures, treated and untreated, along with the polypropylene pellets, were subjected to the staining protocol at the same time.

The appearance of stain is evident when tissue is present and stain has been applied. Figure 13 shows rabbit tissue that has been treated with stain, evident by the coloration within the tissue. These results confirm that the staining protocol employed in these experiments is effective in staining proteinaceous materials.

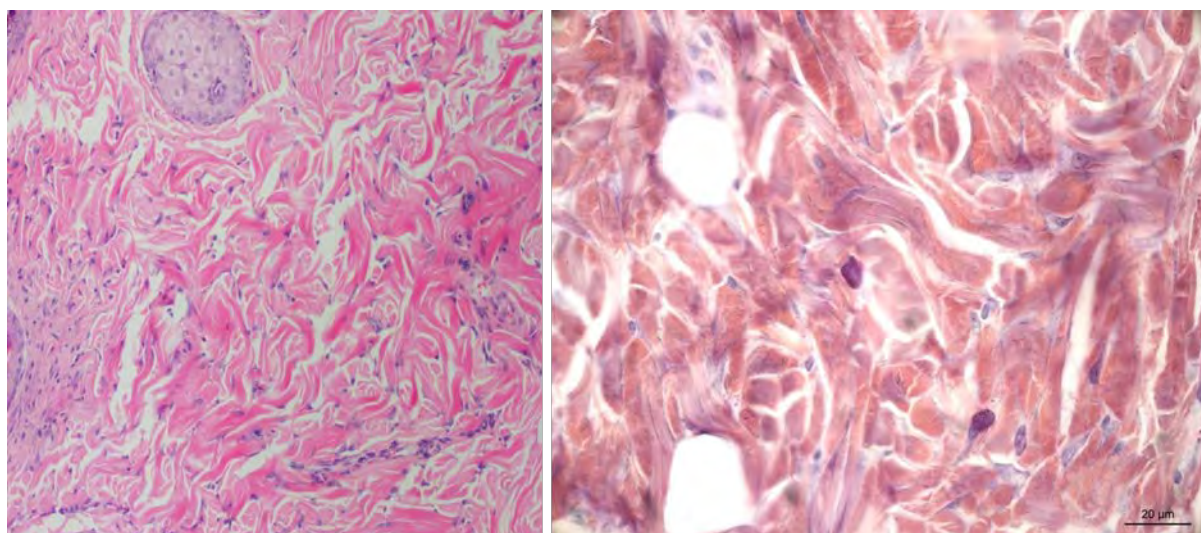


Figure 13. Processed and sectioned tissue that has been subjected to the staining protocol and is modified by the H&E stain. Representative images of rabbit tissue embedded in paraffin (left) and resin (right) are shown.²⁶

Serum-Coated PROLENE—PROLENE with Protein-Rich Coating

PROLENE coated with FBS and stored in formalin was also subjected to the staining protocol. The protein-rich serum coating around the pristine PROLENE mesh was found to stain, as expected, while the PROLENE fiber itself did not stain. The color of the stain on the serum coating is similar to that of the positive control of rabbit skin. Representative images of serum-

²⁶ All images collected as part of our experiments are given as an Appendix to this report.

coated TVT and hernia mesh are shown in Figure 14. In Figure 14b, a segment of serum is observed adjacent to the bottom of the PROLENE fiber in the top half of the image. Upon closer inspection, blue granules are visible within the serum coating, creating an illusion that blue granules are present in the exterior coating, when really they are separate, distinct materials. The illusion is created by both the fiber and serum segment being partially in focus. Additional examples that demonstrate this effect are given in Figure 15. Figure 15A shows the fiber in focus; the serum segment overlaid with the fiber is not. However, blue granules from a PROLENE fiber are visible within the protein-rich serum coating or “bark” as Dr. Iakovlev asserts, giving the illusion of stained PROLENE.²⁷

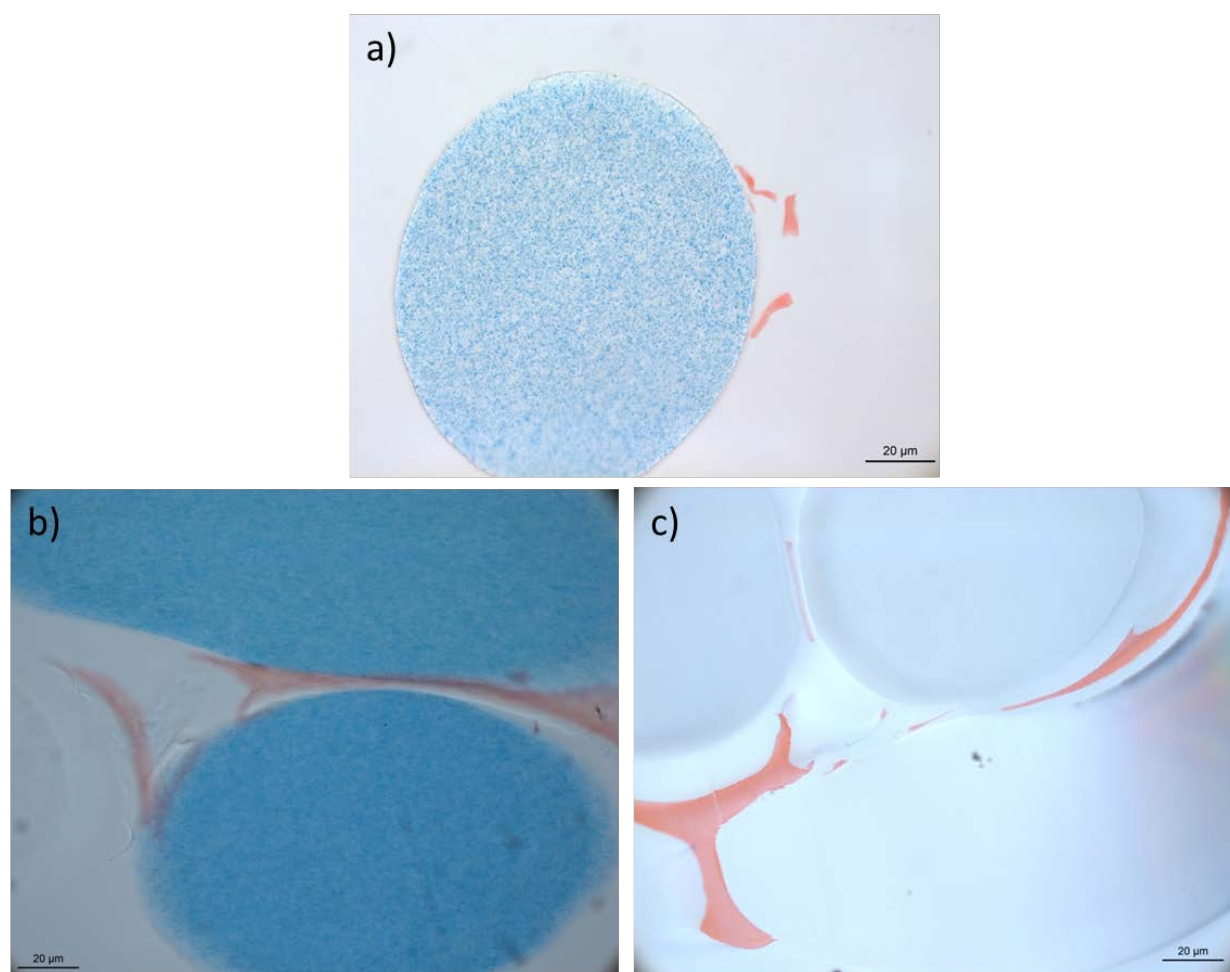


Figure 14. Serum-coated PROLENE fibers. (a) Paraffin embedded and (b) resin embedded are from TVT devices. (c) Resin embedded is from a hernia device. All samples were subjected to the staining protocol.

²⁷ Expert report of Dr. Vladimir Iakovlev dated January 29, 2016, p. 88, 94.

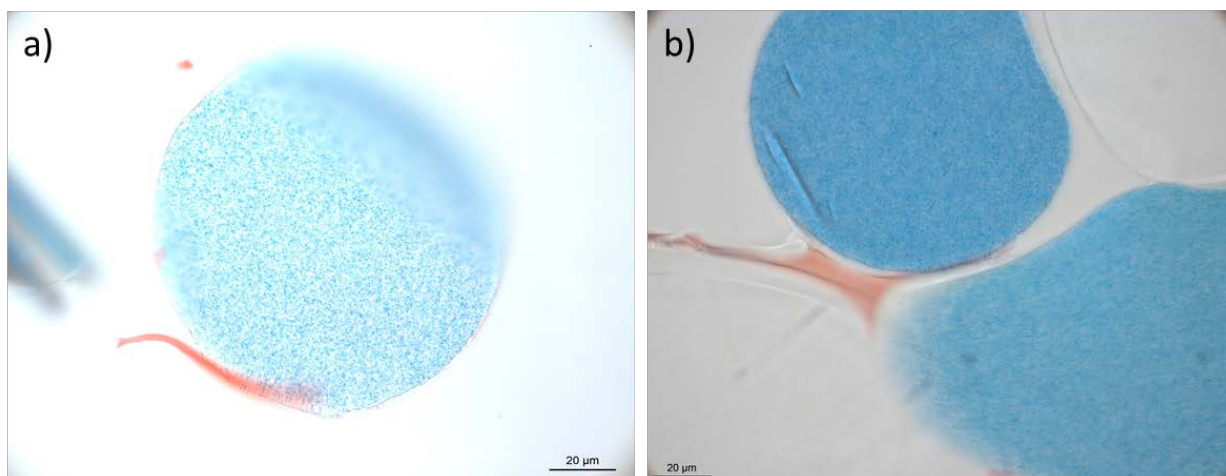


Figure 15. Blue granules from a PROLENE fiber are visible within the protein-rich serum coating, giving the illusion of stained PROLENE.

Non-oxidized Control—Out-of-the-Box PROLENE Mesh

In contrast, pristine PROLENE material processed using the same protocol and subjected to H&E staining protocol did not stain. The absence of staining is indicated by the absence of any pink coloration of the mesh fibers in samples embedded in either paraffin or resin (Figure 16).

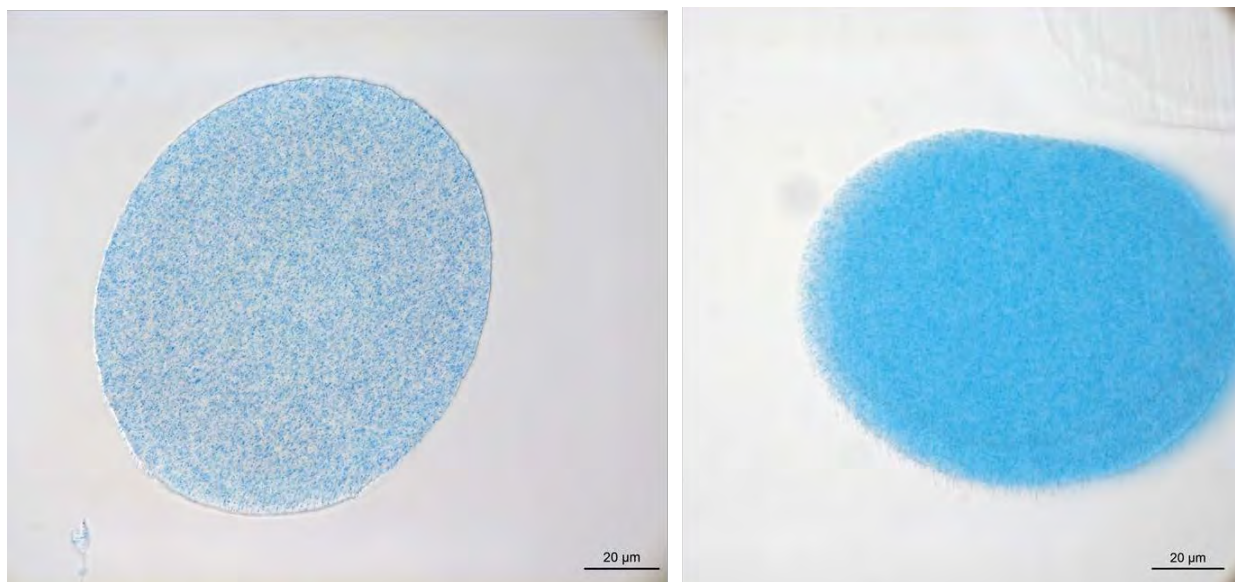


Figure 16. Pristine mesh fiber embedded in paraffin and subjected to Dr. Iakovlev's protocol (left). Pristine mesh fiber embedded in Technovit resin and subjected to staining (right). Both samples show an absence of H&E dye being absorbed.

Intentionally Oxidized PROLENE—Chemical Oxidation

The chemically treated PROLENE was not modified by the H&E stain in any of the five PROLENE devices examined, thereby confirming the flawed methodology of Dr. Iakovlev. The cobalt-based crystallites observed to cover the fiber surface when imaged with SEM appeared to be preserved in the cross-sections. The crystals that coat the surface of the PROLENE fibers appear pink. They also appear pink/purple in micrographs taken after the samples were embedded in paraffin and sectioned but before they were subjected to the staining protocol, as shown in Figure 17. The pink color appears enriched in the image of the stained fiber, likely because cobalt chloride is an ionic compound and therefore susceptible to accepting H&E stain.

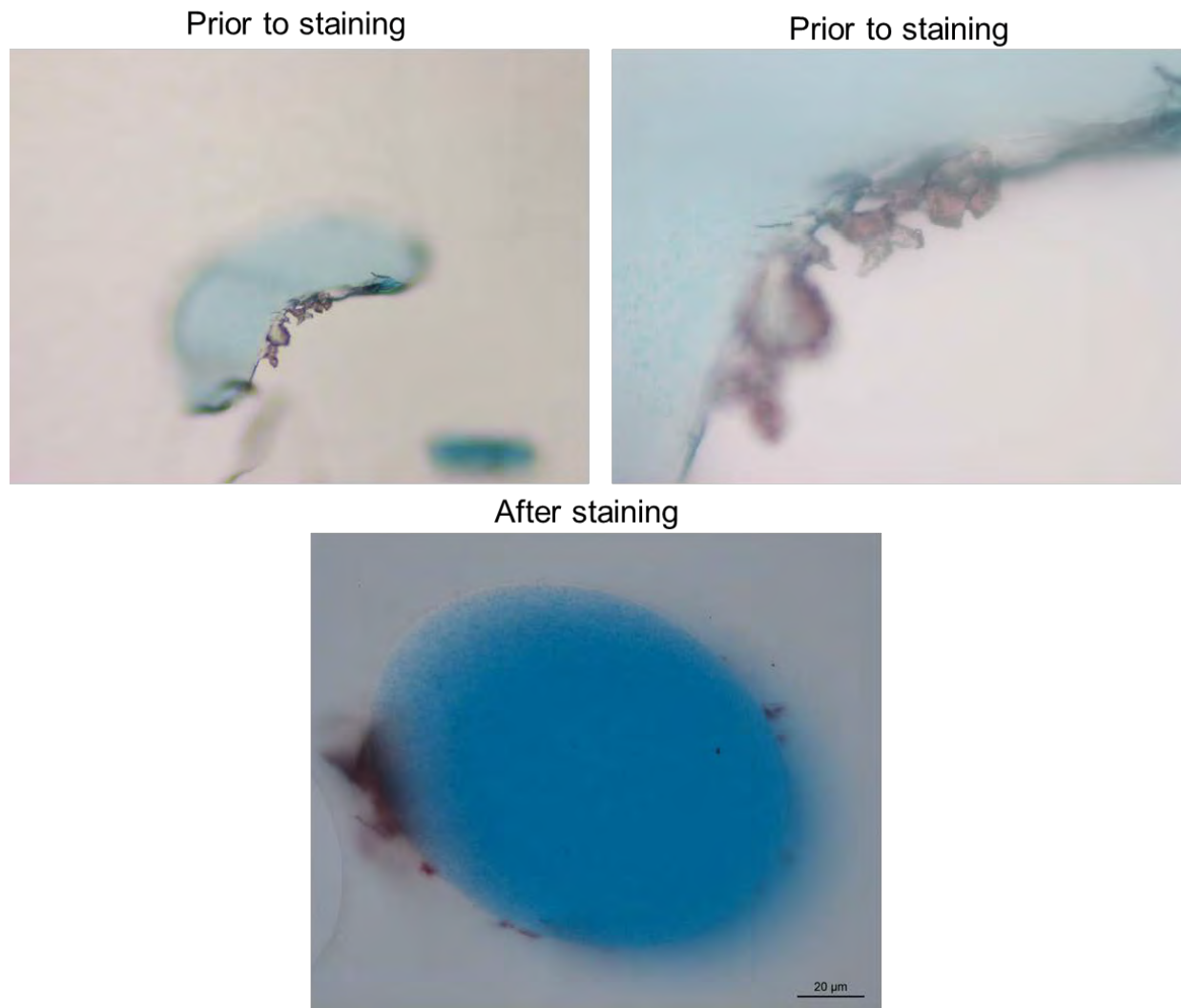


Figure 17. Cobalt-based crystallites adhered to the fiber surface are observed to be pink prior to being exposed to stain and after being stained.

Furthermore, cobalt-based crystallites appeared to be easily lodged between mesh fibers embedded in resin. An example is shown in Figure 18. An image of the fibers illuminated under cross-polarized light is also shown.

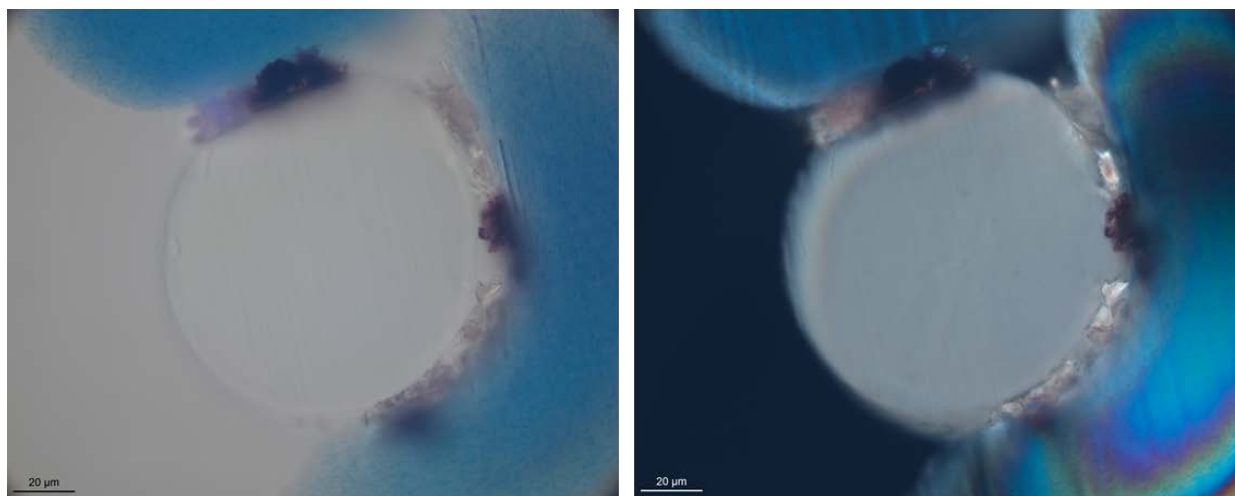


Figure 18. Cobalt-based crystallites are lodged between fibers. A bright field image is shown (left) as well as an image of the same fibers under cross-polarized light (right).

Intentionally Oxidized PROLENE—UV Oxidation

Exemplar PROLENE mesh samples exposed to QUV oxidation were also subjected to the Iakovlev staining protocol. As shown in Figure 19, despite the fact that fibers are extensively cracked and should have trapped stain, according to Dr. Iakovlev, the QUV-oxidized PROLENE did not accept the H&E stain. This finding further supports the conclusion that Dr. Iakovlev's methodology is flawed. Despite multiple observations, using high and low magnifications, polarized and nonpolarized light, no evidence of the stain being trapped, captured, or otherwise bound within the cracks of the damaged mesh was observed in any of the five different PROLENE devices examined.

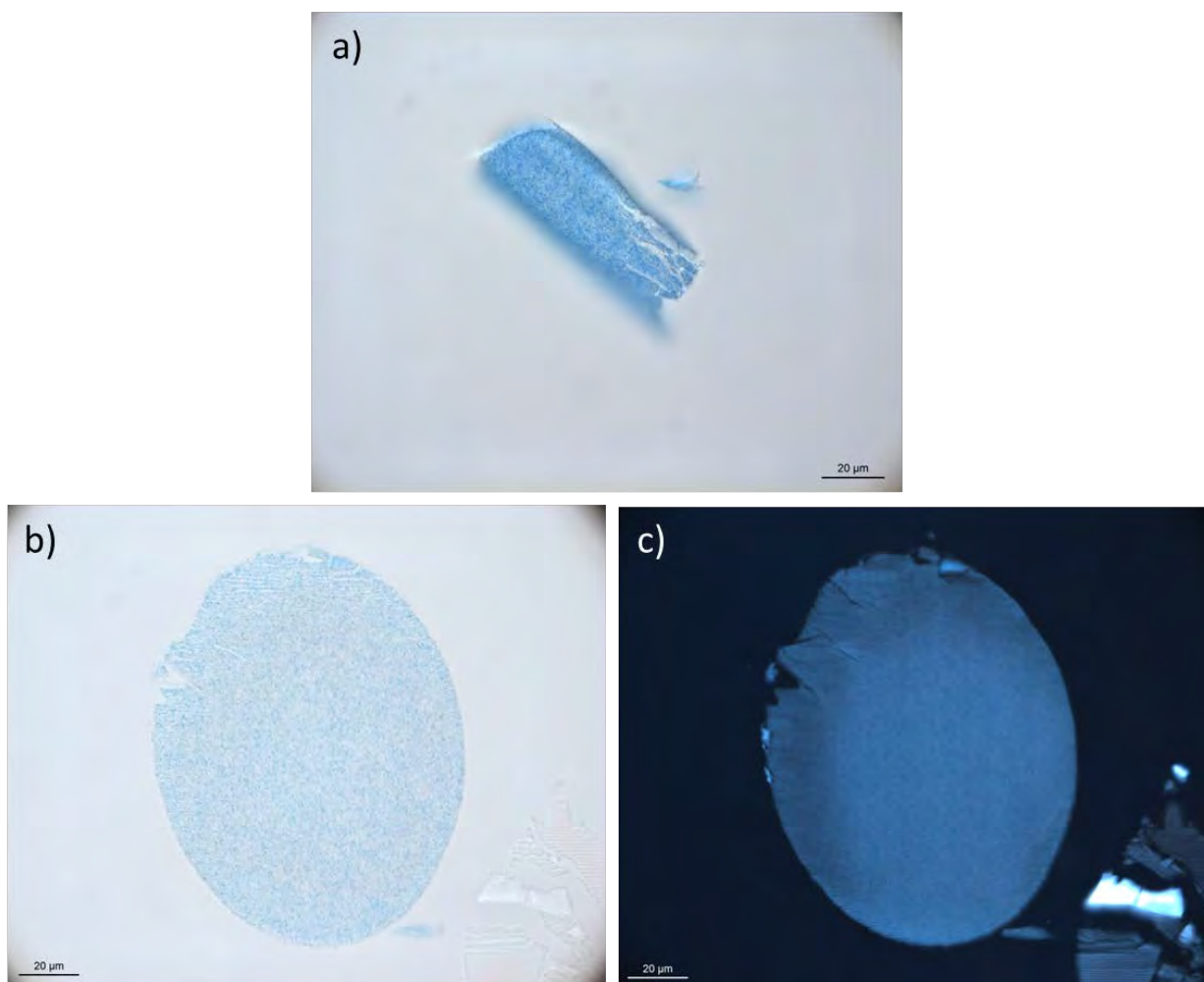


Figure 19. QUV-oxidized PROLENE fibers with several cracks embedded in paraffin. No staining is evident. Mesh fibers are shown under bright field light (a) and (b) and illuminated under cross-polarized light (c).

Imaging Artifacts

Microtome slicing of polymeric samples is a technique that I am familiar with and has been used in the field of polymer science for decades.^{28,29,30} Observation of thin-sliced polymeric specimens, including those that have been dyed, requires an understanding of potential artifacts that can exist as a result of the cutting process.

²⁸ Wang, X., & Zhou, W. (2002). Glass transition of microtome-sliced thin films. *Macromolecules*, 35(18), 6747–6750.

²⁹ Stiftinger, M., Buchberger, W., & Klampfl, C. W. (2013). Miniaturised method for the quantitation of stabilisers in microtome cuts of polymer materials by HPLC with UV, MS or MS2 detection. *Analytical and bioanalytical chemistry*, 405(10), 3177–3184.

³⁰ Janeschitz-Kriegl, H., Krobath, G., Roth, W., & Schausberger, A. (1983). On the kinetics of polymer crystallization under shear. *European polymer journal*, 19(10), 893–898.

In some instances during this study, select images appeared to have a pink background when viewed on two separate computer monitors. An example of this is shown in Figure 20. The image on the left is the actual image file. The image on the right is a photograph of the same image file being displayed on a different monitor. A photograph was taken to capture the color difference. This perceived change in hue is one example of how optics, lighting, and related artifacts may influence visual observations.

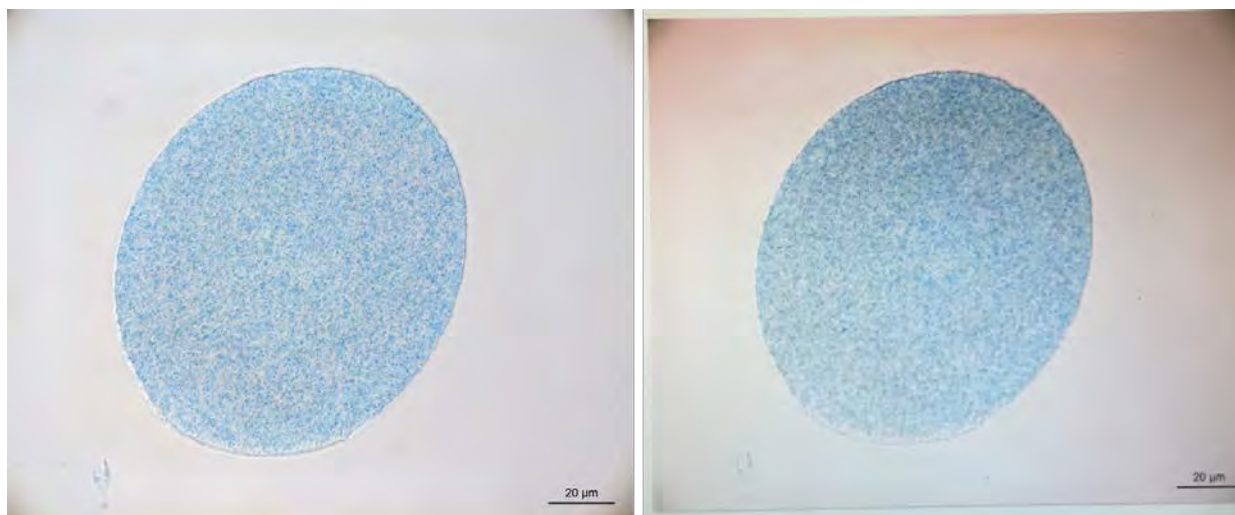


Figure 20. Same micrograph image of pristine PROLENE shown on two different computer monitors. A photograph of the image on the screen of monitor 2 was taken to preserve the observed pink coloring artifact.

Thickness Variation and Stain Pooling

When high-aspect ratio samples (such as fibers) are sectioned with a microtome, simple geometry dictates that the thickness will be variant if the microtome knife is not orthogonal to the sample's long axis. This geometric artifact is exhibited schematically in Figure 21, which illustrates that the edges of the sliced specimen are thinner when viewed under the microscope.

This same effect can result in stain pooling, which is also illustrated schematically in Figure 21. The cylindrical fibers that compose the mesh (A) can be cut in an oval shape depending on the angle at which the blade encounters the block (B). When the resulting section (C) is placed on a glass slide and stained, the angle between the section and the glass forms a small pocket in which stains can accumulate (D), giving the appearance of “true” staining (E)—that is, of chemical interactions between dyes and their ligands. In reality, this is merely a mechanical entrapment of the staining solution.

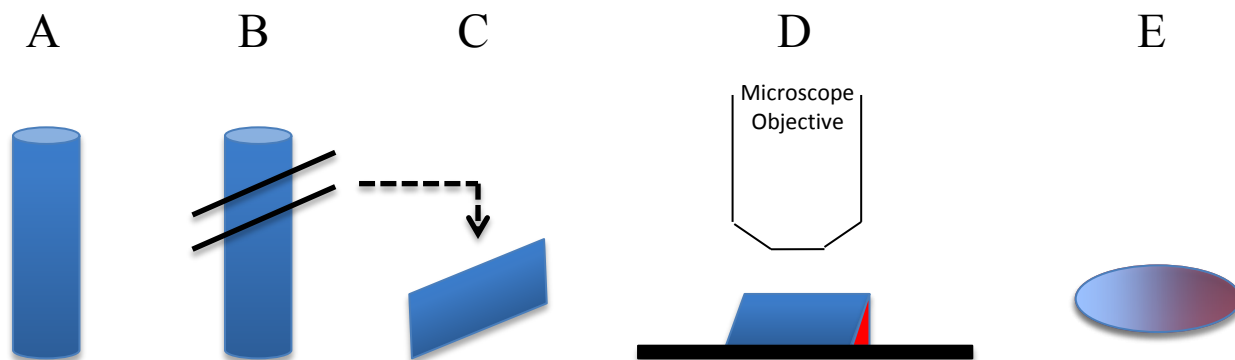


Figure 21. Potential formation mechanism of pooling artifact. A mesh fiber (A) can encounter the microtome blade at an angle (B), forming a section with an angled ledge (C), under which stain can pool (D) and give the appearance of true staining (E).

Stain pooling was observed in several fiber cross sections examined as part of this study. An example of stain pooling, as observed in a pristine TVT device not expected to stain, is given in Figure 22. Different planes of focus for the fiber cross section are given in Figure 22 that include an image of the plane of the fiber nearest the reader in focus (A) and the plane farther away from the reader, underneath the pristine fiber where the stain is pooled (B).

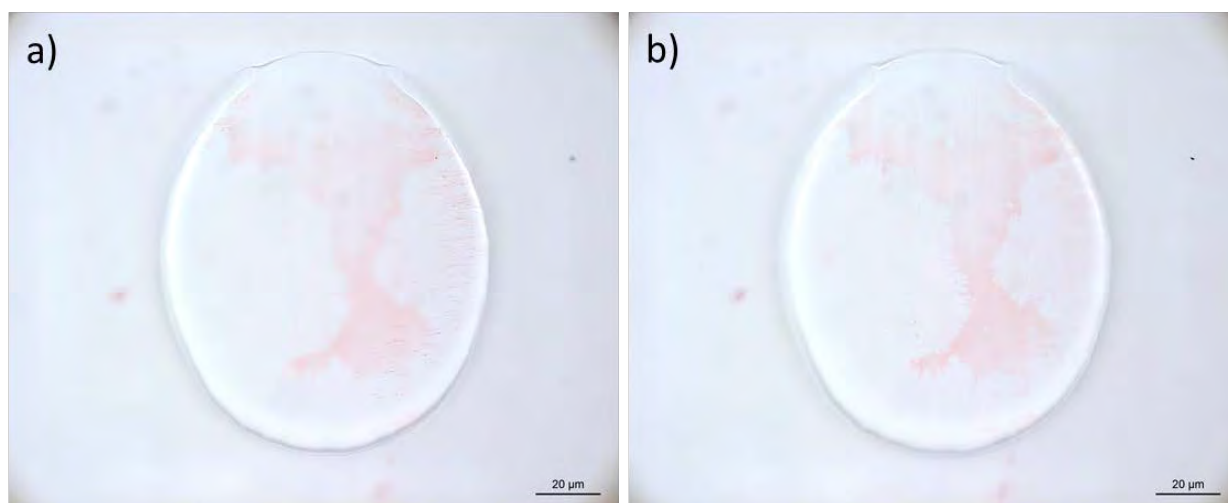


Figure 22. Example of stain pooling is shown. A fiber cross section from a pristine TVT mesh, not expected to stain, is shown with different planes of focus. For image (a), the plane nearest the reader is in focus. For image (b), the stain pooled underneath the fiber is in focus.

Polarizing Artifact

Polarized microscopy is a powerful tool in polymer science.³¹ With good optics and proper alignment, it allows for the visualization of anisotropic structures, making them appear under varying shades of brightness with a polarizing filter in the microscope's light path.³² The brightness of the sample when imaged under polarization depends on factors such as sample alignment. The brightness is greatest when the object is aligned at a 45° angle to the polarizers. On the other hand, the object can become difficult to see when aligned parallel to one of the two polarization planes.³³

The thickness variation resultant from microtoming, as well as the tendency of an anisotropic fiber to tear away from a surrounding matrix, can create edge artifacts under polarized light. An example of such an artifact is displayed in Figure 23, which is a micrograph of a *nonoxidized* (no possible “bark”) pristine PROLENE mesh fiber subjected to the H&E staining protocol. In Figure 23B and Figure 23C, the fiber is shown under polarized light, and a dark ring of false “bark” is visible on a portion of the fiber exterior. The images in Figure 23 show the same region with and without the polarizer.

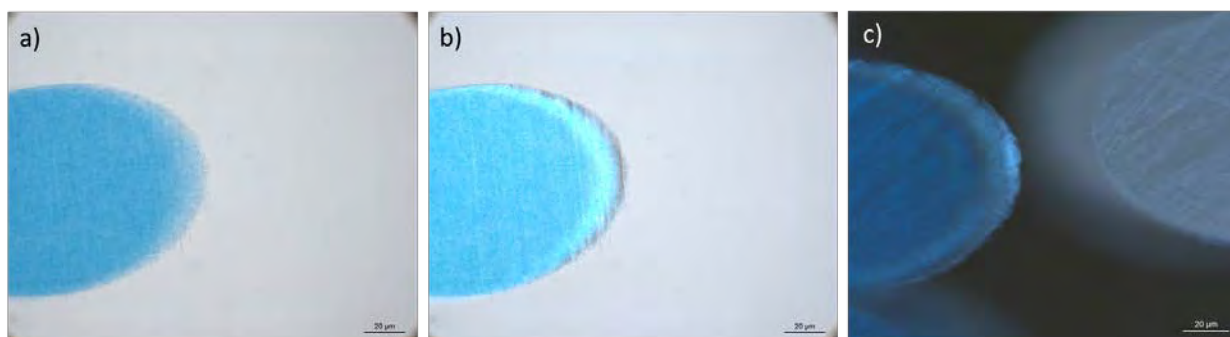


Figure 23. Pristine, nonoxidized PROLENE mesh after staining with H&E. Image (a) was obtained without polarized light. Images (b) and (c) were acquired with polarized light.

³¹ Collins, E.A, Bares, J., and Billmeyer, F.W. (1973) Experiments in Polymer Science, John Wiley & Sons.

³² Wolman, M. (1975). Polarized light microscopy as a tool of diagnostic pathology. Journal of Histochemistry & Cytochemistry, 23(1), 21–50.

³³ Ibid.

Mechanical Behavior of PROLENE Fibers

Dr. Iakovlev opines that oxidation of the PROLENE mesh causes the formation of “a continuous brittle sheath around the mesh filaments contributing to mesh stiffening while the contracting forces acted to deform the mesh. Additionally, degradation of a substance indicates its breakdown into smaller molecules, and in cases of implanted materials, the products of degradation are released into the tissue adding to the complex pathological interactions between the mesh and the human body.”³⁴ Dr. Iakovlev also notes that his alleged “bark” layer showed large nanocavities (cracks) that indicate brittleness.

From a fundamental polymer science perspective, Dr. Iakovlev’s above-stated opinions are flawed for a number of reasons. First, if we assume, for sake of argument, that the “bark” layer is more stiff than the underlying material, if it is filled with cracks (or nanopores and nanocavities as Dr. Iakovlev calls them), it is by definition discontinuous and therefore mechanistically cannot contribute to an increase in stiffening.³⁵ Dr. Iakovlev cannot have it both ways, either the material is stiff and uniform and leads to mesh stiffening, or it cracks and forms pores and traps dyes; the two are mutually exclusive. Second, if the PROLENE is actually being broken down into smaller molecules, it will tend to become less stiff, not more. Again, Dr. Iakovlev cannot have it both ways (indeed, by stating degradation into smaller molecules leads to stiffening, Dr. Iakovlev underscores the flawed nature of his reasoning).

³⁴ Expert report of Dr. Vladimir Iakovlev dated May 23, 2015, p. 54.

³⁵ Had he chosen to do so, with even a fundamental knowledge of mechanics, Dr. Iakovlev could have easily calculated that a continuous (without his observed pores and cracks) bark of the thickness he has measured could not meaningfully contribute to an increase in mesh stiffness.

Conclusion and Opinions

Based on my analysis, as well as my education, training and experience in mechanics of materials, polymer science and mechanical engineering, I have formed the following opinions to a reasonable degree of engineering and scientific certainty. If additional information becomes available, I reserve the right to supplement or amend any or all of these opinions.

- Dr. Iakovlev has not used any reliable scientific methods to conclusively determine that an outer oxidized PROLENE layer stains when exposed to H&E. Dr. Iakovlev's assertion that the mesh material has degraded *in vivo* is solely based on visual and microscopic observations of "bark" microcracking. He has conducted no quantitative experiments to confirm his visually based allegation that the mesh material is degraded or oxidized.
- Dr. Iakovlev has not performed any control experiments nor cited any scientific studies that support his belief that degraded PROLENE is capable of being histologically stained with H&E stains, and for these reasons, his conclusions are flawed and suspect.
- Through a series of controlled oxidation, microtoming and microscopy experiments, Exponent demonstrated that oxidized PROLENE mesh fibers and sutures do not become stained with Hematoxylin & Eosin dyes. This fact is supported by polymer science first principles, given that PROLENE does not possess chemical groups amenable to binding with the H&E stain molecules.
- Artifacts can easily be introduced during sample preparation, sectioning, staining, and imaging, giving the appearance of darkened outer layers.
- A brittle outer layer will not contribute to the stiffness of the mesh if it is thin, cracked, and discontinuous. Dr. Iakovlev's opinion that a thin, cracked, porous outer layer causes an increase in mesh stiffness is not consistent with polymer science first principles and contradicted by the measured modulus data from Ethicon's seven year dog study.

If you have any questions or require additional information, please do not hesitate to contact me.

A handwritten signature in black ink, appearing to read "S MacLean", is centered on the page.

Steven MacLean, Ph.D., P.E.
Senior Managing Engineer

Appendix A: Histology Protocols

Paraffin-embedded samples

1. Samples were processed and embedded in an automated tissue processor according to the following schedule:

Processing Step	Incubating Solution	Number of Changes	Duration of Each Incubation Step
1	70% Reagent Alcohol	2	1 hour each
2	80% Reagent Alcohol	1	1 hour
3	95% Reagent Alcohol	1	1 hour
4	100% Reagent Alcohol	3	1.5 hours each
5	Xylene substitute (ProPar, Manufacturer)	3	1.5 hours each
6	Leica EM400 Paraffin wax	2	2 hours each

2. Tissues were embedded in paraffin blocks using Leica EM400 wax
3. The paraffin blocks were trimmed as necessary and cut at 4-6 μm -thick sections
4. The paraffin sections were briefly floated in a water bath set to 40-45°C to remove wrinkles and allow them to flatten
5. The sections were mounted onto adhesive-coated glass slides, then air-dried for 30 minutes and baked in a 45-50°C oven overnight

6. Paraffin-embedded samples were stained by hand using the following protocol:

Processing Step	Incubating Solution	Duration of Each Incubation Step
1	65°C	10 min
2	Xylene	3 min
3	Xylene	2 min
4	Xylene	2 min
5	100% Alcohol	1 min
6	100% Alcohol	1 min
7	95% Alcohol	1 min
8	Water	1 min
9	Harris Hematoxylin	10 min
10	Wash station	1 min
11	Acid Alcohol	30 sec
12	Water	2 min
13	Ammonia Water	1 min
14	Water	1 min
15	Eosin	2 min
16	Water	20 sec
17	100% Alcohol	1 min
18	100% Alcohol	1 min
19	100% Alcohol	1 min
20	Xylene	1 min
21	Xylene	1 min

Resin-embedded samples

1. Samples were processed and embedded according to the following schedule:

Processing Step	Incubating Solution	Number of Changes	Duration of Each Incubation Step
1	70% Reagent Alcohol	2	1 hour each
2	80% Reagent Alcohol	1	1 hour
3	95% Reagent Alcohol	1	1 hour
4	100% Reagent Alcohol	3	1.5 hours each
5	Technovit 7200	3	3 hours each

2. The resin samples were polymerize using a visible light polymerization unit
3. The blocks were trimmed as necessary, cut using a diamond saw blade, then ground and polished to 10 – 61 μm with a mean thickness of approximately 30 μm .
4. Resin-embedded samples were stained by hand using the following protocol:

Processing Step	Incubating Solution	Duration of Each Incubation Step
1	Water	1 min
2	Harris Hematoxylin	4 hours ³⁶
3	Water	1 min
4	Acid Alcohol	30 sec
5	Water	1 min
6	Ammonia water	1 min
7	Water	1 min
8	Eosin	1 min
9	Water	30 sec

³⁶ The intensity of the stain was monitored microscopically every 15 minutes until the positive control, rabbit skin, was dark enough.

Appendix B: Steven MacLean, Ph.D., P.E. CV

Professional Profile

Dr. Steven MacLean is a Senior Managing Engineer in Exponent's Polymer Science and Materials Chemistry practice. Dr. MacLean's research and professional interests lie in the area of chemical and physical behavior of polymeric materials in end-use applications. His specialties include part design and analysis, failure analysis, and assessing candidate materials through end-use testing. He has studied various polymer failure mechanisms including stress overload, creep rupture, fatigue, environmental stress cracking, and weathering. Throughout his career he has evaluated the suitability of materials for the automotive, sporting goods, medical, business equipment, and construction industries. Dr. MacLean is proficient in a variety of analytical techniques including finite element analysis, statistical methods, as well as empirical approaches to long-term reliability and durability.

Dr. MacLean has considerable practical experience in the conversion of raw materials into finished goods. Throughout his career, he has worked with polymer conversion processes such as injection molding, compression molding, blow molding, extrusion, thermoforming, and laminating. In addition, he has worked on numerous projects involving common secondary operations used throughout the plastics industry such as metallic plating, adhesive joining, painting, as well as vibration and ultrasonic welding.

Dr. MacLean is well versed in voluntary standards and national regulations and codes that often prescribe the technical performance of plastic materials in various industries. Standards organizations and regulatory bodies with which he has interacted include Underwriters Laboratories (UL), International Electrotechnical Commission (IEC), US EPA, California Air Resource Board, NSF International, and ASTM International. He has also participated in numerous sustainability and life cycle assessments (LCAs) per ISO 14040 standards to quantify the environmental impact of manufactured products and raw materials.

Prior to joining Exponent, Dr. MacLean spent 16 years in the plastics industry at General Electric Plastics and SABIC Innovative Plastics where he held several technical positions of

increasing responsibility. His activities included material selection and testing for high-demand applications, product safety assessments, failure analysis, and intellectual property analysis.

Academic Credentials and Professional Honors

Ph.D., Materials Science, University of Rochester, 2007

M.S., Materials Science and Engineering, Rochester Institute of Technology, 2001

M.E., Mechanical Engineering, Rensselaer Polytechnic Institute, 1997

B.S., Mechanical Engineering, Rensselaer Polytechnic Institute (with honors), 1993

Tau Beta Pi; Pi Tau Sigma; Society of Plastics Engineers ANTEC Best Paper Award

Licenses and Certifications

Registered Professional Engineer, New York, #16-079001

Registered Professional Engineer, Maryland, #41593

National Council of Examiners for Engineering and Surveying, Record #47204

Certified Six Sigma Black Belt

Publications

MacLean SB, et al. Fractographic examination and tensile property evaluation of 3D printed acrylonitrile butadiene styrene (ABS). Proceedings, ANTEC, 2015.

MacLean SB, et al. Fractographic examination of failures in polycarbonate and polyoxymethylene due to impact, tensile, fatigue and creep mechanisms. Proceedings, ANTEC, 2013.

MacLean SB, et al. Comparison of mass transit material flammability requirements and trends for aircraft and train applications in Europe and North America. Proceedings, ANTEC, 2012.

MacLean SB, et al. Comparison of mass transit material flammability requirements and trends for aircraft and train applications in Europe and North America. Proceedings, EUROTEC, 2011.

MacLean SB, et al. Root cause investigation of cracked polycarbonate blender jars. Proceedings, ANTEC, 2010.

MacLean SB. Plastics, electronics and the environment: How new global regulations affect material choices. Kunststoffe International 2008 Sept; 97–100.

MacLean SB. Plastics, electronics and the environment: How new global regulations affect material choices. Telepati Aylik Telekom 2008 Mar; 74–77.

MacLean SB, et al. Monolayer barrier for small engine fuel tanks. *Plastics Technology Online* 2007 June.

MacLean SB. Environmental effects of poly(phenylene ether) blends due to long-term exposure to potable hot water. Ph.D. Dissertation, University of Rochester, 2007.

MacLean SB, et al. The effects of recycling and heat history for select high polymers. *Proceedings, ANTEC* 2001.

MacLean SB, et al. Poly(phenylene ether) engineering thermoplastic provides creep resistance, toughness and fire resistance required for high performance pallets. *Proceedings, ANTEC* 2000.

Presentations

MacLean SB, Moll J. The importance of polymer structure-property relationships in preventing failure in medical devices. *Medical Grade Polymers Conference*, Woburn, MA, 2015.

MacLean SB. Fundamentals of plastics fractography. *ANTEC*, Cincinnati, OH, 2013.

MacLean SB. Challenges associated with replacing metal with plastic. *Material Science and Technology Conference*, Pittsburgh, PA, 2012.

MacLean SB, et al. Fractography of unfilled thermoplastic materials subjected to common mechanical failure modes. *Material Science and Technology Conference*, Pittsburgh, PA, 2012.

MacLean SB. Common analytical techniques for failure analysis – A Resin Manufacturer's Perspective. *ANTEC*, Boston, MA, 2011.

MacLean SB, et al. Plastic failure analysis and prevention expert panel. *ANTEC*, Boston, MA, 2011.

MacLean SB. Root cause investigation of cracked polycarbonate blender jars. *ANTEC*, Orlando, FL, 2010.

MacLean SB. Diffusion of potable hot water in poly(phenylene ether) blends. *American Chemical Society Conference*, Binghamton, NY, 2006.

MacLean SB. Changes in polycarbonate and ABS mechanical properties due to multiple heat histories. *Society of Plastics Engineers ANTEC*, Dallas, TX, 2001 (with Korzen).

MacLean SB. Yield Improvement for gas assist panels using statistical methods. *Society for the Plastics Industry Conference*, Vancouver, BC, 2000.

MacLean SB. Design methodologies for metal to plastic conversion. *General Electric Plastics Innovation Seminar*, Columbus OH, 2000.

MacLean SB. Fundamentals of polymer science. *General Electric Plastics Customer Design Workshop*, Pittsfield, MA, 1998, 1999.

MacLean SB. Designing for injection molded parts. General Electric Plastics Customer Design Workshop, Pittsfield, MA, 1998, 1999.

MacLean SB. Mechanical behavior of polymeric materials. General Electric Plastics Engineering Workshop, Pittsfield, MA, 1997.

Prior Experience

Director, Global Agency Relations & Product Safety, SABIC Innovative Plastics,
2007-2011

Global Technical Manager, General Electric Plastics, 2003–2007

Six Sigma Black Belt, General Electric Plastics, 2001–2003

Senior Application Development Engineer, General Electric Plastics, 1998–2001

Plastic Design and Analysis Leader, General Electric Plastics, 1996–1998

Edison Engineer, Lockheed Martin Corporation, (Formerly General Electric Aerospace),
1994–1996

Professional Affiliations

Society of Plastics Engineers (Senior Member)

SPE Failure Analysis & Prevention Group – Board Member and Treasurer

ASTM D20 Plastics Committee Member

Appendix C: Testimony of Steven MacLean, Ph.D., P.E.

Workhorse Custom Chassis, LLC v. Robert Bosch LLC (Marion Superior Court of Indiana), October 2012 (Deposition)

Trice, et al. v. **Toyota Motor Corporation**, et al. (United States District Court – District of Minnesota), August 2013 (Deposition), January 2015 (Trial)

Alberto, et al. v. **Toyota Motor Corporation**, et al. (Genesee County, Michigan), November 2013 (Deposition)

Metropolitan Property & Casualty Insurance v. **LG Electronics**, et al. (United States District Court – District of Arizona), August 2014 (Deposition)

Nease v. **Ford Motor Company** (United States District Court of West Virginia - Huntington Division), December 2014 (Deposition), March 2015 (Trial)

Wubker, et al. v. **A&A Manufacturing Company**, et al. (Santa Fe County, New Mexico), January 2015 (Deposition)

Promethean Insulation Technology LLC v. **Reflectix, Inc.**, et al. (United States District Court of Eastern Texas - Marshall Division), June 2015 (Deposition), October 2015 (Trial)

Nettleton, et al. v. **Ford Motor Company** (United States District Court Northern District of California - San Francisco Division), July 2015 (Deposition)

Mullins, et al. v. **Ethicon** (United States District Court Southern District of West Virginia - Charleston Division), September 2015 (Deposition)

Hower v. **Excel Industries, Inc.**, et al. (United States District Court Western District of Missouri - Southern Division), November 2015 (Deposition)

Brunswick Woodworking Company, Inc. et al. v. **Slocum Adhesives Corp.**, et al., (Circuit Court for Montgomery County, Maryland) January 2016 (Deposition)

Appendix D: List of Documents Reviewed

Literature

A Dictionary of Computing, Oxford University Press, 2004.

Additives: Antioxidants; 7972F/1208; Equistar; pp 1-2.

Anderson, J. M., McNally, A. K. Biocompatibility of Implants: Lymphocyte/macrophage Interactions. *Seminars in Immunopathology*, (2011) 33(3):221–233.

Anderson, J. M., Rodriguez, A., Chang, D. T. Foreign Body Reaction to Biomaterials. *Seminars in Immunology*, (2008) 20(2):86–100.

Atta, A., Modulation of Structure, Morphology and Wettability of Polytetrafluoroethylene Surface by Low Energy Ion Beam Irradiation, *Nuclear Instruments and Methods in Physics Research Section B: Beam Interactions with Materials and Atoms* (2013) 300:46-53.

Bell, B., Beyer, D. E., Maecker, N. L., Papenfus, R. R., Priddy, D. B., Permanence of polymer stabilizers in hostile environments, *Journal of Applied Polymer Science* (1994) 54:1605-1612.

Bell, G. R., Microtoming: An Emerging Tool for Analyzing Polymer Structures. *Plastics Engineering* (1979) August.

Bezwada, R. S., Jamiolkowski, D. D., Lee, I-Y., Vishvaroop, A., Persivale, J., Trenka-Bethnin, S., Erneta, M., Suryadevara, J., Yang, A., Liu, S., Monocryl suture, a new ultra-pliable absorbable monofilament suture, *Biomaterials* (1995) 16:1141-1146.

Birch, C., The Use of Prosthetics in Pelvic Reconstructive Surgery. *Best Practice & Research Clinical Obstetrics and Gynecology* (2005) 19(6):979-997.

Blais, P., The Photo-Oxidation of Polypropylene Monofilaments, Part II: Physical Changes and Microstructure, *Textile Research Journal*, (1976) 46(9):641-648.

Bracco, P., Brunella, V., Trossarelli, L., Coda, A., Botto-Micca, F., Comparison of polypropylene and polyethylene terephthalate (Dacron) meshes for abdominal wall hernia repair: A chemical and morphological study. *Hernia* (2005) 9:51-55.

Carlsson, D. J., Wiles, D. M. The Photodegradation of Polypropylene Films. III. Photolysis of Polypropylene Hydroperoxides. *Macromolecules*, (1969) 2(6):597–606.

Chan, J. K. C. The Wonderful Colors of the Hematoxylin-Eosin Stain in Diagnostic Surgical Pathology. *International Journal of Surgical Pathology*, (2014) 22(1):12–32.

Chemical Book, accessed August 23, 2015.

http://www.chemicalbook.com/ChemicalProductProperty_EN_CB3712869.htm

Chen, Z., Hay, J. N., Jenkins, M. J. FTIR Spectroscopic Analysis of Poly(ethylene Terephthalate) on Crystallization. *European Polymer Journal*, (2012) 48(9):1586–1610.

Chowbey, Pradeep, ed. *Endoscopic Repair of Abdominal Wall Hernias* (2nd Edn.): Revised and Enlarged Edition. Byword Books Private Limited, 2012.

Clavé, A., Yahi, H., Hammou, J.-C., Montanari, S., et al. Polypropylene as a Reinforcement in Pelvic Surgery Is Not Inert: Comparative Analysis of 100 Explants. *International Urogynecology Journal*, (2010) 21(3):261–270.

Cojocari, D. pKa Data, *CRC Handbook of Chemistry* 2010, University of Toronto (2011).

Cosson, M., Lambaudie, E., Boukerrou, M., Lobry, P., et al. A Biomechanical Study of the Strength of Vaginal Tissues. *European Journal of Obstetrics & Gynecology and Reproductive Biology*, (2004) 112(2):201–205.

Costello, C. R., Bachman, S. L., Ramshaw, B. J., Grant, S. A. Materials Characterization of Explanted Polypropylene Hernia Meshes. *Journal of Biomedical Materials Research Part B: Applied Biomaterials*, (2007) 83B(1):44–49.

Costello, C., Characterization of Heavyweight and Light weight Polypropylene Prosthetic Mesh Explants From a Single Patient, *Surgical Innovation* (2007) 14(3):168-176.

Cozad, M. J., Materials Characterization of Explanted Polypropylene, Polyethylene Terephthalate, and Expanded Polytetrafluoroethylene Composites: Spectral and Thermal Analysis, *Journal of Biomedical Materials Research Part B: Applied Biomaterials* (2010) 94(2):455-462.

Cundiff, G. W., Varner, E., Visco, A. G., Zyczynski, H. M., et al. Risk Factors for Mesh/suture Erosion Following Sacral Colpopexy. *American Journal of Obstetrics and Gynecology*, (2008) 199(6):688.e1–688.e5.

Dällenbach, P. “To Mesh or Not to Mesh: A Review of Pelvic Organ Reconstructive Surgery.” *Int. J. Womens Health*, (2015) 331-343.

de Tayrac, R., Letouzey, V. Basic Science and Clinical Aspects of Mesh Infection in Pelvic Floor Reconstructive Surgery. *International Urogynecology Journal*, (2011) 22(7):775–780.

de Tayrac, R., Sentilhes, L. Complications of Pelvic Organ Prolapse Surgery and Methods of Prevention. *International Urogynecology Journal*, (2013) 24(11):1859–1872.

DeBord, J. R. Prostheses in Hernia Surgery: A Century of Evolution. *Abdominal Wall Hernias*. Ed. Robert Bendavid, Jack Abrahamson, Maurice E. Arregui, Jean Bernard Flament, et al. New York, NY: Springer New York, 2001. 16–32.

Deeken, C. R., Abdo, M. S., Frisella, M. M., Matthews, B. D., Physicomechanical evaluation of polypropylene, polyester, and polytetrafluoroethylene meshes for inguinal hernia repair, *American College of Surgeons*, (2011) 212:68-79.

Edwards, S.L., Werkmeister, J.A., Rosamilia, A., Ramshaw, J.A.M., et al. Characterization of Clinical and Newly Fabricated Meshes for Pelvic Organ Prolapse Repair. *Journal of the Mechanical Behavior of Biomedical Materials*, (2013) 2353–61.

Elneil, S., Cutner, A. S., Remy, M., Leather, A. T., et al. Abdominal Sacrocolpopexy for Vault Prolapse without Burial of Mesh: A Case Series. *BJOG: An International Journal of Obstetrics and Gynaecology*, (2005) 112(4):486–489.

Fayolle, L., Oxidation Induced Embrittlement in Polypropylene – a Tensile Testing Study, *Polymer Degradation and Stability* (2000) 70:333-340.

FDA Draft ISO 10993

FDA Guidance for the Preparation of a Premarket Notification Application for a Surgical Mesh, Accessed July 25, 2015, Available at:

<http://www.fda.gov/MedicalDevices/DeviceRegulationandGuidance/GuidanceDocuments/ucm073790.htm>.

FDA Guidelines on Premarket Approval of Medical Devices, Accessed July 25, 2015, Available at:

<http://www.fda.gov/MedicalDevices/DeviceRegulationandGuidance/HowtoMarketYourDevice/PremarketSubmissions/PremarketApprovalPMA/ucm050490.htm#bio>.

Fotopoulou, K. N., Surface Properties of Beached Plastics, *Environmental Science and Pollution Research*, (2015) 22(14):11022-11032.

Garton, A., Carlsson, D. J., Wiles, D. M. Role of Polymer Morphology in the Oxidation of Polypropylene. *Journal of Polymer Science: Polymer Chemistry Edition*, (1978) 16(1):33–40.

Gensler, R., Plummer, C. J., Kausch, H.-H., Kramer, E., et al. Thermo-Oxidative Degradation of Isotactic Polypropylene at High Temperatures: Phenolic Antioxidants versus HAS. *Polymer Degradation and Stability*, (2000) 67(2):195–208.

George, G. A., Celina, M., Vassallo, A. M., Cole-Clarke, P. A. Real-Time Analysis of the Thermal Oxidation of Polyolefins by FT-IR Emission. *Polym. Degrad. Stab.*, (1995) 48(2):199–210.

Gijsman, P., Hennekens, J., Vincent, J. The Mechanism of the Low-Temperature Oxidation of Polypropylene. *Polymer Degradation and Stability*, (1993) 42(1):95–105.

Godbey, W. *An Introduction to Biotechnology The Science, Technology and Medical Applications*. Elsevier, 2014.

Guelcher, S. A., Dunn, R. F. Oxidative Degradation of Polypropylene Pelvic Mesh in Vitro. *Int Urogynecol J*, (2015) 26(Suppl 1):S55–S56.

Helander, K. G. Kinetic Studies of Formaldehyde Binding in Tissue. *Biotechnic & Histochemistry*, (1994) 69(3):177–179.

Hewitson, T. D., Wigg, B., Becker, G. J. *Tissue Preparation for Histochemistry: Fixation, Embedding, and Antigen Retrieval for Light Microscopy. Histology Protocols*. Ed. Tim D. Hewitson and Ian A. Darby. Vol. 611. Totowa, NJ: Humana Press, 2010. 3–18.

Hirsh, S. L., McKenzie, D. R., Nosworthy, N. J., Denman, J. A., et al. The Vroman Effect: Competitive Protein Exchange with Dynamic Multilayer Protein Aggregates. *Colloids and Surfaces B: Biointerfaces*, (2013) 103395–404.

Iakovlev, V. V., Guelcher, S. A., Bendavid, R. Degradation of Polypropylene in Vivo : A Microscopic Analysis of Meshes Explanted from Patients. *J. Biomed. Mater. Res. B Appl. Biomater.*, (2015) 000–000.

Imel, A., Malmgren, T., Dadmun, M., Gido, S., Mays, J., In vivo oxidative degradation of polypropylene pelvic mesh, *Biomaterials*, (2015) 73:131-141.

ISO 10993-1+Cor1-2010

ISO 10993-1-2009

ISO 10993-18-2005

ISO 10993-55.009(e) v.1

ISO 12891-1

ISO 12891-2

ISO 12891-3

Janeschitz-Kriegl, H., Krobath, G., Roth, W., Schausberger, A. On the Kinetics of Polymer Crystallization under Shear. *Eur. Polym. J.*, (1983) 19(10-11):893–898.

Jansen, J. A. Environmental Stress Cracking - The Plastic Killer. *Advanced Materials & Processes*, June 2004.

Janzen, W., Ehrenstein, G. W. Microtomy of Polymeric Materials Part 2: Application of Microtomy. *Practical Metallography*, (1989) 26549–558.

Jongebloed, W.L., Worst, J.F., Degradation of Polypropylene in the Human Eye: a SEM-study (1986) 64(1):143-52.

Jongeblood, W. L., Figueras, M. J., Humalda, D., Blanksma, L. J., Worst, J. G. F., Mechanical and biochemical effects of man-made fibres and metals in the human eye, a SEM-study, *Documenta Ophthalmologica* (1986) 61:303-312.

Julian, T. M. The Efficacy of Marlex Mesh in the Repair of Severe, Recurrent Vaginal Prolapse of the Anterior Midvaginal Wall. *American Journal of Obstetrics and Gynecology*, (1996) 175(6):1472–1475.

Kanagarajah, P., Ayyathirai, R., & Gomez, C. (2012). Evaluation of Current Synthetic Mesh Materials in Pelvic Organ Prolapse Repair. *Current urology reports*, 13(3): 240-246.

Kawaguchi, T., Nishimura, H., Miwa, F., Kuriyama, T., et al. Environmental Effects. *Plastics Failure Analysis and Prevention*. Elsevier, 2001. 73–78.

Keys, T., Aboushwareb, T., Badlani, G., Re: Post-Implantation Alterations of PP in Humans.

Klinge, U., Klosterhalfen, B., Conze, J., Limberg, W., et al. Modified Mesh for Hernia Repair That Is Adapted to the Physiology of the Abdominal Wall. *European Journal of Surgery*, (2003) 164(12):951–960.

Klink, C.D., Junge, K., Binnebösel, M., Alizai, H.P., Otto, J., Neumann, U.P., Klinge, U. Comparison of Long-Term Biocompatibility of PVDF and PP Meshes. *Journal of Investigative Surgery*, (2011) 24(6):292-299.

Kurtz, J., Rael, B., Lerma, J., Wright, C., Khraishi, T., Auyang, E. D., Effects of reactive oxygen species on the physical properties of polypropylene surgical mesh at various concentrations: a model for inflammatory reaction as a cause for mesh embrittlement and failure, *Surg. Endosc.* (2015).

Kyriakides, T. R. Molecular Events at Tissue–Biomaterial Interface. Host Response to Biomaterials. Elsevier, 2015. 81–116.

Lai, M., Lü, B. Tissue Preparation for Microscopy and Histology. *Comprehensive Sampling and Sample Preparation*. Elsevier, 2012. 53–93.

Lappan, U., Geißler, U., Häußler, L., Jehnichen, D., et al. Radiation-Induced Branching and Crosslinking of Poly(tetrafluoroethylene) (PTFE). *Nuclear Instruments and Methods in Physics Research Section B: Beam Interactions with Materials and Atoms*, (2001) 185(1-4):178–183.

Lappan, U., Geißler, U., Lunkwitz, K. Changes in the Chemical Structure of Polytetrafluoroethylene Induced by Electron Beam Irradiation in the Molten State. *Radiation Physics and Chemistry*, (2000) 59(3):317–322.

Lenz, R. W. Experiments in Polymer Science, Edward A. Collins, Jan Bares, Fred W. Billmeyer, Jr., Wiley-Interscience, New York, 1973. 530 Pp. \$16.95. *J. Polym. Sci. Polym. Lett. Ed.*, (1974) 12(9):535–536.

Liebert, T. C., Chartoff, R. P., Cosgrove, S. L., McCuskey, R. S. Subcutaneous Implants of Polypropylene Filaments. *Journal of Biomedical Materials Research*, (1976) 10(6):939–951.

Lubliner, J, Papadopoulos, P. Introduction to Solid Mechanics an Integrated Approach. New York: Springer, 2014.

Maher, C., Feiner, B., Baessler, K., Schmid, C. Surgical Management of Pelvic Organ Prolapse in Women. *Cochrane Database of Systematic Reviews*. Ed. The Cochrane Collaboration. Chichester, UK: John Wiley & Sons, Ltd, 2013.

Maier, C.; Calafut, T. Polypropylene: the Definitive User's Guide and Databook; PDL Handbook Series: Plastics Design Library: Norwich, NY, 1998.

Mary, C., Marois, Y., King, M. W., Laroche, G., et al. Comparison of the In Vivo Behavior of Polyvinylidene Fluoride and Polypropylene Sutures Used in Vascular Surgery: *ASAIO Journal*, (1998) 44(3):199–206.

McInnes, E. Artefacts in Histopathology. *Comparative Clinical Pathology*, (2005) 13(3):100–108.

McKeen, L. W. Plastics Used in Medical Devices. *Handbook of Polymer Applications in Medicine and Medical Devices*. Elsevier, 2014. 21–53.

Mei, G., Herben, P., Cagnani, C., Mazzucco, A. The Spherizone Process: A New PP Manufacturing Platform. *Macromolecular Symposia*, (2006) 245-246(1):677–680.

Miller, J.M., Kimmel, L.E. Clinical Evaluation of Monofilament Polypropylene Suture. *The American Surgeon*, (1967) 33(8):666-670.

Moore, P. F., Schrenzel, M. D., Affolter, V. K., Olivry, T., et al. Canine Cutaneous Histiocytoma Is an Epidermotropic Langerhans Cell Histiocytosis That Expresses CD1 and Specific Beta 2-Integrin Molecules. *The American Journal of Pathology*, (1996) 148(5):1699–1708.

Morgan, C., Some Effects of the Microtome Knife and the Electron Beam on Methacrylate-Embedded Thin Sections. *J Biophys. and Biochem Cyto.*, (1956) 2(4):21-28.

Movasaghi, Z., Rehman, S., ur Rehman, D. I. Fourier Transform Infrared (FTIR) Spectroscopy of Biological Tissues. *Applied Spectroscopy Reviews*, (2008) 43(2):134–179.

Mowbray, S. L., Chang, S.-H., Casella, J. F. Estimation of the Useful Lifetime of Polypropylene Fiber in the Anterior Chamber. *American Intra-Ocular Implant Society Journal*, (1983) 9(2):143–147.

Nair, L. S., Laurencin, C. T., Biodegradable polymers as biomaterials, *Progress in Polymer Science*, (2007) 32:762-798.

Natta, G., Pasquon, I., Zambelli, A., Gatti, G. Dependence of the Melting Point of Isotactic Polypropylenes on their Molecular Weight and Degree of Stereospecificity of Different Catalytic Systems, *Macromolecular Chemistry and Physics*, (1964) 70 (1):191-205.

Nelson, B. A., King, W. P. Temperature Calibration of Heated Silicon Atomic Force Microscope Cantilevers. *Sensors and Actuators A: Physical*, (2007) 140(1):51–59.

Odian, G.G., *Principles of Polymerization*. 4th ed. Hoboken, N.J: Wiley-Interscience, 2004.

Ostergard, D.R., Degradation, Infection and Heat Effects on Polypropylene Mesh for Pelvic Implantation: What was Known and When it was Known, *Clinical Opinion*, (2011) 22(7):771-774.

Oswald, H. J., Turi, E. The Deterioration of Polypropylene by Oxidative Degradation. *Polymer Engineering and Science*, (1965) 5(3):152–158.

PA Consulting Group, Investigating Mesh Erosion in Pelvic Floor Repair (June 22, 2011)

Pandit, A. S. and Henry, J. A., Design of Surgical Meshes – An Engineering Perspective. *Technology and Health Care*, (2004) 12(1): 51-65.

Plastics Additives: An A-Z Reference. Ed. G. Pritchard. 1st ed. London ; New York: Chapman & Hall, 1998.

Postlethwait, R. W., Five year study of tissue reaction to synthetic sutures. *Ann. Surg.* (1979) 190:54-57.

Pott, P. P., Schwarz, M. L. R., Gundling, R., Nowak, K., Hohenberger, P., Roessner, E. D., Mechanical Properties of Mesh Materials Used for Hernia Repair and Soft Tissue Augmentation. *PLOS|ONE*, 7(10):e46978.

Process Analytics in Polypropylene (PP) Plants, Siemens AG; 2007, pp:1-9.

Puchtler, H., Meloan, S. N. On the Chemistry of Formaldehyde Fixation and Its Effects on Immunohistochemical Reactions. *Histochemistry*, (1985) 82(3):201–204.

Pugmire, D. L., Wetteland, C. J., Duncan, W. S., Lakis, R. E., et al. Cross-Linking of Polytetrafluoroethylene during Room-Temperature Irradiation. *Polymer Degradation and Stability*, (2009) 94(9):1533–1541.

Rosa, D.S., The Use of Optical Microscopy to Follow the Degradation of Isotactic Polypropylene (iPP) Subjected to Natural and Accelerated Ageing. *Polymer Testing*. (2005) 24(8):1022-1026.

Rosato, D. V., Mattia, D. P., Rosato, D. V. *Designing with Plastics and Composites: A Handbook*. Boston, MA: Springer US, 1991.

Salem, D. R. *Structure Formation in Polymeric Fibers*. Munich : Cincinnati: Hanser Gardner Publications, 2001.

Sastri, V. R. *Commodity Thermoplastics. Plastics in Medical Devices*. Elsevier, 2014. 73–120.

Schmidt, H., Witkowska, B., Kaminska, I., Twarowska-Schmidt, K., et al. Comparison of the Rates of Polypropylene Fibre Degradation Caused by Artificial Light and Sunlight. *Fibres & Textiles in Eastern Europe*, (2011) 19(4):53–58.

Schubert, M. A., Wiggins, M. J., Anderson, J. M., Hiltner, A. Role of Oxygen in Biodegradation of Poly(etherurethane Urea) Elastomers. *Journal of Biomedical Materials Research*, (1997) 34(4):519–530.

Stiftinger, M., Buchberger, W., Klampfl, C. W. Miniaturised Method for the Quantitation of Stabilisers in Microtome Cuts of Polymer Materials by HPLC with UV, MS or MS2 Detection. *Anal. Bioanal. Chem.*, (2013) 405(10):3177–3184.

Sussman, E. M., Halpin, M. C., Muster, J., Moon, R. T., et al. Porous Implants Modulate Healing and Induce Shifts in Local Macrophage Polarization in the Foreign Body Reaction. *Annals of Biomedical Engineering*, (2014) 42(7):1508–1516.

Thavarajah, R., Chemical and Physical Basics of Routine Formaldehyde Fixation, *Journal of Oral and Maxillofacial Pathology* (2012) 16(3):400-405.

Theory and Practice of Histological Techniques. Ed. Kim S. Suvarna, Christopher Layton, and John D. Bancroft. 7. ed. Edinburgh: Elsevier Churchill Livingstone, 2013.

Trofimova, N.F., Zinov'ye, V.V., Kharitonov, V.V., Kinetic Regularities of the Oxidative Degradation of Solid Polypropylene. *Polymer Science U.S.S.R.*, (1981) 23(5):1239-1247.

Usher, F. C., Ochener, J., Tuttle, L. L. D., Use of matrix mesh in the repair of incisional hernias. *The American Surgeon*, (1958) 24:969-974.

Veuthey, T. Dyes and Stains: From Molecular Structure to Histological Application. *Front. Biosci.*, (2014) 19(1):91.

Vroman, L., Adams, A. L. Findings with the Recording Ellipsometer Suggesting Rapid Exchange of Specific Plasma Proteins at Liquid/solid Interfaces. *Surface Science*, (1969) 16438–446.

Vroman, L., Adams, A. L. Identification of Rapid Changes at Plasma-Solid Interfaces. *Journal of Biomedical Materials Research*, (1969) 3(1):43–67.

Wang, X., Zhou, W. Glass Transition of Microtome-Sliced Thin Films. *Macromolecules*, (2002) 35(18):6747–6750.

Wieslawa Urbaniak-Domagala (2012). The Use of the Spectrometric Technique FTIR-ATR to Examine the Polymers Surface. (INTECH Open Access Publisher).

Winters, J. C., Fitzgerald, M. P., Barber, M. D. The Use of Synthetic Mesh in Female Pelvic Reconstructive Surgery. *BJU International*, (2006) 98(s1):70–76.

Wolman, M. Polarized Light Microscopy as a Tool of Diagnostic Pathology. *J. Histochem. Cytochem.*, (1975) 23(1):21–50.

Woo, L., Ling, M., Khare, A. R., Ding, Y. S. Polypropylene degradation and durability estimates based on the master curve concept. (2001).

Woo, L., Khare, A. R., Sandford, C. L., Ling, M. T. K., Ding, Y. S. Relevance of High Temperature Oxidative Stability testing to long term polymer durability. *J. Thermal Analysis and Calorimetry*, (2001) 64:539-548.

Wood, A. J., Cozad, M. J., Grant, D. A., Ostdiek, A. M., et al. “Materials Characterization and Histological Analysis of Explanted Polypropylene, PTFE, and PET Hernia Meshes from an Individual Patient.” *J. Mater. Sci. Mater. Med.*, (2013) 24(4):1113–1122.

Wright, D. C., Rapra Technology Limited. Environmental Stress Cracking of Plastics. Shrewsbury: Rapra Technology, 1996. 3.

Wypych, G. Introduction. *Handbook of Plasticizers*. Burlington: Elsevier Science, 2013. 1–6.

Yang, C. Q., Martin, L. K. Photo- and Thermal-Oxidation of the Nonwoven Polypropylene Fabric Studied by FT-IR Photoacoustic Spectroscopy. *Journal of Applied Polymer Science*, (1994) 51(3):389–397.

Zakharov, V., Echevskaya, L., Mikenas, T., Matsko, M., et al. Supported Ziegler-Natta Catalyst for Ethylene Slurry Polymerization and Control of Molecular Weight Distribution of Polyethylene. *Chinese Journal of Polymer Science*, (2008) 26(05):553.

Zalevsky, Z., Sarafis, V., “Phase Imaging in Plant Cells and Tissues,” *Biomedical Optical Phase Microscopy and Nanoscopy*, chapter 4. Oxford, UK: Elsevier, 2013.

Zhao, Q. H., McNally, A. K., Rubin, K. R., Renier, M., et al. Human Plasma Macroglobulin Promotes in Vitro Oxidative Stress Cracking of Pellethane 2363-80A: In Vivo And in Vitro Correlations. *Journal of Biomedical Materials Research*, (1993) 27(3):379–388.

Production Materials

[DEPO.ETH.MESH.00006437-39]

[DEPO.ETH.MESH.00006440-42]

[DEPO.ETH.MESH.00006443-45]

[DEPO.ETH.MESH.00006446-49]

[DEPO.ETH.MESH.00006450-52]

[DEPO.ETH.MESH.00006453-55]

[DEPO.ETH.MESH.00006456-58]

[DEPO.ETH.MESH.00006459-61]

[DEPO.ETH.MESH.00006462-64]

[DEPO.ETH.MESH.00006465-67]

[DEPO.ETH.MESH.00006468-70]

[DEPO.ETH.MESH.00006471-73]

[DEPO.ETH.MESH.00006474-76]

[DEPO.ETH.MESH.00006477-79]

[ETH.MESH.04091125-26]

[ETH.MESH.06195201-05]

[ETH.MESH.09269739-40]

[ETH.MESH.09273600-01]

[ETH.MESH.12009027-35]

[ETH.MESH.15406846-999]

[ETH.MESH.15955438-73]

Gynecare Instructions Eth.Mesh.03427878

10/0 Prolene explanted after 4½ years in eye (Ref. Ethicon Notebook 1962/73) Project 47201
[ETH.MESH.15958495-8502]

10/0 Prolene suture removed from patients eye after 4½ years (Product Management) Project 47201
[ETH.MESH.15958512-8517] [ETH.MESH.15958518-8523]

10-0 Prolene suture removed from patient's eye after 4½ years, Dr. Drews (Ethicon, Inc. Analytical Chemistry Department) Project 47201 [ETH.MESH.15958524]

25 2-24512 fourier transform-infrared examination of prolene microcrack and photo-oxidized polypropylene

[DEPO.ETH.MESH.00006304-06]

Bry Prolene Explants, Dr. S. Garg Pr. # 16102 [ETH.MESH.15958470-8477]

China Mesh EGS-August 2009 Update [ETH.MESH.10492861-63]

Clinical Expert Report: Prolene Polypropylene Mesh [ETH.MESH.03712324-44]

Completion Report: Design Verification for Soft Prolene Mesh/ Mesh Curling
[ETH.MESH.02182839-44]

Cracks in lens surface near haptic, Christine Jordan PR. #41001 [ETH.MESH.15958492-8494]

ERF 82-147 Microscopic Examination of Prolene (polypropylene) suture and dacron graft returned for norfolk surgical group, ltd (human Retrieval) [DEPO.ETH.MESH.00006307-08]

ERF 83-352 Human retrieval samples from Dr. Gregory, Norfolk Surgical Group
[DEPO.ETH.MESH.00006309]

ERF 84-533 PROLENE 7 Year Explant [DEPO.ETH.MESH.00006310-
DEPO.ETH.MESH.00006311]

ERF 84-533 prolene polypropylene suture explant from Dr. Drewes
[DEPO.ETH.MESH.00006312]

Examination of 5 0 and 6 0 Cardiovascular PROLENE Suture Explanted after 2 to 6 years implantation [DEPO.ETH.MESH.00006313-15]

Examination of Ends of PREP and Prolene Sutures Reported to Have Broken in Animals [ETH.MESH.15958433-8444]

Examination of Ends of PREP and PROLENE Sutures Reported to Have Broken in animals.pdf [DEPO.ETH.MESH.00006316-24]

Expert Report of Howard Jordi w/ exhibits from a NJ case dated 5.20.14 (under New Jersey cases expert reports)

Expert Report of Vladimir Iakovlev (Richard Schmidt)

Explanted after 2 to 6 years. Nine samples were submitted by Research Foundation through Dr. Lunn. The results were provided in the memo. (DX25875)

FDA Reclassification of Prolene Sutures (1990) (ETH.MESH.10665538)

Figures included in seven year report (dog studies) [ETH.MESH.11336505-6525]

Handwritten Notes for project 16102 re: Measurement of cracks in explanted Prolene sutures. Investigator E. Lindemann [DEPO.ETH.MESH00004769-4772]

Handwritten notes for Project No. 45702 (May go with DEPO.ETH.MESH00004761 as it indicates "cont.p.99) "Development of procedure to ____ cracks in ____ explanted suture." Investigator E. Lindemann [DEPO.ETH.MESH00004768]

Handwritten notes for project no. 45702 re: Development of procedure to ____ of cracks in Prolene Suture." Appears to describe method and result from examination of sutures. Investigator E. Lindemann [DEPO.ETH.MESH00004761-4766]

Handwritten notes from Dan Burkley lab notebook regarding Gudoin prolene explants (September 22, 1987) (DEPO.ETH.MESH.000000367 - 368)

Handwritten notes regarding completion and conclusion from the investigation/examination of 23 Prolene sutures. Second page is dated 02/01/1988 but appears to go with document. Investigator: not legible [DEPO.ETH.MESH00004757-4758]

Intra ocular lens, C. Jordan PR. #41001 [ETH.MESH.15958481-8485]

Intraocular lenses, C. Jordan PR. #41001 [ETH.MESH.15958486-8491]

John Karl's January 23, 2003 Memo titled Prolene Resin Manufacturing Specifications and Additive Package (ETH.MESH.02268619)

July 6, 2007 email from Dr. Engel re "How inert is polypropylene?" (ETH.MESH.05447475)

June 15, 1982 memo from Anthony Lunn regarding Crack Depth in Explanted Prolene Polypropylene Sutures (ETH.MESH.12831405-406)

Laboratory Notebook of D. Burkley covering March 20, 1984 to October 23, 1984 [DEPO.ETH.MESH00000347 -375]

Ledger and attached slides [ETH.MESH15406846-6977]

Listing of explants, SEM evaluation and SEM number with attached slides containing handwritten information. [ETH.MESH.15406978-6999]

March 12, 2012 Memo re Response to email from Clare Huntington 26 January 2012 regarding publication by Clavé et al., Polypropylene as a reinforcement in pelvic surgery is not inert: comparative analysis of 100 explants" (ETH.MESH.07226481)

Meeting Minutes: TVT Development-Team-Meeting 7.28.1999 [ETH.MESH.08165497-99]

Memo Burkley to A.J. Melveger re: IR Microscopy of Explanted Prolene Received from Prof. R. Guiddin [ETH.MESH 12831391-1404]

Memo by Matlaga, Sheffield & Fetter to P. Marshall re: Human Retrieval Specimens from Dr. Roger Gregory, Norfolk Surgical Group. Samples were submitted from evaluation. The results are included in the memo. [ETH.MESH.1595440-5442]

Memo Dr. Borysko to Melveger et al. re: Examination of 5/0 and 6/0 Cardiovascular Prolene Sutures [ETH.MESH15958410-8432]

Memo Frick to Matlage enclosing specimens of graft and suture material from two of Dr. Roger Gregory's patients. [ETH.MESH15955443-5452]

Memo from Burkley to J. McDivitt re: Fourier Transform-Infrared Examination of Prolene Microcrack and Photo-Oxidized Polypropylene [ETH.MESH15958336-8395]

Memo Garfield Jones to E.A. Block re: Prolene Polypropylene Suture/Tissue Specimens. Enclosing Prolene suture explants received from Dr. Margaret Billingham with attached letter regarding the sutures. [ETH.MESH 15955472-5473]

Memo Lunn to Melveger re: Crack Depth in Explanted Prolene Polypropylene Sutures [ETH.Mesh 12831405-1407]

Memo Matlaga and Sheffield to Dr. R.L. Kronenthal re: Examination of Prolene (Polypropylene) Sutures from Human Cardiovascular Explants received from Dr. Margaret Bellingham for evaluation. The results are included in the memo. [ETH.MESH15955462-5468]

Memo Matlaga to Dr. A. Lunn re: Prolene (Polypropylene) Microcracks. Matlaga reviewed histological preparation from past samples more critically and provided the results. [ETH.MESH15955438-5439]

Memo Matlaga to P. Marshall re: Human Retrieval Samples [ETH.MESH15958400-8404]

Memo Matlaga to R.L. Kronenthal re: Prolene Polypropylene Suture Explant from Dr. Drewes [ETH.MESH15958405-8407]

Memo Moy to A. Melveger re: Prolene Microcrack Experiments [ETH.MESH 15958445-8451]

Memo Moy to A.J. Melveger re: Prolene Microcracking [ETH.MESH15958452-8469]

Memo R.J. Reinhardt to Dr. D.C. Marshall re: Prolene Polypropylene Suture. Included was a dissected surgical specimen of a graft sutured with Prolene suture received from Dr. Richard J. Sanders of Denver, Colorado. [ETH.MESH15955469-5471]

Memo Schiller to T. Davidson et al. re: Polene 7 year explant ERF Accession #84-533 [ETH.MESH15958408-8409]

Memo to Dr. A. Melveger re: Optical examination of 7 /12 year Prolene Explant, ERF Acc. #84-194. Examination results included along with Handwritten notes Microscopic Examination of Prolene (Polypropylene) Suture and Dacron Graft Returned for Norfolk Surgical Group, LTD (Human Retrieval) (ERF Accession No. 82-147) [ETH.MESH.15958396-8399]

Page from Prolene IFU re: Degradation

Project No 47201 (16 - 1983.05.25 - ETH.Mesh.15958400-8404)

Prolene – 7 year Explant from Dr. Drews (ERF Acc. #84-533) [ETH.MESH.15958503-8507]

Prolene Microcrack Experiments.pdf [DEPO.ETH.MESH.00006325-31]

prolene microcracking [DEPO.ETH.MESH.00006386]

Prolene Package Insert re: Degradation (ETH.MESH.09634318)

Prolene Suture (treated and un-treated) (Dr. Guidain) [ETH.MESH.15958478-8480]

Quebec Explants - SEM Evaluation [DEPO.ETH.MESH.00004755]

Risk Assessment Summary for Product in the Gynecare TVT Secure System
[ETH.MESH.11353422-39]

Satya Garg's November 12, 1987 Memo regarding Gudoin prolene explants Study Meeting
Minutes 10/8/87 (ETH.MESH.12831407)

Second Iolab job – requested by Sal Romano Project #45702-509 [ETH.MESH.15958510-
8511]

SEM 10551-10572 83D057-83D960-83D035-84D007-84D010-83D067-83TM020
[DEPO.ETH.MESH.00006332-39]

SEM 1205-1208 and 1211-1212 and 1215-1216 PROLENE - tissue digestion treatment
[DEPO.ETH.MESH.00006340-41]

SEM 4088-4101 Intra-ocular Lens for SR29477 [DEPO.ETH.MESH.00006342-46]

SEM 4102-4117 Intra-ocular Lens for SR29477 [DEPO.ETH.MESH.00006347-52]

SEM 4749-4754 Intra-ocular Lens cracks near haptic for SR29477
[DEPO.ETH.MESH.00006353-55]

SEM 5627-5641 10-0 PROLENE explants [DEPO.ETH.MESH.00006356-63]

SEM 7467-7478 7 year explant ERF 84-533 [DEPO.ETH.MESH.00006364-68]

SEM Negatives 4696-4701 Intra-ocular Lens [DEPO.ETH.MESH.00006369-70]

SEM Negatives 4736-4741 Intra-ocular Lens [DEPO.ETH.MESH.00006371-72]

SEM Negatives 5627-5641 10-0 PROLENE Explants [DEPO.ETH.MESH.00006373-78]

SEM Negatives 5627-5641 10-0 PROLENE Explants [DEPO.ETH.MESH.00006379-84]

Seven Year Dog Study (Lewis trial exhibit no. 1291) (Complete)

Seven Year Dog Study (Used as exhibit at the 30(b)(6) deposition of Thomas Barbolt [ETH.MESH.11336184 -]

SR14154 10-0 PROLENE explant [DEPO.ETH.MESH.00006385]

Sunoco MSDS (ETH.MESH.02026591)

The Use of Mesh in Hernia Repair by L. Thomas Divilio, MD, FACS [ETH.MESH.14442958-76]

Third type sample from Iolab Corp., Intra-Ocular Lens Project #47416 [ETH.MESH.15958508-8509]

NDA – 4.16.1969 PROLENE FDA Approval (ETH.MESH.09625731-09625737)

PROLENE suture NDA Preclinical Studies.pdf (ETH.MESH.09626242 – 09626359)

1973 Rabbit Study for PROLENE Mesh.pdf (ETH.MESH.10575607 – 10575613)

PSE 97-0197.pdf (ETH.MESH.05315240 – 05315295)

Eth Mesh 04384112 – Biocompatibility Risk Assessment for the TVT-L Device – June 6 2001.pdf (ETH.MESH.04384112 – 04284125)

Crack Depth in Explanted PROLENE Polypropylene Sutures memo (ETH.MESH.123831405 – 123831406)

Human Retrieval Specimens from Dr. Roger Gregory, Norfolk Surgical Group memo1983.03.29 (ETH.MESH.15955440-15955442)

Ethicon's Seven Year Dog Study ETH.MESH.09888187

Ethicon's Seven Year Dog Study ETH.MESH.09888189

Ethicon's Seven Year Dog Study ETH.MESH.09888218-222

Ethicon's Seven Year Dog Study ETH.MESH.09888188

Ethicon's Seven Year Dog Study ETH.MESH.11336183

Ethicon's Seven Year Dog Study ETH.MESH.11336181

Ethicon's Seven Year Dog Study ETH.MESH.11336081-082

Ethicon's Seven Year Dog Study ETH.MESH.11336166-168

Ethicon's Seven Year Dog Study ETH.MESH.09888191

Tensile Strength Study of Colorless and Pigmented Monofilament Polypropylene Sutures in the Rat (ETH.MESH.09626336 - 09626345)

Histological Evaluation and Comparison of Mechanical Pull Out Strength of Prolene Mesh and Prolene Soft Mesh in a Rabbit Model (ETH.MESH.10039989 - 10040024)

Monofilament Prolene In Vivo Breaking Strength Loss (ETH.MESH.10575510)

Prolene Polypropylene Sutures: Breaking Strength of Prolene Sutures After Subcutaneous Implantation in Rats (ETH.MESH.10575614)

Non-Absorbable Sutures; In Vivo Tensile Strength Values of Production Non-Absorbable Sutures Tested To Supply Reference Tensile Strength Values (ETH.MESH.10665625 - 10665661)

NDA - Approved Labeling - Prolene Sutures - 1969 (ETH.MESH.09629447 - 09629448)

NDA - FDA Prolene NDA Supplement with Transitory Language (ETH.MESH.09630649)

NDA - Librojo Affidavit

NDA - Prolene NDA - Insert Changes Approvals

NDA - Prolene NDA with Blue Composition (ETH.MESH.09625606 - 09625632)

Cytotoxicity Risk Assessment for the TVT (Ulmsten) Device 8-8-1997 (ETH.MESH.00349228 - 00349237)

Bellew Case Materials

Expert Reports

Ducheyne, Paul

Iakovlev, Vladimir

Jordi, Howard

Klinge, Uwe

Muehl, Thomas

Thames, Shelby

Depositions

Iakovlev, Vladamir [8.12.2014] (Corbett)

Jordi, Howard C., MD [8.19.2014]

Thames, Shelby F., Ph.D. [9.4.2014]

Trial

Iakovlev, Vladimir [03.05.2015]

Miscellaneous

All FTIR spectra (Four charts dated 6/17/2014)

Invoice #9475 from Jordi Labs to Anderson Law offices

Invoice #9685 from Jordi Labs to Anderson Law offices

NIST Polystyrene Standard (dated 6/18/2014)

Ong, Kevin SEM Images

Huskey Case Materials

Depositions

Iakovlev, Vladamir [3.18.2014] (Huskey-Edwards)

Trial Transcript (Guelcher Testimony) w/ Exhibits [8.25.2014]

Trial Transcript (Thames Testimony) w/ Exhibits [9.2.2014]

Expert Reports

Dunn, Russell (Huskey-Edwards)

Dunn, Russell (Rebuttal) (Huskey-Edwards)

Guelcher, Scott (Huskey-Edwards)

Guelcher, Scott (Rebuttal)

Guelcher, Scott (2nd Supplemental) (Huskey-Edwards)

Ong, Kevin (Huskey-Edwards)

Pandit, Abhay (Huskey-Edwards)

Thames, Shelby (Huskey-Edwards)

Miscellaneous

Plaintiff's slides used with Guelcher

Lewis Case Materials

Expert Reports

Jordi, Howard

Jordi, Howard (Rebuttal)

Ong, Kevin

Thames, Shelby

Guelcher, Scott (Rebuttal)

TVT NJ Case Materials

Expert Reports

Ducheyne, Paul

Elliott, Daniel

Iakovlev, Vladimir

Jordi, Howard

Klinge, Uwe

Muehl, Thomas

Rosenzweig, Bruce

Pence, Peggy

Carlino Case Materials

Dr. Iakovlev's Expert Report 8-28-15

Civil Action Complaint – Short Form

Ethicon's Response to Request for Production 8-24-15

McGee Case Materials

Dr. Klinge's Expert Report 10-13-13

11.9.15 (TVM) McGee - letter to counsel enclosing plaintiff expert reports

Complaint and Jury Demand (J&J McGee, Kathryn)_18144909_1

Wave 1 Case Materials

Expert Reports

Jordi, Howard (Wave 1, Lewis, Bellew)

Guelcher, Scott

Guelcher, Scott (corrected)

Klinge, Uwe (SUI, POP)

Mays, Jimmy

Priddy, Duane

Ostergard, Donald

Iakovlev, Vladimir (General)

Iakovlev, Vladimir (Adams, Beach, Bennett, Boggs, Daino, Destefano-Raston, Dimock, Fox, Frye (original), Frye (supplemental), Funderburke, Georgilakis, Hankins, Hooper, Hoy, Justus, Kaiser, Kropf, Loustaunau, Massey, McBrayer, Nix, Phelps, Ruebel, Ruiz, Smith, Smith, Stone, Stubblefield, Taylor, Teasley, Vignos-Ware, White, Wolfe, Wroble)

Muehl, Thomas

Depositions

Priddy, Duane (3-8-2016)

Mays, Jimmy (3-2-16)

Other Materials

Mpathy Medical Devices, Ltd. Minimesh® polypropylene mesh. 510(k) #K041632

Sofradim Production. Parietene™ Duo Polypropylene mesh and Parietene™ Quadra Polypropylene mesh. 510(k) #K072951

Coloplast A/S. Restorelle™ polypropylene mesh. 510(k) #K103568

C.R. Bard, Inc. Bard® InnerLace™ BioUrethral Support System. 510(k) #K031295

C.R. Bard, Inc. Avaulta™ Solo Support System and Avaulta™ Plus Biosynthetic Support System. 510(k) #K063712

American Medical Systems. BioArc TOTM Subfascial Hammock. 510(k) #K040538

American Medical Systems. AMS Large Pore Polypropylene mesh. 510(k) #K033636

MentorCorp. Mentor ObTape™ Trans-obdurator Surgical Kit. 510(k) #042851

MLE, Inc. Suture Fixation Device. 510(k) #K021834

Boston Scientific Corp. Pinnacle Pelvic Floor Repair Kit II. 510(k) #081048

Boston Scientific Corp. Pinnacle Lite Pelvic Floor Repair Kit. 510(k) #122459

Island Biosurgical, Inc. Island Biosurgical Bolster. 510(k) #K960101

Ethicon, Inc. Modified PROLENE Polypropylene Mesh Nonabsorbable Synthetic Surgical Mesh. 510(k) #962530

Ethicon, Inc. Gynemesh PROLENE Soft (Polypropylene) Mesh. 510(k) # K013718

ATR – Theory and Applications.pdf Pike Technologies

EAG FTIR Technique Note

Education Guide: Special Stains and H&E Second Edition, Editors: George L. Kumar and John A. Kiernan., 2010 Dako North America, Carpinteria, California

Myers, R. (2011). The Basic Chemistry of Hematoxylin. Available from:
<http://www.leicabiosystems.com/pathologyleaders/the-basic-chemistry-of-hematoxylin/>

TVT Classic 510(K) (ETH.MESH.08476210 - 08476342)

ISO_10993_Testing

ASTM D3895

Trial Testimony of Vladimir Iakovlev (Cardenas) 8.18.2014

Trial Transcript of Eghnayem v. Boston Scientific 11.6.2014

Iakovlev, Vladimir Expert Report of (Iholts)

Iakovlev FULL REPORT ETH MDL Consolidated Case -8-24-15

Jordi FULL REPORT ETH MDL Consolidated Case 8-24-15

Guelcher FULL REPORT ETH MDL Consolidated Case 8-24-15

Klinge ETH MDL Consolidated Case-Expert Report 8-24-15

Muhl ETH MDL Consolidated Case-Expert Report-8-24-15

Iakovlev, Vladimir Expert Report - Clowe

Thames, Shelby Expert Report – Contrell

Thames, Shelby Trial Testimony - Batiste

Barbolt 30(b)(6) deposition exhibit--list of studies 1-8-14

Scott, Guelcher Trial Testimony and Exhibits - Perry

Barbolt New Jersey Cases deposition 9-9-2012

Barbolt New Jersey Cases deposition day II 9-10-2012

Barbolt Pelvic Repair System Products Liability Litigation deposition 8-14-2013

Barbolt Pelvic Repair System Products Liability Litigation deposition day II 8-14-2013

Barbolt Pelvic Repair System Products Liability Litigation deposition 1-7-2014

Barbolt Pelvic Repair System Products Liability Litigation deposition day II 1-7-2014

Rosenzweig, Bruce Final Cantrel report 6-6-14

Rosenzweig, Bruce Final Corbet Report

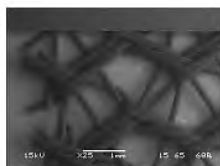
Burkley, Dan deposition day 1, dated 5-22-2013

Burkley, Dan deposition day 2, dated 5-23-2013

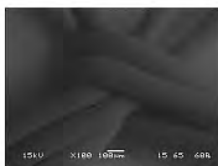
Appendix E: Compensation

In 2016, Exponent charges for my time at a rate of \$380/hour. No portion of my compensation is dependent on the outcome of this matter.

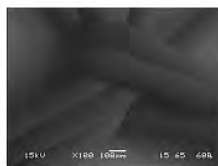
Appendix F: Study Images



HerniaMeshR_01



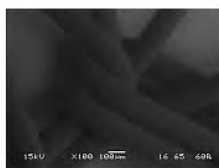
HerniaMeshR_02



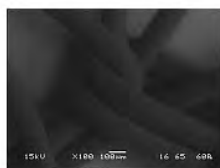
HerniaMeshR_03



HerniaP-01



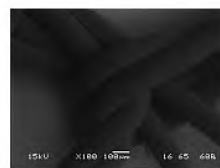
HerniaP-02



HerniaP-03



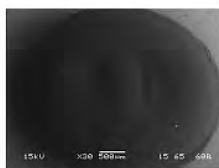
HerniaR-01



HerniaR-02



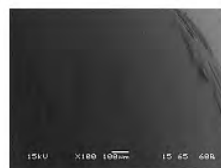
HerniaR-03



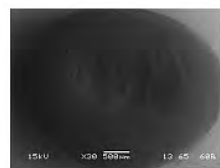
PelletP-01



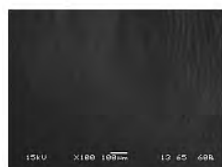
PelletP-02



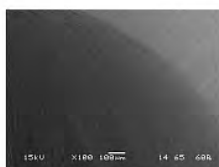
PelletP-03



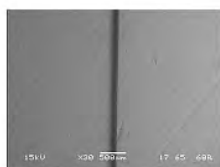
PelletR-01



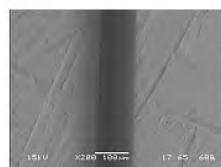
PelletR-02



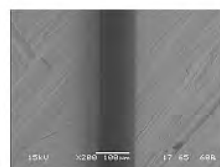
PelletR-03



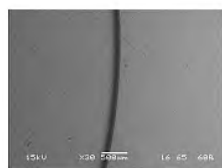
SutureP-01



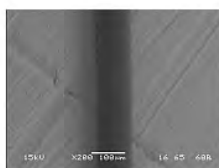
SutureP-02



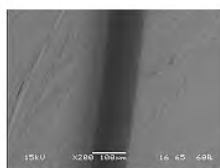
SutureP-03



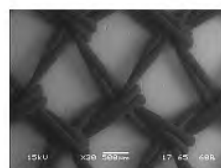
SutureR-01



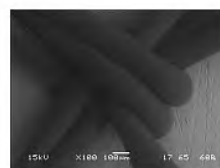
SutureR-02



SutureR-03



TVT1P-01



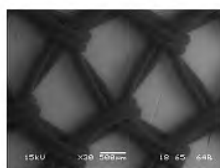
TVT1P-02



TVT1P-03



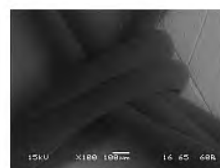
TVT1P-04



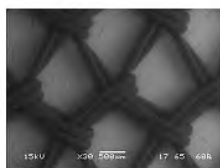
TVT1R-01



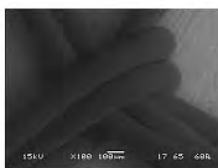
TVT1R-02



TVT1R-03



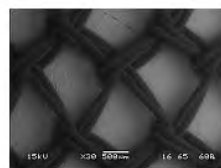
TVT2P-01



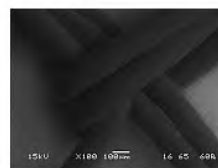
TVT2P-02



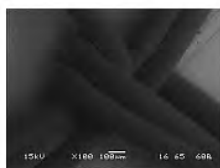
TVT2P-03



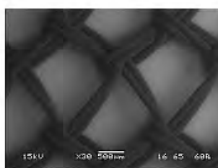
TVT2R-01



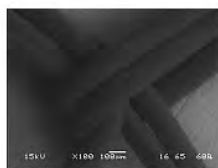
TVT2R-02



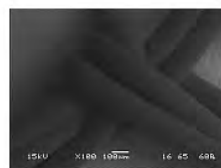
TVT2R-03



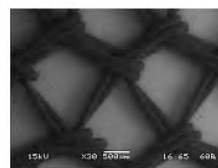
TVT3P-01



TVT3P-02



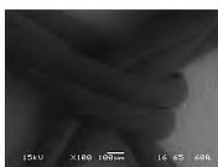
TVT3P-03



TVT3R-01



TVT3R-02



TVT3R-03



DSC_5380



DSC_5381



DSC_5388



DSC_5389



DSC_5398



DSC_5399



DSC_5410



DSC_5411



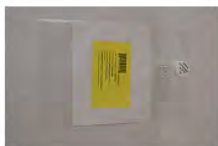
DSC_5421



DSC_5422



DSC_5423



DSC_5432



DSC_5433



DSC_5384



DSC_5385



DSC_5402



DSC_5403



DSC_5414



DSC_5415



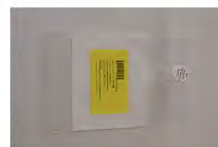
DSC_5426



DSC_5427



DSC_5436



DSC_5437



DSC_5443



DSC_5444



DSC_5473



DSC_5474



DSC_5475



DSC_5386



DSC_5387



DSC_5404



DSC_5405



DSC_5416



DSC_5417



DSC_5428



DSC_5429



DSC_5438



DSC_5439



DSC_5445



DSC_5446



DSC_5382



DSC_5383



DSC_5400



DSC_5401



DSC_5412



DSC_5413



DSC_5424



DSC_5425



DSC_5434



DSC_5435



DSC_5441



DSC_5442



DSC_5462



DSC_5463



DSC_5464



DSC_5465



DSC_5466



DSC_5467



DSC_5468



DSC_5469



DSC_5470



DSC_5471



DSC_5476



DSC_5477



DSC_5478



DSC_5479



DSC_5480



DSC_5481



DSC_5482



DSC_5483



DSC_5484



DSC_5485



DSC_5486



DSC_5487



DSC_5488



DSC_5489



DSC_5490



DSC_5491



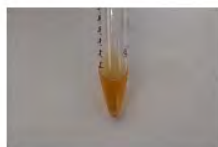
DSC_5492



DSC_5493



DSC_5494



DSC_5495



DSC_5496



DSC_5497



DSC_5498



DSC_5499



DSC_5500



DSC_5501



DSC_5502



DSC_5503



DSC_5504



DSC_5505



DSC_5506



DSC_5507



DSC_5508



DSC_5509



DSC_5510



DSC_5511



DSC_5512



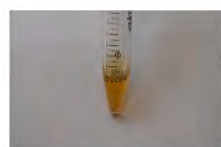
DSC_5513



DSC_5514



DSC_5515



DSC_5516



DSC_5517



DSC_5518



DSC_7023



DSC_7024



DSC_7025



DSC_7026



DSC_7027



DSC_7028



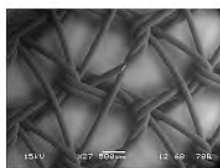
DSC_7029



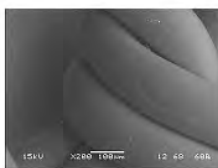
DSC_7030



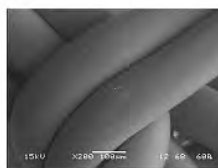
DSC_7031



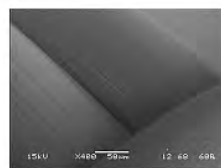
Hernia_mesh_P-01



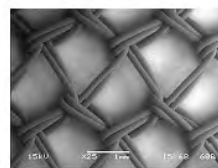
Hernia_mesh_P-02



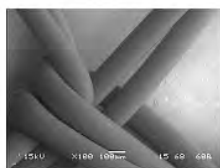
Hernia_mesh_P-03



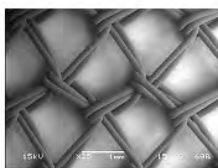
Hernia_mesh_P-04



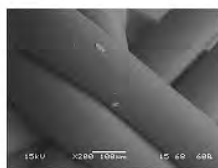
TVT_mesh3_P-01



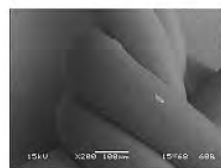
TVT_mesh3_P-02



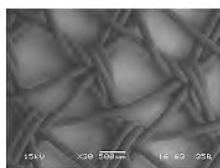
TVT_mesh3_P-03



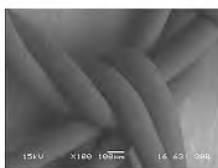
TVT_mesh3_P-04



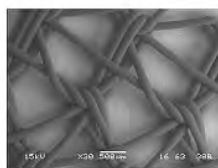
TVT_mesh3_P-05



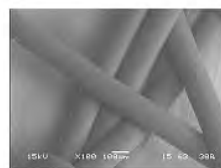
Hernia Mesh_48 hrs-01



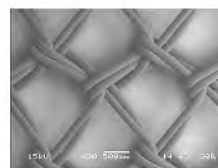
Hernia Mesh_48 hrs-02



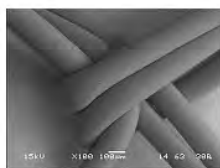
Hernia Mesh_48 hrs-03



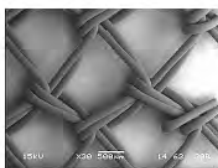
Hernia Mesh_48 hrs-04



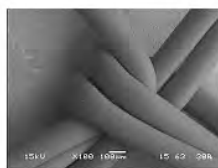
TVT Mesh 3_48 hrs-01



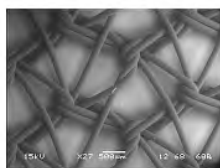
TVT Mesh 3_48 hrs-02



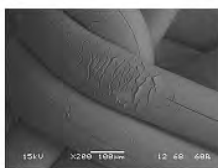
TVT Mesh 3_48 hrs-03



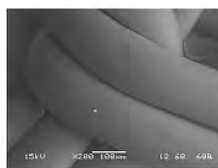
TVT Mesh 3_48 hrs-04



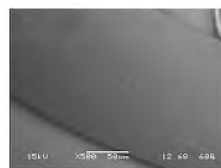
Hernia_mesh_P-01



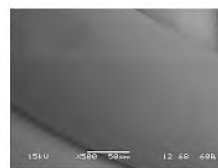
Hernia_mesh_P-02



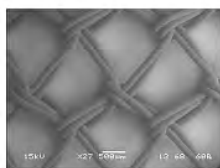
Hernia_mesh_P-03



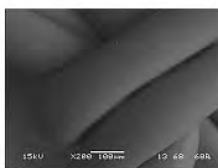
Hernia_mesh_P-04



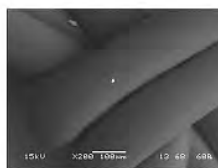
Hernia_mesh_P-05



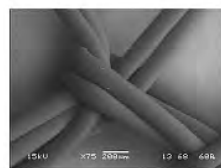
TVT3_mesh-01



TVT3_mesh-02



TVT3_mesh-03



TVT3_mesh-04



IMG_2077



IMG_2078



IMG_2079



IMG_2080



IMG_2081



IMG_2082



IMG_2083



IMG_2084



IMG_2085



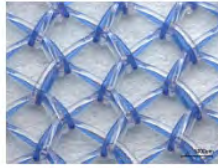
IMG_2086



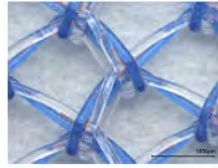
IMG_2087



157164_TVT#1_Paraffin_01



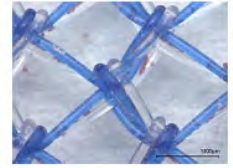
157164_TVT#1_Paraffin_02



157164_TVT#1_Paraffin_03



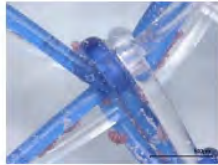
157165_TVT#1_Resin_01



157165_TVT#1_Resin_02



157165_TVT#1_Resin_03



157165_TVT#1_Resin_04



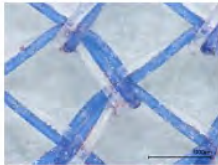
157172_TVT#2_Paraffin_01



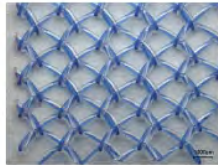
157172_TVT#2_Paraffin_02



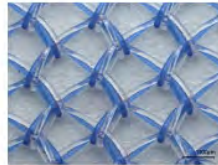
157172_TVT#2_Paraffin_03



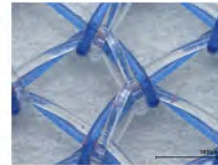
157172_TVT#2_Paraffin_04



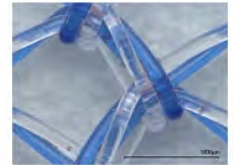
157173_TVT#2_Resin_01



157173_TVT#2_Resin_02



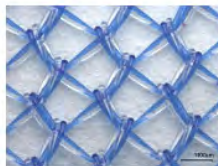
157173_TVT#2_Resin_03



157173_TVT#2_Resin_04



157180_TVT#3_Paraffin_01



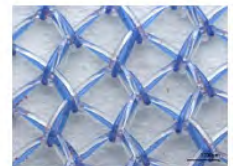
157180_TVT#3_Paraffin_02



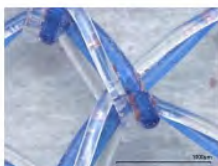
157180_TVT#3_Paraffin_03



157181_TVT#3_Resin_01



157181_TVT#3_Resin_02



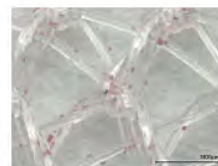
157181_TVT#3_Resin_03



57188_HerniaMesh_Paraffin_0



57188_HerniaMesh_Paraffin_0



57188_HerniaMesh_Paraffin_0



57189_HerniaMesh_Resin_01



157189_HerniaMesh_Resin_02



157189_HerniaMesh_Resin_03



57196_Suture_Paraffin-Resin_C



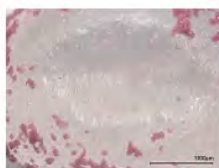
57196_Suture_Paraffin-Resin_C



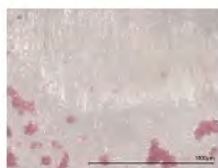
57196_Suture_Paraffin-Resin_C



157232_pellet_Paraffin_01



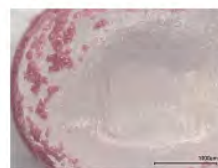
157232_pellet_Paraffin_02



157232_pellet_Paraffin_03



157233_pellet_Resin_01



157233_pellet_Resin_02



157233_pellet_Resin_03



157164_TVT#1_Paraffin_01



157164_TVT#1_Paraffin_02



157164_TVT#1_Paraffin_03



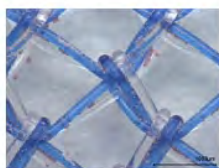
157164_TVT#1_Paraffin_04



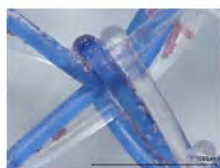
157165_TVT#1_Resin_01



157165_TVT#1_Resin_02



157165_TVT#1_Resin_03



157165_TVT#1_Resin_04



157172_TVT#2_Paraffin_01



157172_TVT#2_Paraffin_02



157172_TVT#2_Paraffin_03



157172_TVT#2_Paraffin_04



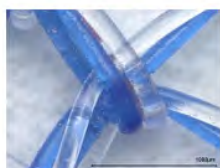
157173_TVT#2_Resin_01



157173_TVT#2_Resin_02



157173_TVT#2_Resin_03



157173_TVT#2_Resin_04



157180_TVT#3_Paraffin_01



157180_TVT#3_Paraffin_02



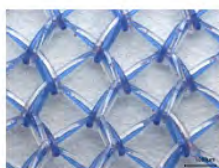
157180_TVT#3_Paraffin_03



157180_TVT#3_Paraffin_04



157181_TVT#3_Resin_01



157181_TVT#3_Resin_02



157181_TVT#3_Resin_03



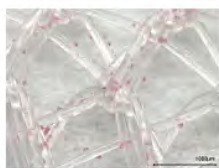
157181_TVT#3_Resin_04



57188_HerniaMesh_Paraffin_0



57188_HerniaMesh_Paraffin_0



57188_HerniaMesh_Paraffin_0



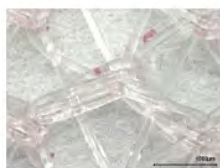
57188_HerniaMesh_Paraffin_0



157189_HerniaMesh_Resin_01



157189_HerniaMesh_Resin_02



157189_HerniaMesh_Resin_03



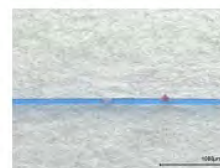
157189_HerniaMesh_Resin_04



57196_Suture_Paraffin-Resin_C



57196_Suture_Paraffin-Resin_C



57196_Suture_Paraffin-Resin_C



57196_Suture_Paraffin-Resin_C



157232_pellet_Paraffin_01



157232_pellet_Paraffin_02



157232_pellet_Paraffin_03



157233_pellet_Resin_01



157233_pellet_Resin_02



157233_pellet_Resin_03



IMG_2153



IMG_2154



IMG_2155



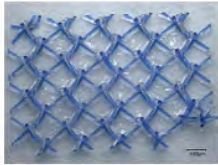
IMG_2156



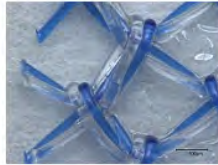
IMG_2157



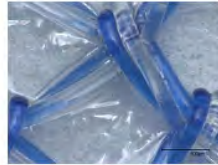
IMG_2158



157166_TVT1_Serum-P_01



57166_TVT1_Serum-P_100x_0



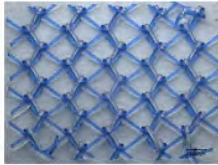
57166_TVT1_Serum-P_150x_0



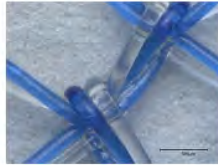
57166_TVT1_Serum-P_150x_0



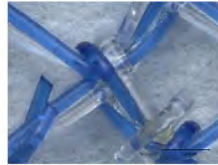
57166_TVT1_Serum-P_150x_0



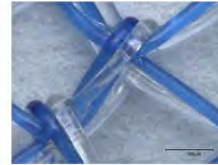
57167_TVT1_Serum-R_030x_0



57167_TVT1_Serum-R_150x_0



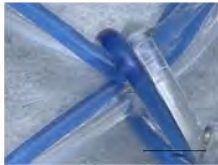
57167_TVT1_Serum-R_150x_0



57167_TVT1_Serum-R_150x_0



57167_TVT1_Serum-R_150x_0



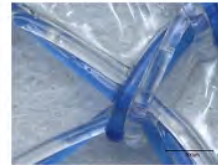
57167_TVT1_Serum-R_200x_0



57174_TVT2_Serum-P_030x_0



174_TVT2_Serum-P_030x_stitch



57174_TVT2_Serum-P_150x_0



57174_TVT2_Serum-P_150x_0



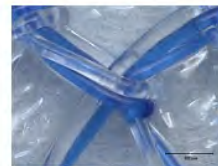
57175_TVT2_Serum-R_030x_0



175_TVT2_Serum-R_030x_stitch



57175_TVT2_Serum-R_150x_0



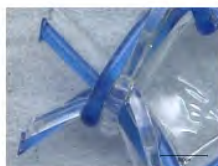
57175_TVT2_Serum-R_150x_0



57175_TVT2_Serum-R_150x_0



57182_TVT3_Serum-P_030x_0



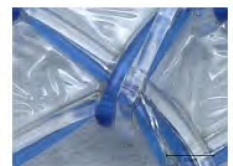
57182_TVT3_Serum-P_150x_0



57182_TVT3_Serum-P_150x_0



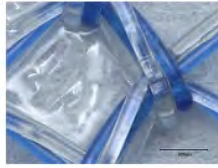
57182_TVT3_Serum-P_150x_0



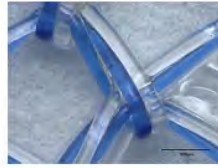
57182_TVT3_Serum-P_150x_0



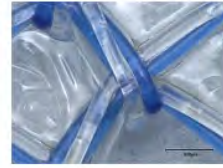
57183_TVT3_Serum-R_030x_0



57183_TVT3_Serum-R_150x_0



57183_TVT3_Serum-R_150x_0



57183_TVT3_Serum-R_150x_0



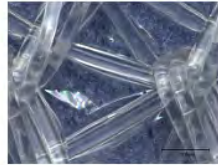
57190_Hernia_Serum-P_030x_0



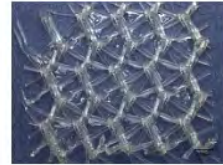
57190_Hernia_Serum-P_150x_0



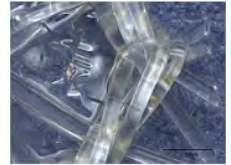
57190_Hernia_Serum-P_150x_0



57190_Hernia_Serum-P_150x_0



57191_Hernia_Serum-R_030x_0



57191_Hernia_Serum-R_150x_0



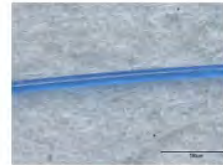
57191_Hernia_Serum-R_150x_0



57191_Hernia_Serum-R_150x_0



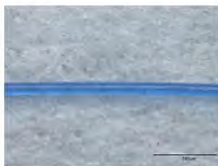
57198_Suture_Serum-P_030x_0



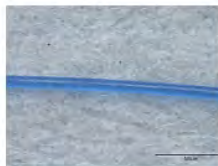
57198_Suture_Serum-P_200x_0



57198_Suture_Serum-P_200x_0



57198_Suture_Serum-P_200x_0



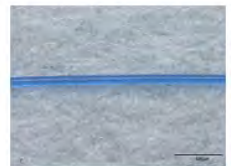
57198_Suture_Serum-P_200x_0



57199_Suture_Serum-R_030x_0



57199_Suture_Serum-R_200x_0



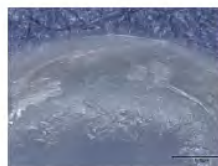
57199_Suture_Serum-R_200x_0



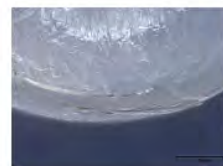
57199_Suture_Serum-R_200x_0



157234_Pellet 3_050x_01



157234_Pellet 3_150x_02



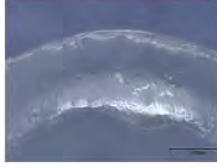
157234_Pellet 3_150x_03



157234_Pellet 3_150x_04



157235_Pellet 4_050x_01



157235_Pellet 4_150x_02



157235_Pellet 4_150x_03



IMG_1022



IMG_1023



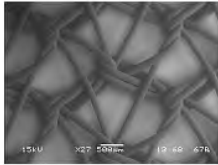
IMG_1024



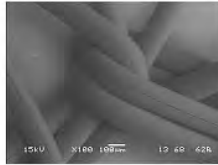
IMG_1025



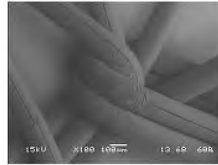
IMG_1026



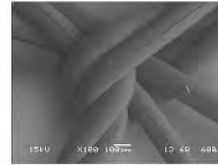
Hernia_mesh_P-01



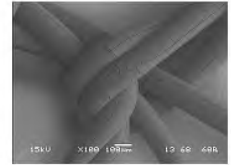
Hernia_mesh_P-02



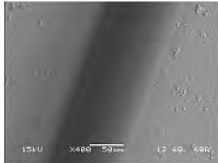
Hernia_mesh_P-03



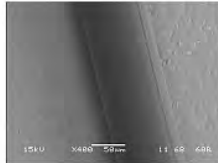
Hernia_mesh_P-04



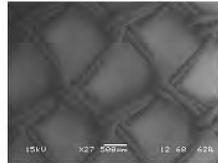
Hernia_mesh_P-05



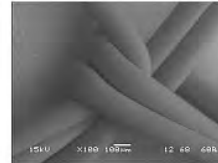
Suture_P-01



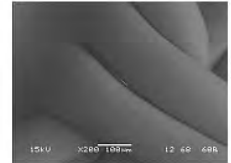
Suture_R-01



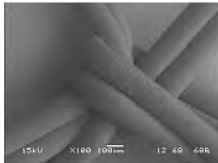
TVT3_mesh-01



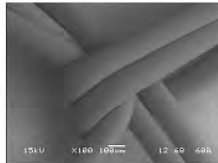
TVT3_mesh-02



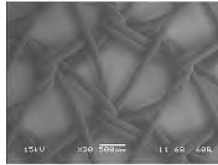
TVT3_mesh-03



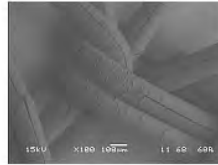
TVT3_mesh-04



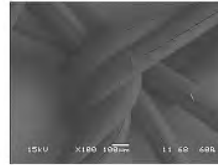
TVT3_mesh-05



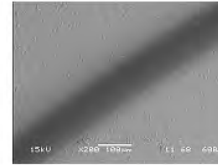
Hernia_mesh_P-01



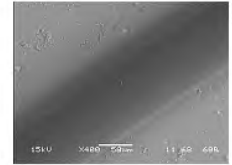
Hernia_mesh_P-02



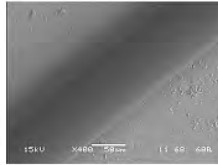
Hernia_mesh_P-03



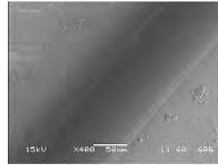
Suture_P-01



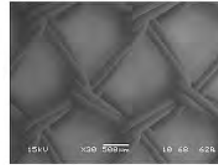
Suture_P-02



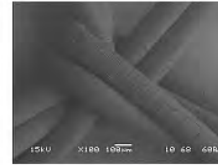
Suture_P-03



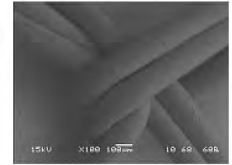
Suture_P-04



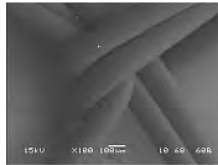
TVT3_mesh-01



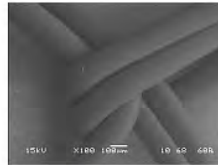
TVT3_mesh-02



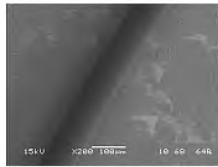
TVT3_mesh-03



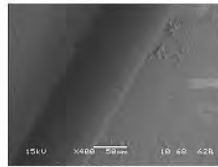
TVT3_mesh-04



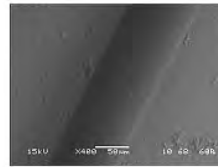
TVT3_mesh-05



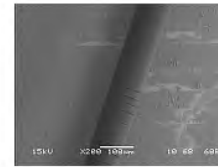
Suture_P-01



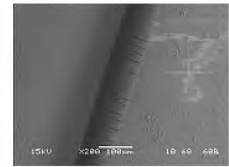
Suture_P-02



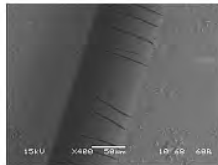
Suture_P-03



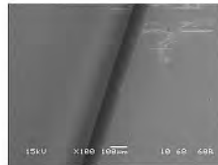
Suture_P-04



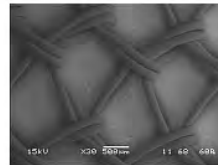
Suture_P-05



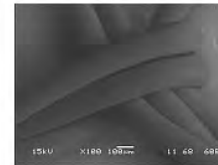
Suture_P-06



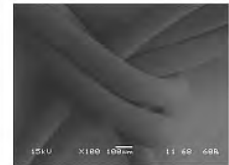
Suture_P-07



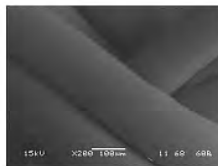
TVT2_mesh-P-01



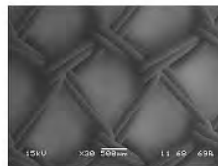
TVT2_mesh-P-02



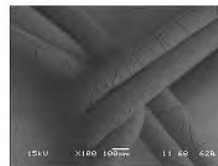
TVT2_mesh-P-03



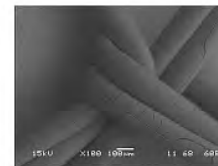
TVT2_mesh-P-04



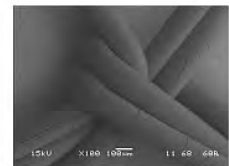
TVT3_mesh-P-01



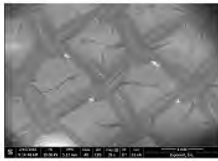
TVT3_mesh-P-02



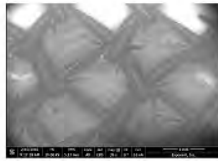
TVT3_mesh-P-03



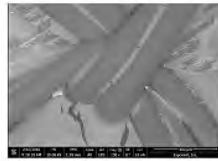
TVT3_mesh-P-04



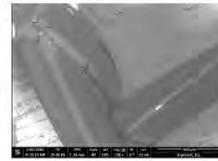
157166_TVT1-P_001



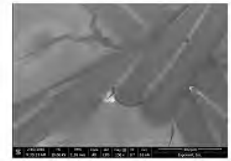
157166_TVT1-P_002



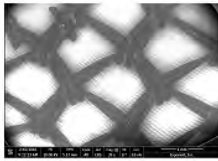
157166_TVT1-P_003



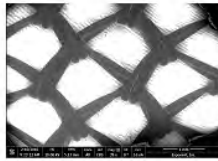
157166_TVT1-P_004



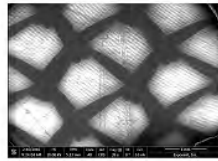
157166_TVT1-P_005



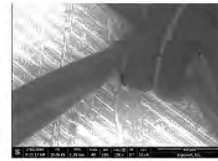
157167_TVT1-R_001



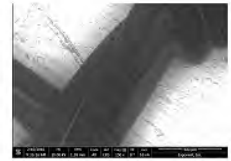
157167_TVT1-R_002



157167_TVT1-R_003



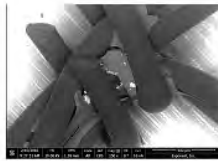
157167_TVT1-R_004



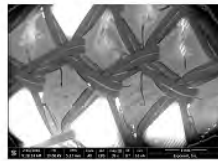
157167_TVT1-R_005



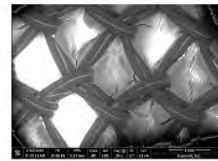
157167_TVT1-R_006



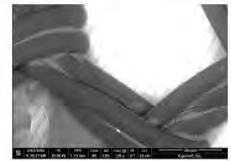
157167_TVT1-R_007



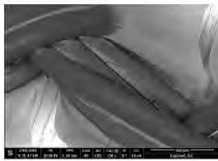
157174_TVT2-P_001



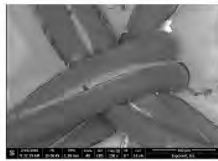
157174_TVT2-P_002



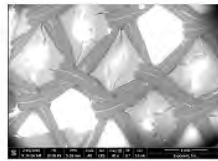
157174_TVT2-P_003



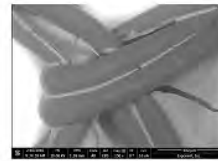
157174_TVT2-P_004



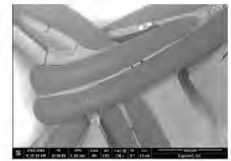
157174_TVT2-P_005



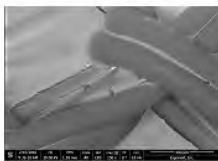
157175_TVT2-R_001



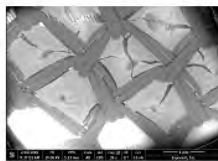
157175_TVT2-R_002



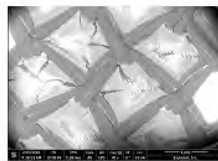
157175_TVT2-R_003



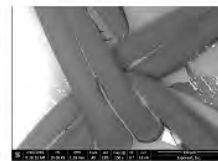
157175_TVT2-R_004



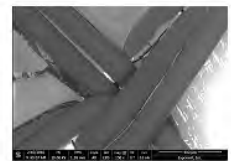
157182_TVT3-P_001



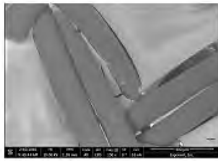
157182_TVT3-P_002



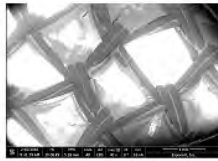
157182_TVT3-P_003



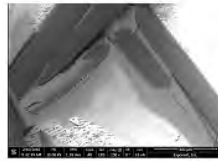
157182_TVT3-P_004



157182_TVT3-P_005



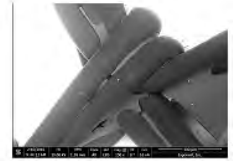
157183_TVT3-R_001



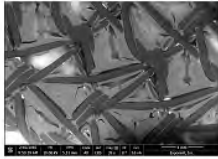
157183_TVT3-R_002



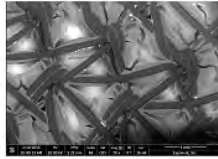
157183_TVT3-R_003



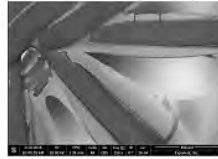
157183_TVT3-R_004



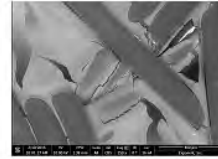
157190_Hernia-P_001



157190_Hernia-P_002



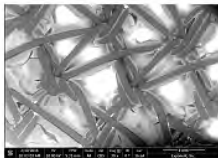
157190_Hernia-P_003



157190_Hernia-P_004



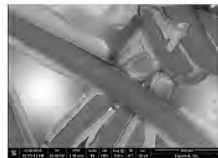
157190_Hernia-P_005



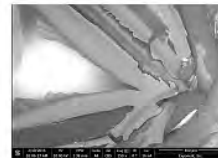
157191_Hernia-R_001



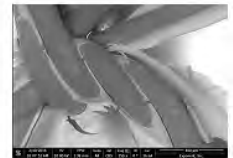
157191_Hernia-R_002



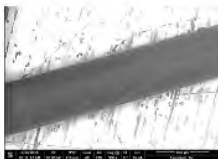
157191_Hernia-R_003



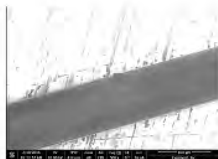
157191_Hernia-R_004



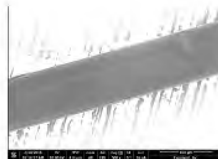
157191_Hernia-R_005



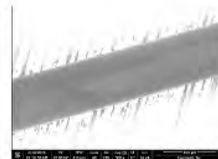
157198_Suture-P_001



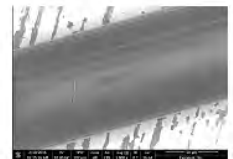
157198_Suture-P_002



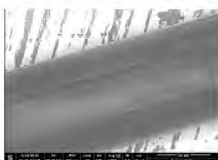
157198_Suture-P_003



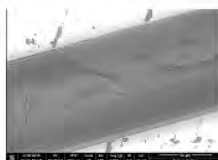
157198_Suture-P_004



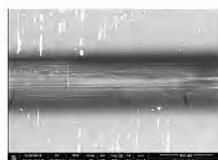
157198_Suture-P_005



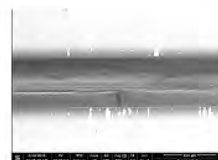
157198_Suture-P_006



157198_Suture-P_007



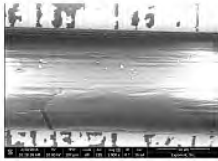
157199_Suture-R_001



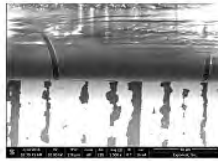
157199_Suture-R_002



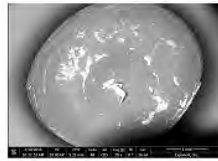
157199_Suture-R_003



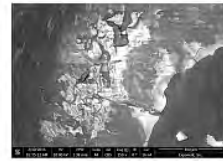
157199_Suture-R_004



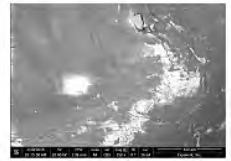
157199_Suture-R_005



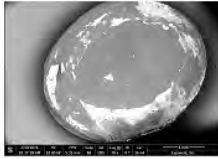
157234_Pellet3_001



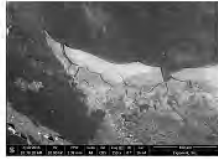
157234_Pellet3_002



157234_Pellet3_003



157235_Pellet4_001



157235_Pellet4_002



157235_Pellet4_003



DSC_7052



DSC_7053



DSC_7054



DSC_7055



DSC_7056



DSC_7057



DSC_7058



DSC_7059



IMG_1008



IMG_1009



IMG_1010



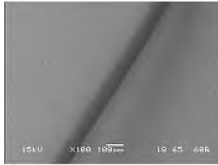
IMG_1011



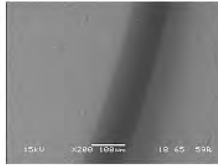
IMG_1012



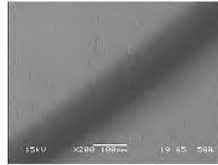
IMG_1013



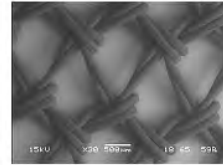
Suture_P_01



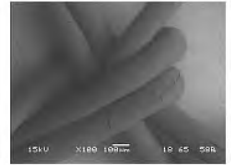
Suture_P_02



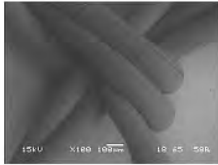
Suture_P_03



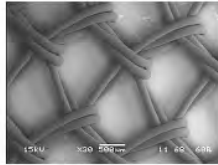
TVT1_Mesh_P_01



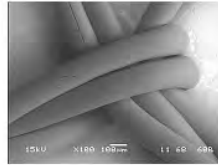
TVT1_Mesh_P_02



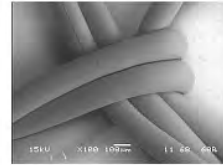
TVT1_Mesh_P_03



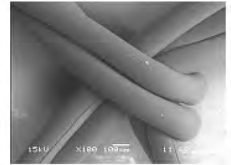
TVT2_mesh-P-01



TVT2_mesh-P-02



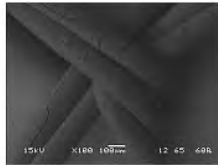
TVT2_mesh-P-03



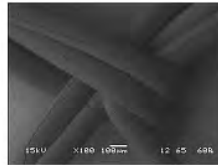
TVT2_mesh-P-04



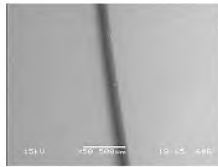
TVT3_Mesh_P_01



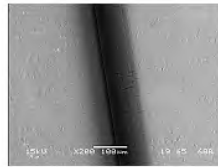
TVT3_Mesh_P_02



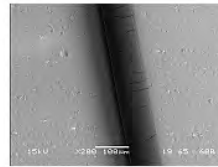
TVT3_Mesh_P_03



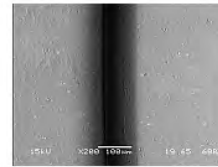
SutureR_01



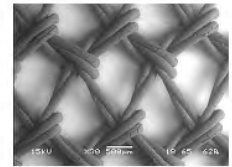
SutureR_02



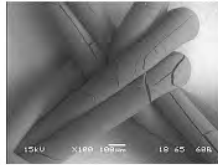
SutureR_03



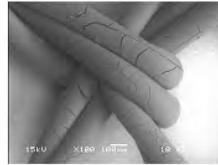
SutureR_04



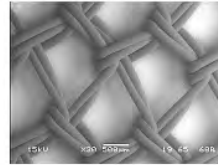
TVT1P_01



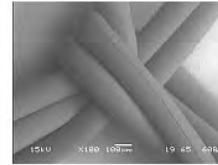
TVT1P_02



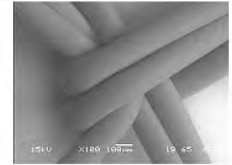
TVT1P_03



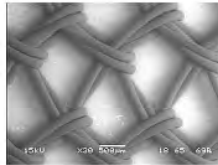
TVT1R_01



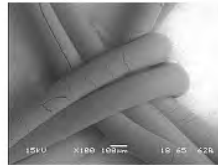
TVT1R_02



TVT1R_03



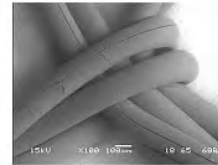
TVT2P_01



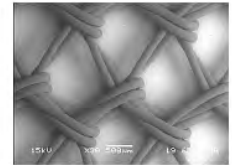
TVT2P_02



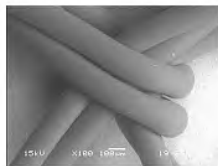
TVT2P_03



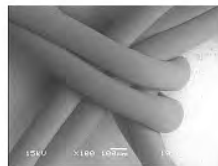
TVT2P_04



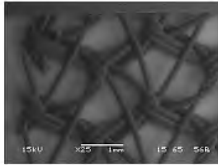
TVT2R_01



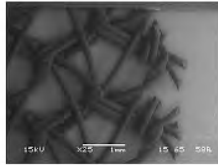
TVT2R_02



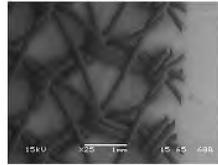
TVT2R_03



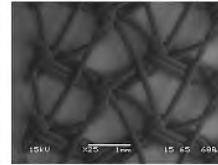
HerniaMeshP_01



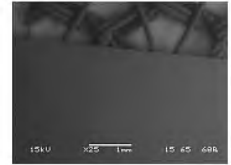
HerniaMeshP_02



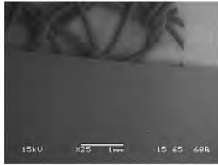
HerniaMeshP_03



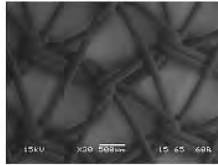
HerniaMeshP_04



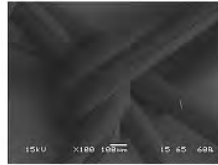
HerniaMeshP_05



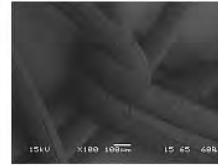
HerniaMeshP_06



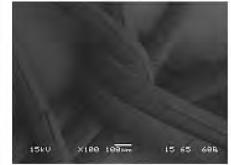
HerniaMeshP_07



HerniaMeshP_08



HerniaMeshP_09



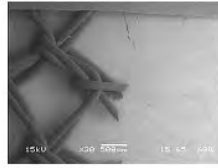
HerniaMeshP_10



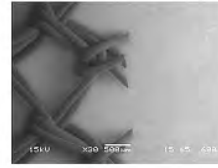
TVT3P_01



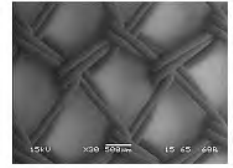
TVT3P_02



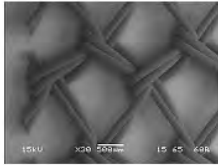
TVT3P_03



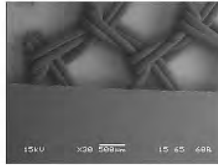
TVT3P_04



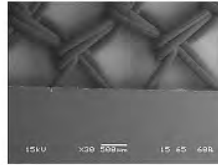
TVT3P_05



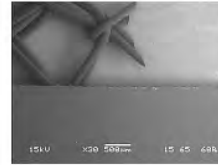
TVT3P_06



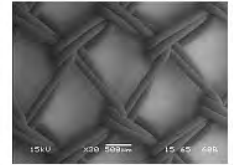
TVT3P_07



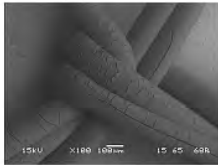
TVT3P_08



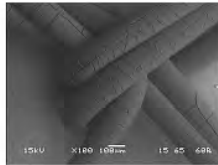
TVT3P_09



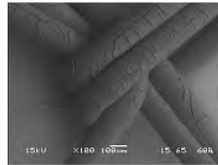
TVT3P_10



TVT3P_11



TVT3P_12



TVT3P_13



IMG_2314



IMG_2315



IMG_2316



IMG_2317



IMG_2318



IMG_2319



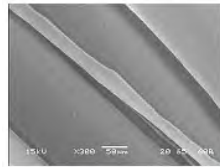
IMG_2320



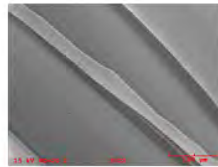
IMG_2321



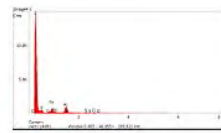
IMG_2322



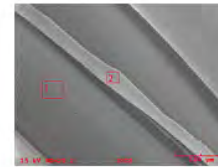
157166_TVT1_P_01



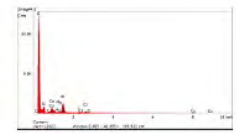
157166_TVT1_P_EDS



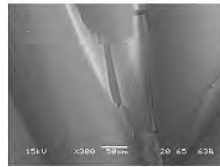
157166_TVT1_P_EDS_Loc1



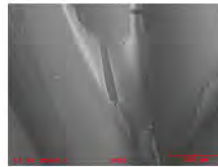
157166_TVT1_P_EDS_Loc1-2



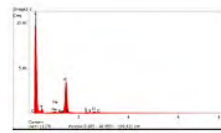
157166_TVT1_P_EDS_Loc2



157173_TVT2_P_01



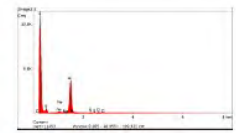
157173_TVT2_P_EDS



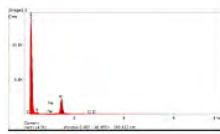
157173_TVT2_P_EDS_Loc1



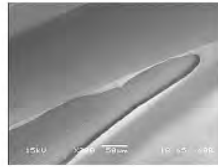
157173_TVT2_P_EDS_Loc1-3



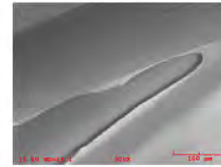
157173_TVT2_P_EDS_Loc2



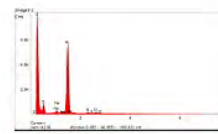
157173_TVT2_P_EDS_Loc3



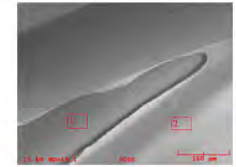
157182_TVT3_P_01



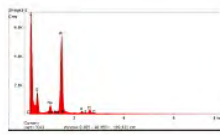
157182_TVT3_P_EDS



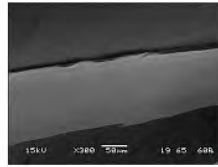
157182_TVT3_P_EDS_Loc1



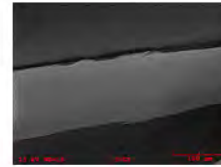
157182_TVT3_P_EDS_Loc1-2



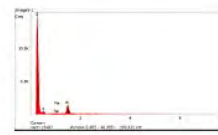
157182_TVT3_P_EDS_Loc2



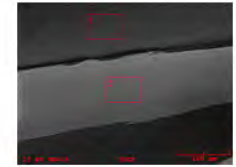
157190_Hernia_P_01



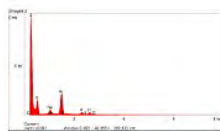
157190_Hernia_P_EDS



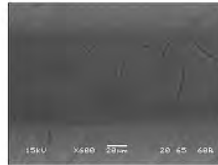
157190_Hernia_P_EDS_Loc1



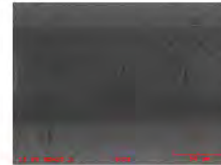
157190_Hernia_P_EDS_Loc1-2



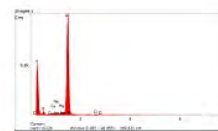
157190_Hernia_P_EDS_Loc2



157198_Suture_01



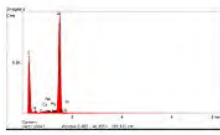
157198_Suture_EDS



157198_Suture_EDS_Loc1



157198_Suture_EDS_Loc1-2



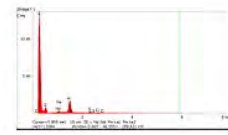
157198_Suture_EDS_Loc2



157234_Pellet3_P_01



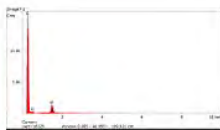
157234_Pellet3_P_EDS



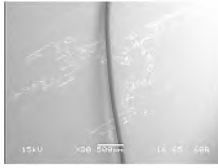
157234_Pellet3_P_EDS_Loc1



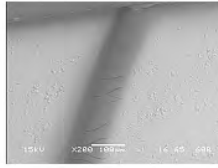
157234_Pellet3_P_EDS_Loc1-2



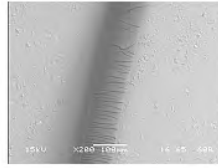
157234_Pellet3_P_EDS_Loc2



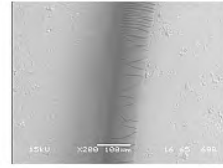
SutureP_01



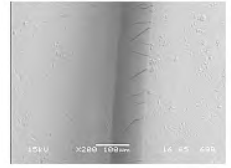
SutureP_02



SutureP_03



SutureP_04



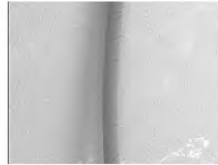
SutureP_05



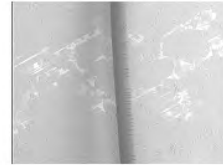
SutureP_06



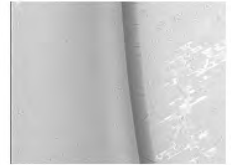
SutureP_07



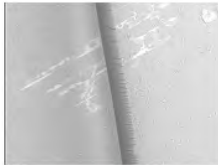
SutureP_08



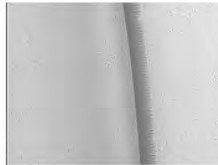
SutureP_09



SutureP_10



SutureP_11



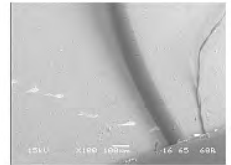
SutureP_12



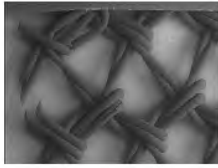
SutureP_13



SutureP_14



SutureP_15



TVT1P_01



TVT1P_02



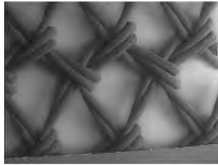
TVT1P_03



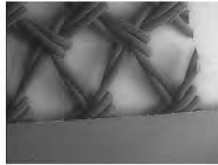
TVT1P_04



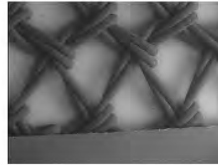
TVT1P_05



TVT1P_06



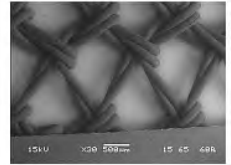
TVT1P_07



TVT1P_08



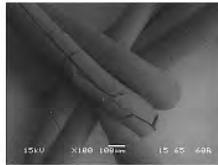
TVT1P_09



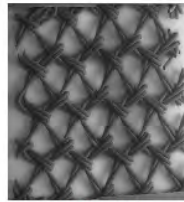
TVT1P_10



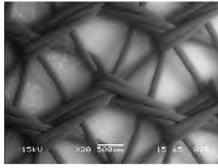
TVT1P_11



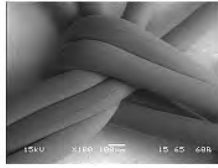
TVT1P_12



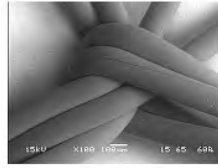
TVT1P_stitch



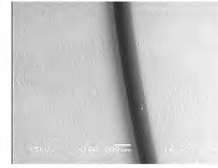
HerniaR_01



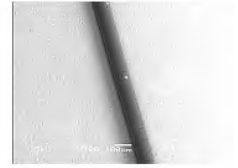
HerniaR_02



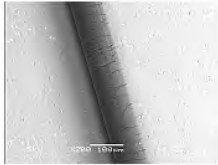
HerniaR_03



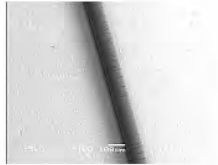
SutureR_01



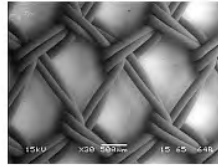
SutureR_02



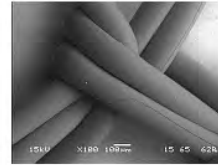
SutureR_03



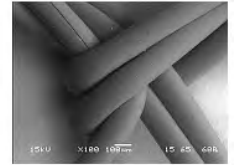
SutureR_04



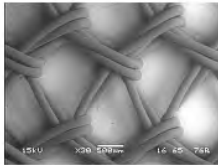
TVT1R_01



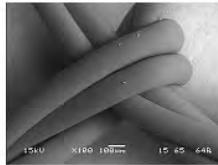
TVT1R_02



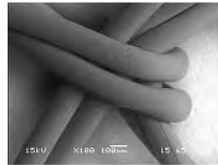
TVT1R_03



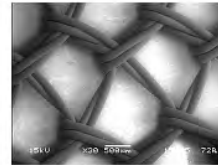
TVT2R_01



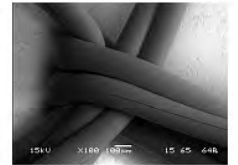
TVT2R_02



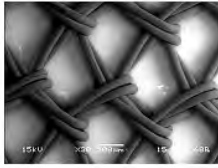
TVT2R_03



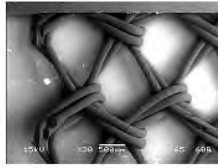
TVT3R_01



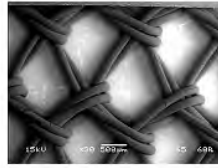
TVT3R_02



TVT2P_01



TVT2P_02



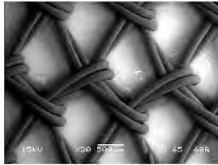
TVT2P_03



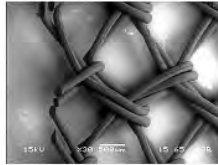
TVT2P_04



TVT2P_05



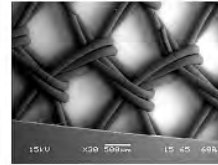
TVT2P_06



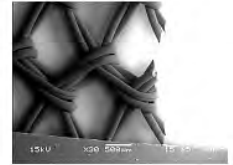
TVT2P_07



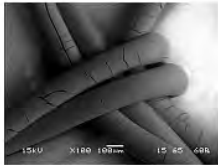
TVT2P_08



TVT2P_09



TVT2P_10



TVT2P_11



TVT2P_12



DSC_7105



DSC_7106



DSC_7107



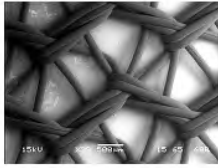
DSC_7108



DSC_7109



DSC_7110



HerniaR_01



HerniaR_02



HerniaR_03



HerniaR_04



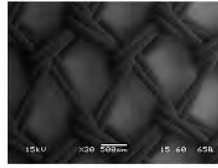
SutureR_01



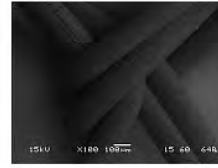
SutureR_02



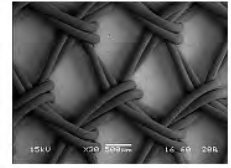
SutureR_03



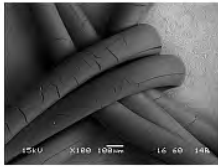
TVT1R_01



TVT1R_02



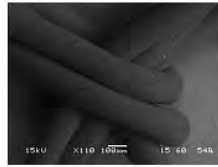
TVT2R_01



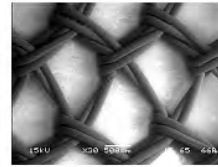
TVT2R_02



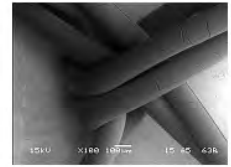
TVT2R_03



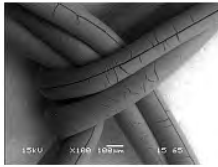
TVT2R_04



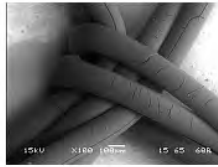
TVT3R_01



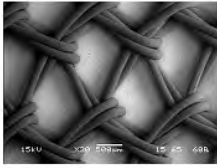
TVT3R_02



TVT3R_03



TVT3R_04



TVT2R_01



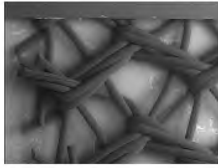
TVT2R_02



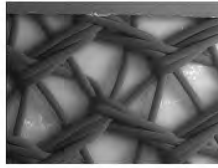
TVT2R_03



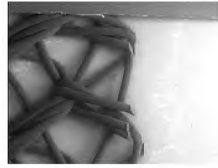
TVT2R_04



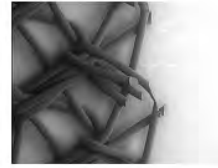
HerniaR_01



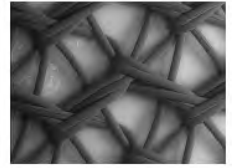
HerniaR_02



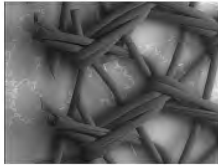
HerniaR_03



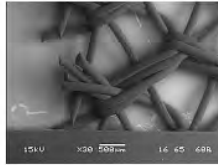
HerniaR_04



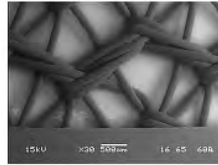
HerniaR_05



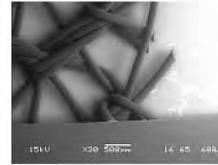
HerniaR_06



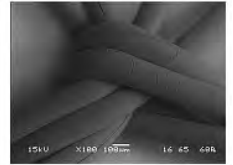
HerniaR_07



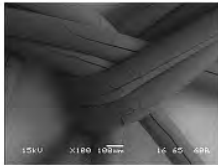
HerniaR_08



HerniaR_09



HerniaR_10



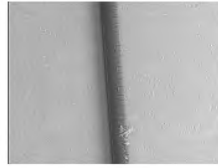
HerniaR_11



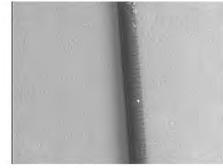
SutureR_01



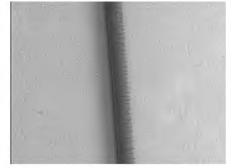
SutureR_02



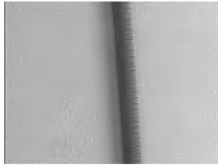
SutureR_03



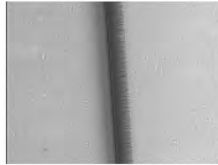
SutureR_04



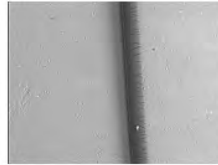
SutureR_05



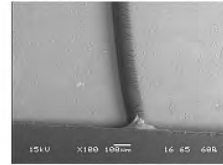
SutureR_06



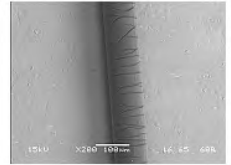
SutureR_07



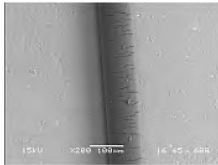
SutureR_08



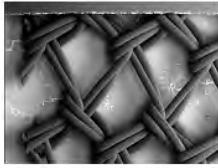
SutureR_09



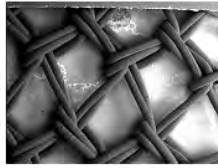
SutureR_10



SutureR_11



TVT1R_01



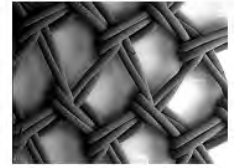
TVT1R_02



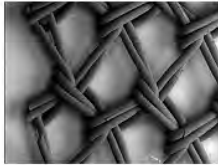
TVT1R_03



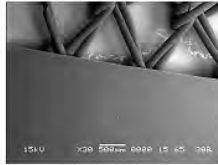
TVT1R_04



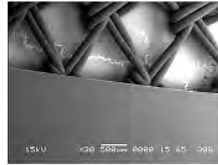
TVT1R_05



TVT1R_06



TVT1R_07



TVT1R_08



TVT1R_09



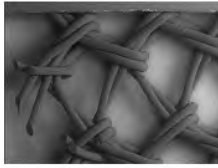
TVT1R_10



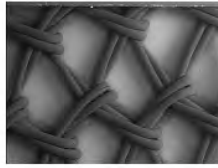
TVT1R_11



TVT1R_stitch



TVT2R_01



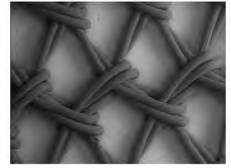
TVT2R_02



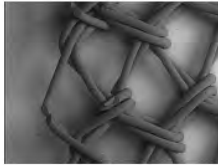
TVT2R_03



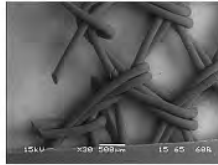
TVT2R_04



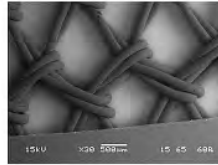
TVT2R_05



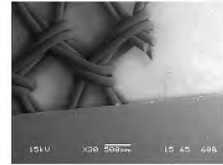
TVT2R_06



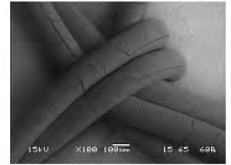
TVT2R_07



TVT2R_08



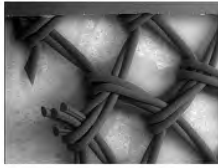
TVT2R_09



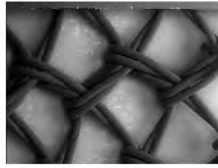
TVT2R_10



TVT2R_11



TVT3R_01



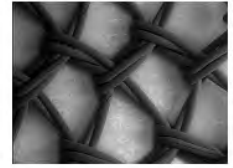
TVT3R_02



TVT3R_03



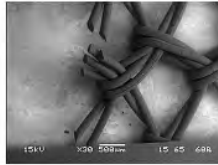
TVT3R_04



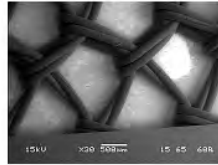
TVT3R_05



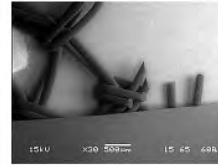
TVT3R_06



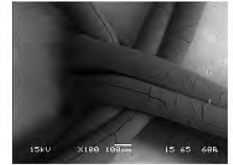
TVT3R_07



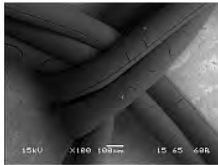
TVT3R_08



TVT3R_09



TVT3R_10



TVT3R_11



DSC_9597



DSC_9598



DSC_9599



DSC_9600



DSC_9601



DSC_9683



DSC_9684



DSC_9685



DSC_9686



DSC_9687



DSC_9688



DSC_9689



IMG_1054



IMG_1055



IMG_1056



IMG_1057



IMG_1058



DSC_9696



DSC_9697



DSC_9698



DSC_9699



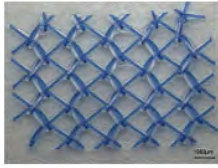
DSC_9700



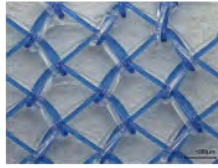
DSC_9701



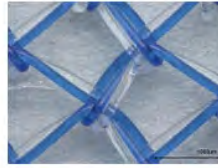
DSC_9702



157166_TVT#1_Paraffin_01



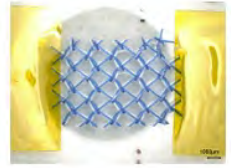
157166_TVT#1_Paraffin_02



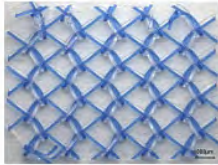
157166_TVT#1_Paraffin_03



157166_TVT#1_Paraffin_04



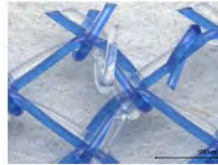
157166_TVT#1_Paraffin_05



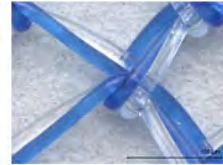
157167_TVT#1_Resin_01



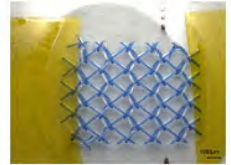
157167_TVT#1_Resin_02



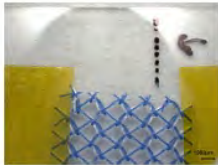
157167_TVT#1_Resin_03



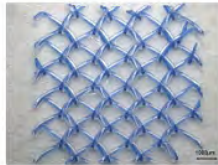
157167_TVT#1_Resin_04



157167_TVT#1_Resin_05



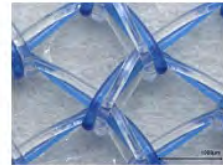
157167_TVT#1_Resin_06



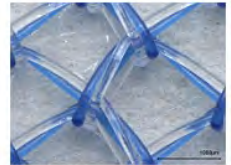
157174_TVT#2_Paraffin_01



157174_TVT#2_Paraffin_02



157174_TVT#2_Paraffin_03



157174_TVT#2_Paraffin_04



157174_TVT#2_Paraffin_05



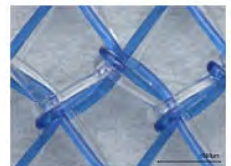
157174_TVT#2_Paraffin_06



157175_TVT#2_Resin_01



157175_TVT#2_Resin_02



157175_TVT#2_Resin_03



157175_TVT#2_Resin_04



157175_TVT#2_Resin_05



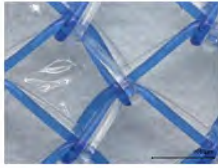
157175_TVT#2_Resin_06



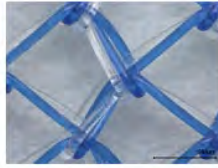
157182_TVT#3_Paraffin_01



157182_TVT#3_Paraffin_02



157182_TVT#3_Paraffin_03



157182_TVT#3_Paraffin_04



157182_TVT#3_Paraffin_05



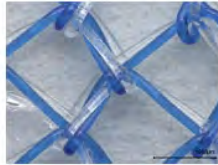
157182_TVT#3_Paraffin_06



157183_TVT#3_Resin_01



157183_TVT#3_Resin_02



157183_TVT#3_Resin_03



157183_TVT#3_Resin_04



157183_TVT#3_Resin_05



157183_TVT#3_Resin_06



57190_HerniaMesh_Paraffin_0



57190_HerniaMesh_Paraffin_0



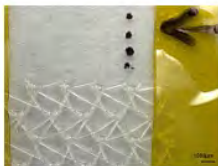
57190_HerniaMesh_Paraffin_0



57190_HerniaMesh_Paraffin_0



57190_HerniaMesh_Paraffin_0



57190_HerniaMesh_Paraffin_0



157191_HerniaMesh_Resin_01



157191_HerniaMesh_Resin_02



157191_HerniaMesh_Resin_03



157191_HerniaMesh_Resin_04



157191_HerniaMesh_Resin_05



157191_HerniaMesh_Resin_06



157198_Suture_Paraffin_01



157198_Suture_Paraffin_02



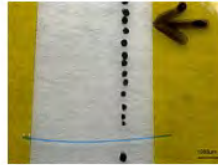
157198_Suture_Paraffin_03



157198_Suture_Paraffin_04



157198_Suture_Paraffin_05



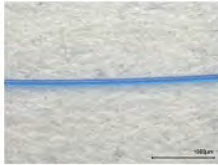
157198_Suture_Paraffin_06



157199_Suture_Resin_01



157199_Suture_Resin_02



157199_Suture_Resin_03



157199_Suture_Resin_04



157199_Suture_Resin_05



157199_Suture_Resin_06



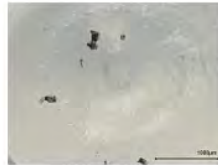
157199_Suture_Resin_07



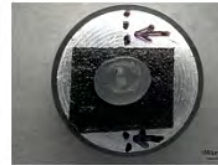
157234_pellet_Paraffin_01



157234_pellet_Paraffin_02



157234_pellet_Paraffin_03



157234_pellet_Paraffin_04



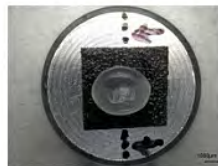
157235_pellet_Resin_01



157235_pellet_Resin_02



157235_pellet_Resin_03



157235_pellet_Resin_04



DSC_4479



DSC_4480



DSC_4481



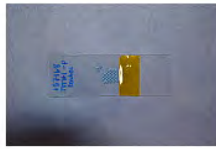
DSC_4482



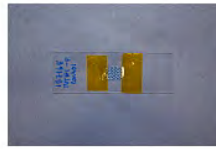
DSC_4483



DSC_4483



DSC_4484



DSC_4485



DSC_4486



DSC_4512



DSC_4513



DSC_4514



DSC_4515



DSC_4516



DSC_4517



DSC_4518



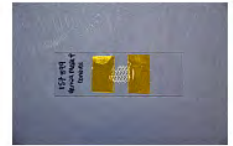
DSC_4519



DSC_4520



DSC_4521



DSC_4522



DSC_4523



DSC_4524



DSC_4525



DSC_4526



DSC_4527



DSC_4528



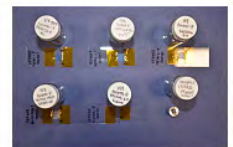
DSC_4529



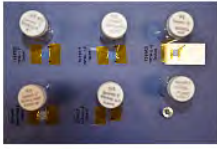
DSC_4530



DSC_4531



DSC_4532



DSC_4533



DSC_4465



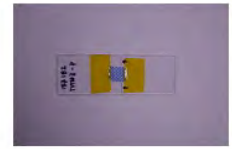
DSC_4466



DSC_4467



DSC_4468



DSC_4469



DSC_4470



DSC_4471



DSC_4472



DSC_4473



DSC_4474



DSC_4475



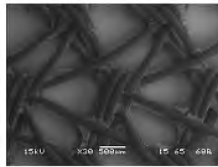
DSC_4476



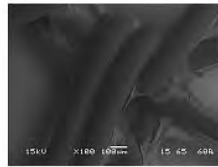
DSC_4477



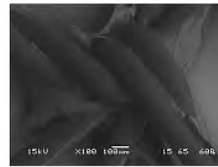
DSC_4478



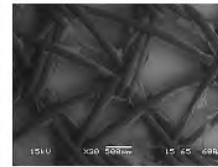
HerniaP-01



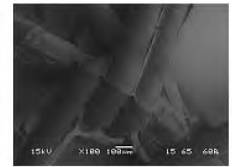
HerniaP-02



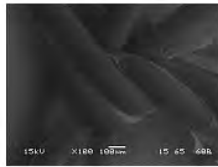
HerniaP-03



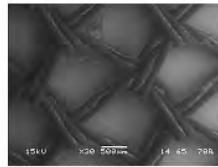
HerniaR-01



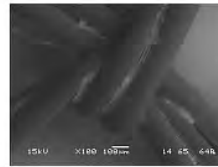
HerniaR-02



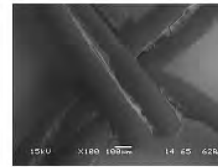
HerniaR-03



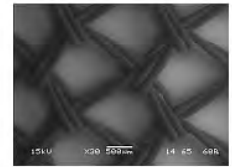
TVT1P-01



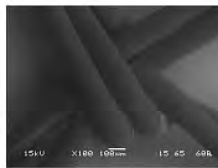
TVT1P-02



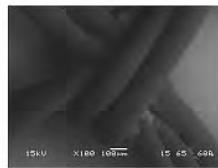
TVT1P-03



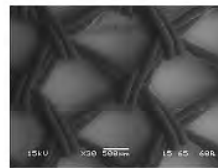
TVT1R-01



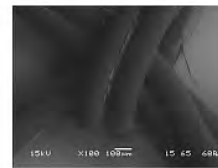
TVT1R-02



TVT1R-03



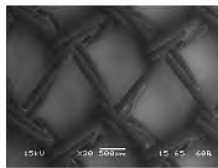
TVT2P-01



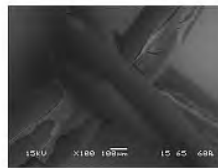
TVT2P-02



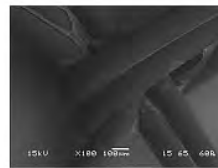
TVT2P-03



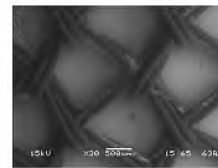
TVT2R-01



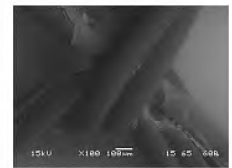
TVT2R-02



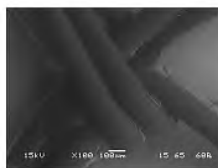
TVT2R-03



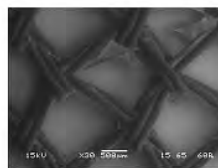
TVT3P-01



TVT3P-02



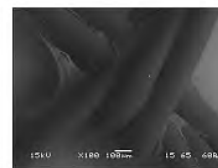
TVT3P-03



TVT3R-01



TVT3R-02



TVT3R-03



DSC_4487



DSC_4488



DSC_4489



DSC_4490



DSC_4491



DSC_4492



DSC_4493



DSC_4494



DSC_4495



DSC_4496



DSC_4497



DSC_4498



DSC_4499



DSC_4500



DSC_4501



DSC_4502



DSC_4503



DSC_4504



DSC_4505



DSC_4506



DSC_4507



DSC_4508



DSC_4509



DSC_4510



DSC_4511



DSC_4560



DSC_4561



DSC_4562



DSC_4563



DSC_4564



DSC_4565



DSC_4566



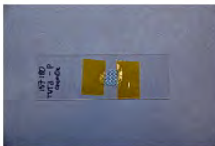
DSC_4567



DSC_4568



DSC_4569



DSC_4570



DSC_4571



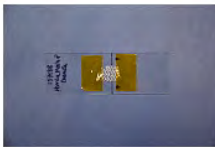
DSC_4572



DSC_4573



DSC_4574



DSC_4575



DSC_4576



DSC_4577



DSC_4578



DSC_4579



DSC_4580



DSC_4581



DSC_4582



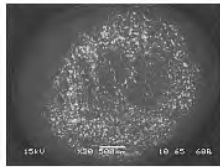
DSC_4583



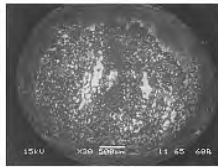
DSC_4584



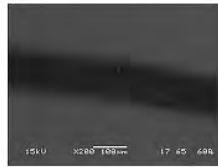
IMG_3190



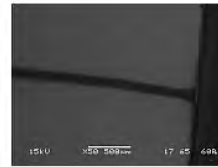
PP Pellet-P-01



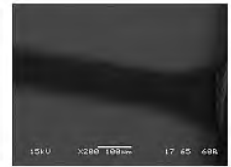
PP Pellet-R-01



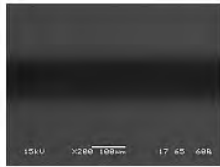
Suture-P-01



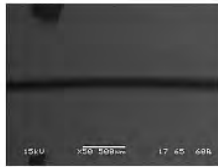
Suture-P-02



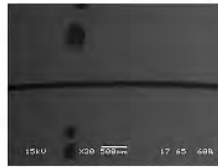
Suture-P-03



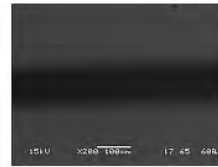
Suture-P-04



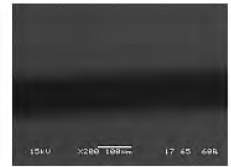
Suture-P-05



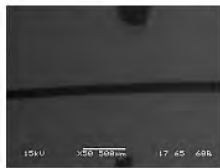
Suture-P-06



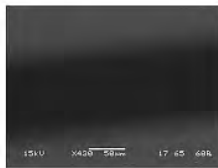
Suture-P-07



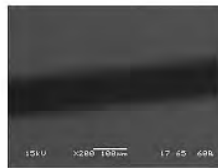
Suture-P-08



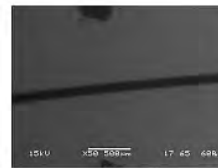
Suture-P-09



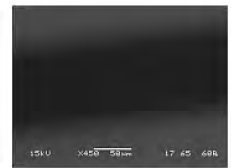
Suture-R-01



Suture-R-02



Suture-R-03



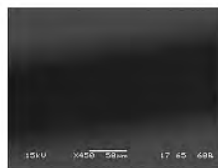
Suture-R-04



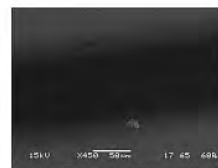
Suture-R-05



Suture-R-06



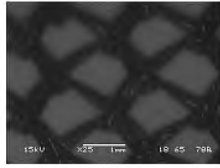
Suture-R-07



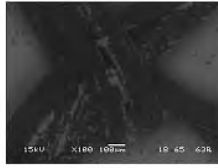
Suture-R-08



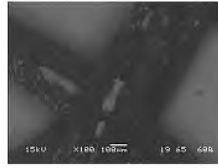
Suture-R-09



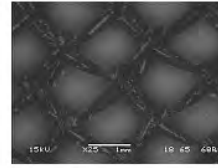
157164-TVT1-Chem Ox-P-01



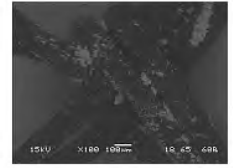
157164-TVT1-Chem Ox-P-02



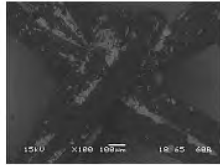
157164-TVT1-Chem Ox-P-03



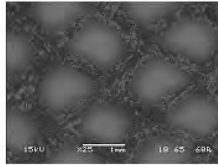
157165-TVT1-Chem Ox-R-01



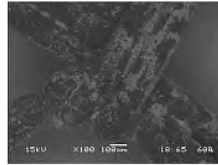
157165-TVT1-Chem Ox-R-02



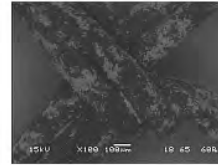
157165-TVT1-Chem Ox-R-03



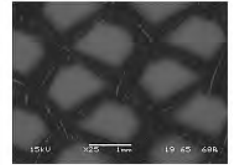
157172-TVT2-Chem Ox P-01



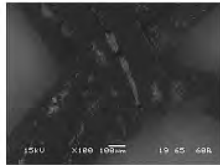
157172-TVT2-Chem Ox P-02



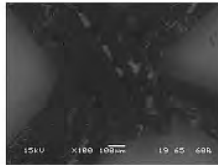
157172-TVT2-Chem Ox P-03



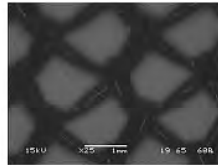
157173-TVT2-Chem Ox R-01



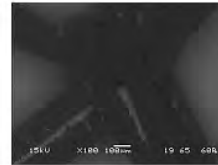
157173-TVT2-Chem Ox R-02



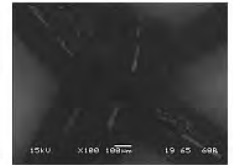
157173-TVT2-Chem Ox R-03



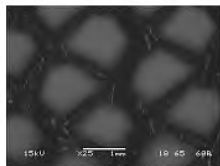
157180-TVT3-Chem Ox-P-01



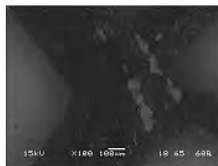
157180-TVT3-Chem Ox-P-02



157180-TVT3-Chem Ox-P-03



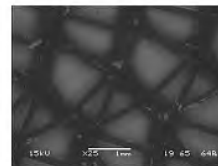
157181-TVT3-Chem Ox-R-01



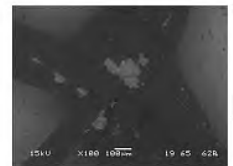
157181-TVT3-Chem Ox-R-02



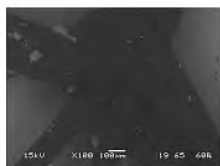
157181-TVT3-Chem Ox-R-03



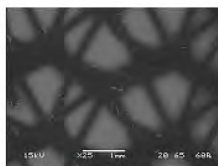
157188-Hernia Chem Ox-P-01



157188-Hernia Chem Ox-P-02



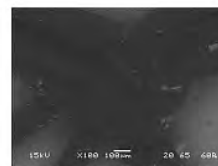
157188-Hernia Chem Ox-P-03



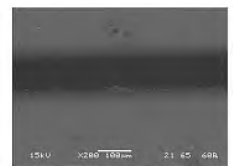
157189-Hernia Chem Ox-R-01



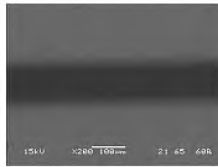
157189-Hernia Chem Ox-R-02



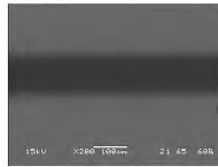
157189-Hernia Chem Ox-R-03



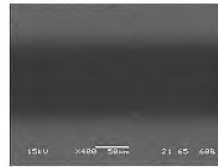
157196-Suture-Chem Ox-01



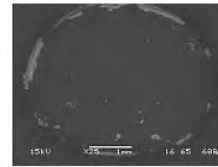
157196-Suture-Chem Ox-02



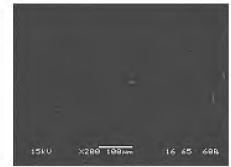
157196-Suture-Chem Ox-03



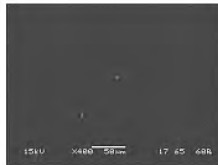
157196-Suture-Chem Ox-04



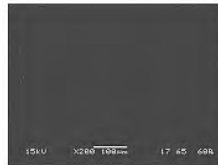
157232-PP Pellet-P-01



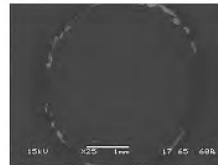
157232-PP Pellet-P-02



157232-PP Pellet-P-03



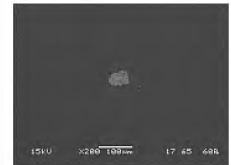
157232-PP Pellet-P-04



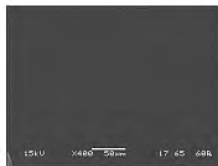
157233-PP Pellet-R-01



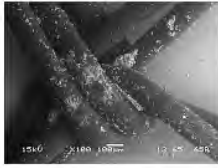
157233-PP Pellet-R-02



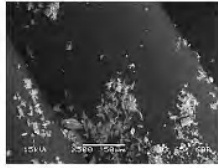
157233-PP Pellet-R-03



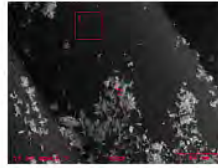
157233-PP Pellet-R-04



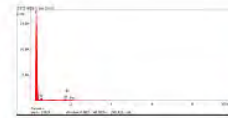
TVT1-01



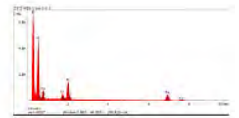
TVT1-02



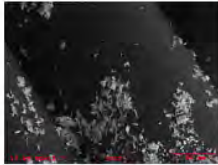
TVT1-EDS 1 Loc 1-2



TVT1-EDS 1 Loc 1-2-1



TVT1-EDS 1 Loc 1-2-2



TVT1-EDS 1



157178_QUV_P_63x_H&E_ana_01-image
Export-01



157178_QUV_P_63x_H&E_ana_02-image
Export-02



157178_QUV_P_63x_H&E_ana_03-image
Export-03



157178_QUV_P_63x_H&E_BF_01-image Export-04



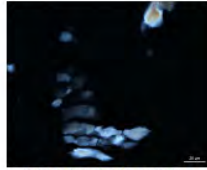
157178_QUV_P_63x_H&E_BF_02-image Export-05



157178_QUV_P_63x_H&E_BF_03-image Export-06



157178_QUV_P_63x_H&E_xpol_01-image
Export-07



157178_QUV_P_63x_H&E_xpol_02-image
Export-08



157178_QUV_P_63x_H&E_xpol_03-image
Export-09



157180_ChemOx_P_63x_H&E_ana_01-image
Export-01



157180_ChemOx_P_63x_H&E_ana_02-image
Export-02



157180_ChemOx_P_63x_H&E_ana_03-image
Export-03



157180_ChemOx_P_63x_H&E_ana_04-image
Export-04



157180_ChemOx_P_63x_H&E_BF_01-image
Export-05



157180_ChemOx_P_63x_H&E_BF_02-image
Export-06



157180_ChemOx_P_63x_H&E_BF_03-image
Export-07



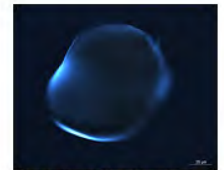
157180_ChemOx_P_63x_H&E_BF_04-image
Export-08



157180_ChemOx_P_63x_H&E_xpol_01-image
Export-09



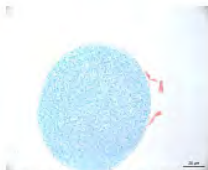
157180_ChemOx_P_63x_H&E_xpol_02-image
Export-10



157180_ChemOx_P_63x_H&E_xpol_03-image
Export-11



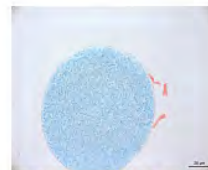
157180_ChemOx_P_63x_H&E_xpol_04-image
Export-12



157182_Serum_P_63x_H&E_ana_01-image
Export-01



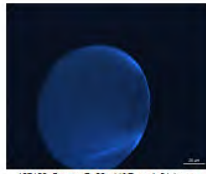
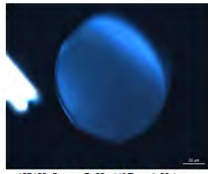
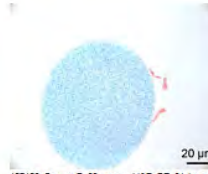
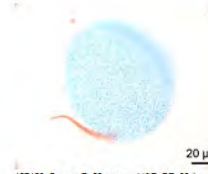
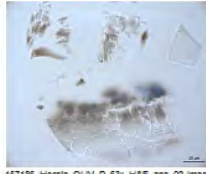
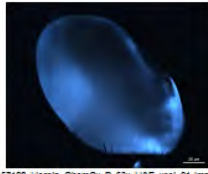
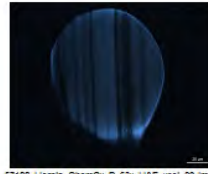
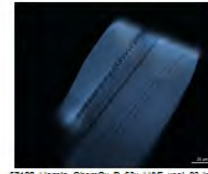
157182_Serum_P_63x_H&E_ana_02-image
Export-02

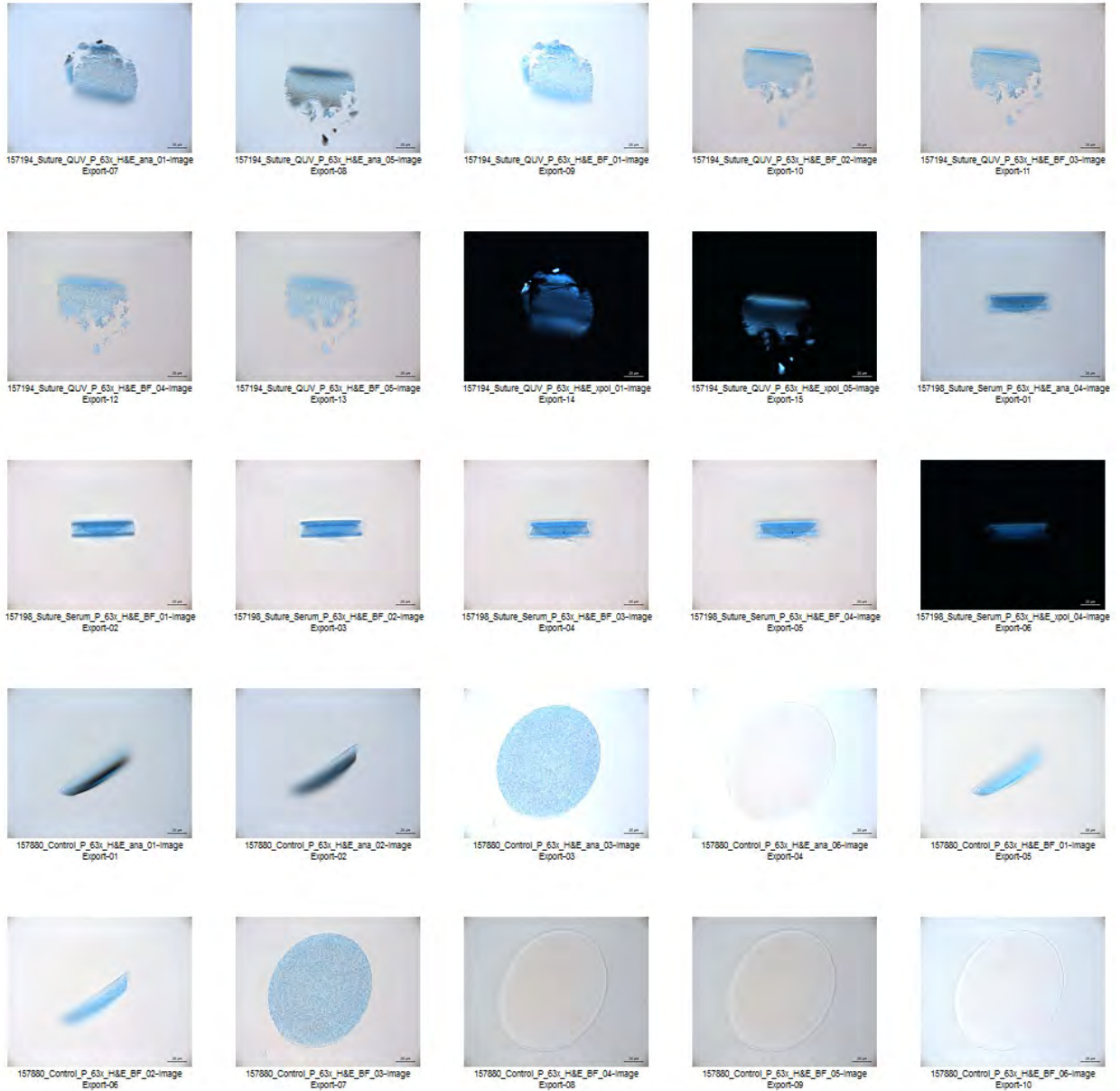


157182_Serum_P_63x_H&E_BF_01-image
Export-03



157182_Serum_P_63x_H&E_BF_02-image
Export-04

157182_Serum_P_63x_H&E_ipol_01-image
Export-06157182_Serum_P_63x_H&E_ipol_02-image
Export-06157182_Serum_P_63x-zoom_H&E_BF_01-image
Export-07157182_Serum_P_63x-zoom_H&E_BF_02-image
Export-06157186_Hemia_QUV_P_63x_H&E_ana_01-image
Export-01157186_Hemia_QUV_P_63x_H&E_ana_02-image
Export-02157186_Hemia_QUV_P_63x_H&E_BF_01-image
Export-03157186_Hemia_QUV_P_63x_H&E_BF_02-image
Export-04157186_Hemia_QUV_P_63x_H&E_ipol_01-image
Export-05157186_Hemia_QUV_P_63x_H&E_ipol_02-image
Export-06157188_Hemia_ChemOx_P_63x_H&E_ana_01-image
Export-01157188_Hemia_ChemOx_P_63x_H&E_ana_02-image
Export-02157188_Hemia_ChemOx_P_63x_H&E_ana_03-image
Export-03157188_Hemia_ChemOx_P_63x_H&E_BF_01-image
Export-04157188_Hemia_ChemOx_P_63x_H&E_BF_02-image
Export-05157188_Hemia_ChemOx_P_63x_H&E_BF_03-image
Export-06157188_Hemia_ChemOx_P_63x_H&E_ana_01-image
Export-07157188_Hemia_ChemOx_P_63x_H&E_ipol_02-image
Export-08157188_Hemia_ChemOx_P_63x_H&E_ipol_03-image
Export-09157190_Hemia_Serum_P_63x_H&E_ana_01-image
Export-01157190_Hemia_Serum_P_63x_H&E_ana_02-image
Export-02157190_Hemia_Serum_P_63x_H&E_BF_01-image
Export-03157190_Hemia_Serum_P_63x_H&E_BF_02-image
Export-04157190_Hemia_Serum_P_63x_H&E_ipol_01-image
Export-05157190_Hemia_Serum_P_63x_H&E_ipol_02-image
Export-06





157880_Control_P_63x_H&E_xpol_01-image
Export-11



157880_Control_P_63x_H&E_xpol_02-image
Export-12



157880_Control_P_63x_H&E_xpol_03-image
Export-13



157880_Control_P_63x_H&E_xpol_06-image
Export-14



157884_Control_P_63x_H&E_ana_01-image
Export-01



157884_Control_P_63x_H&E_ana_04-image
Export-02



157884_Control_P_63x_H&E_BF_01-image
Export-03



157884_Control_P_63x_H&E_BF_02-image
Export-04



157884_Control_P_63x_H&E_BF_03-image
Export-05



157884_Control_P_63x_H&E_BF_04-image
Export-06



157884_Control_P_63x_H&E_xpol_01-image
Export-07



157884_Control_P_63x_H&E_xpol_04-image
Export-08



157885_Control_P_63x_H&E_ana_02-image
Export-01



157885_Control_P_63x_H&E_ana_05-image
Export-02



157885_Control_P_63x_H&E_BF_01-image
Export-03



157885_Control_P_63x_H&E_BF_02-image
Export-04



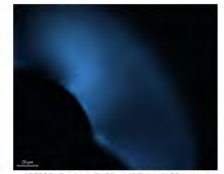
157885_Control_P_63x_H&E_BF_03-image
Export-05



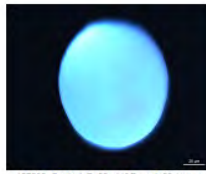
157885_Control_P_63x_H&E_BF_04-image
Export-06



157885_Control_P_63x_H&E_BF_05-image
Export-07



157885_Control_P_63x_H&E_xpol_02-image
Export-08



157885_Control_P_63x_H&E_xpol_05-image
Export-09



157889_Hernia_Control_P_63x_H&E_ana_01-image
Export-01



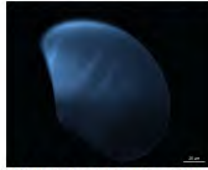
157889_Hernia_Control_P_63x_H&E_ana_02-image
Export-02



157889_Hernia_Control_P_63x_H&E_BF_01-image
Export-03



157889_Hernia_Control_P_63x_H&E_BF_02-image
Export-04



157899_hemia_Control_P_63x_H&E_xpol_01-image Export-06



157899_hemia_Control_P_63x_H&E_xpol_02-image Export-06



159703_Suture_CemOx_P_63x_H&E_ana_01-image Export-06



159703_Suture_CemOx_P_63x_H&E_ana_05-image Export-06



159703_Suture_CemOx_P_63x_H&E_BF_01-image Export-01



159703_Suture_CemOx_P_63x_H&E_BF_02-image Export-02



159703_Suture_CemOx_P_63x_H&E_BF_03-image Export-03



159703_Suture_CemOx_P_63x_H&E_BF_04-image Export-04



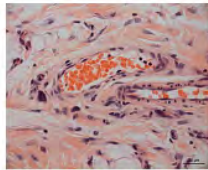
159703_Suture_CemOx_P_63x_H&E_BF_05-image Export-07



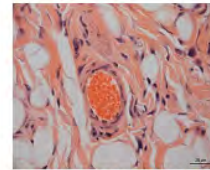
159703_Suture_CemOx_P_63x_H&E_xpol_01-image Export-06



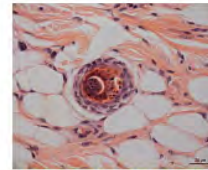
159703_Suture_CemOx_P_63x_H&E_xpol_05-image Export-09



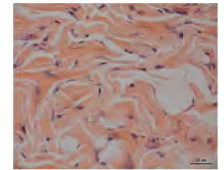
Rabbit skin_63x_H&E_BF_01-image Export-01



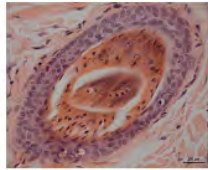
Rabbit skin_63x_H&E_BF_02-image Export-02



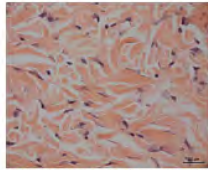
Rabbit skin_63x_H&E_BF_03-image Export-03



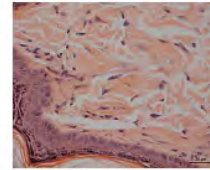
Rabbit skin_63x_H&E_BF_04-image Export-01



Rabbit skin_63x_H&E_BF_05-image Export-02



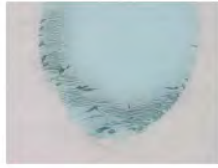
Rabbit skin_63x_H&E_BF_06-image Export-03



Rabbit skin_63x_H&E_BF_07-image Export-04



162_QUV-P_40x_Unstained_BF



162_QUV-P_40x_Unstained_BF



4_ChemOx-P_10x_Unstained_I



4_ChemOx-P_10x_Unstained_I



4_ChemOx-P_10x_Unstained_I



66_Serum-P_10x_Unstained_B



66_Serum-P_40x_Unstained_B



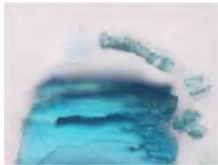
66_Serum-P_40x_Unstained_B



170_QUV-P_10x_Unstained_BF



170_QUV-P_10x_Unstained_BF



170_QUV-P_40x_Unstained_BF



2_ChemOx-P_10x_Unstained_I



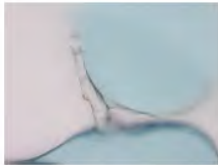
2_ChemOx-P_40x_Unstained_I



2_ChemOx-P_40x_Unstained_I



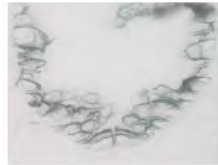
74_Serum-P_40x_Unstained_B



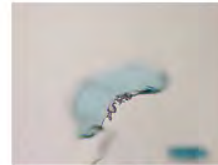
74_Serum-P_40x_Unstained_B



178_QUV-P_10x_Unstained_BF



178_QUV-P_40x_Unstained_BF



0_ChemOx-P_10x_Unstained_I



0_ChemOx-P_10x_Unstained_I



0_ChemOx-P_10x_Unstained_I



0_ChemOx-P_10x_Unstained_I



0_ChemOx-P_40x_Unstained_I



0_ChemOx-P_40x_Unstained_I



0_ChemOx-P_40x_Unstained_I



0_ChemOx-P_40x_Unstained_I



82_Serum-P_10x_Unstained_B



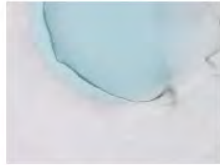
82_Serum-P_10x_Unstained_B



82_Serum-P_10x_Unstained_B



82_Serum-P_40x_Unstained_B



82_Serum-P_40x_Unstained_B



8_ChemOx-P_10x_Unstained_I



ChemOx-Pellet-P_10x_Unstain



ntreatedControl_P_10x_Unstain



ntreatedControl_P_10x_Unstain



ntreatedControl_P_40x_Unstain



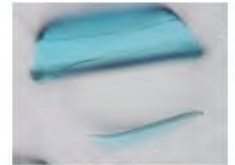
ntreatedControl_P_40x_Unstain



ntreatedControl_P_40x_Unstain



ntreatedControl_P_40x_Unstain



ntreatedControl_P_40x_Unstain



ntreatedControl_P_10x_Unstain



ntreatedControl_P_10x_Unstain



ntreatedControl_P_10x_Unstain



ntreatedControl_P_10x_Unstain



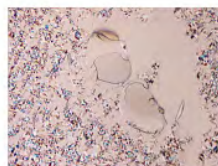
ntreatedControl_P_10x_Unstain



ntreatedControl_P_10x_Unstain



ntreatedControl_P_40x_Unstain



ntreatedControl_P_10x_Unstain



ntreatedControl_P_10x_Unstain



ntreatedControl_P_10x_Unstain



ntreatedControl_P_10x_Unstain



ntreatedControl_P_10x_Unstain



ntreatedControl_P_10x_Unstain



3_ChemOx_P_40x_Unstained_



3_ChemOx_P_40x_Unstained_



157164_ChemOx_P_63x_H&E_ana_01-image
Export-15



157164_ChemOx_P_63x_H&E_BF_01-image
Export-16



157164_ChemOx_P_63x_H&E_BF_02-image
Export-17



157164_ChemOx_P_63x_H&E_xpol_01-image
Export-18



157164_ChemOx_P_63x_H&E_xpol_02-image
Export-19



157172_ChemOx_P_63x_H&E_ana_01-image
Export-29



157172_ChemOx_P_63x_H&E_ana_02-image
Export-30



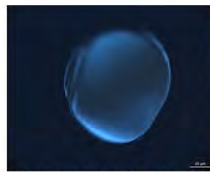
157172_ChemOx_P_63x_H&E_BF_01-image
Export-31



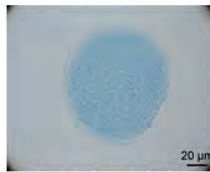
157172_ChemOx_P_63x_H&E_BF_02-image
Export-32



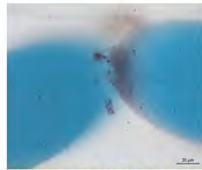
157172_ChemOx_P_63x_H&E_xpol_01-image
Export-33



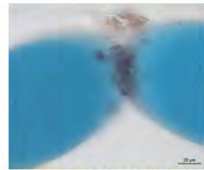
157172_ChemOx_P_63x_H&E_xpol_02-image
Export-34



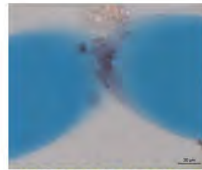
157172_ChemOx_P_63xzoom_H&E_BF_02-image
Export-35



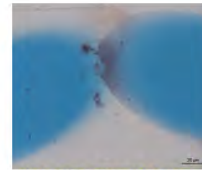
157165_ChemOx_R_63x_H&E_ana_01-image
Export-52



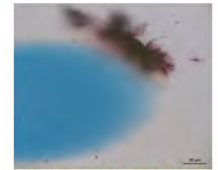
157165_ChemOx_R_63x_H&E_ana_02-image
Export-77



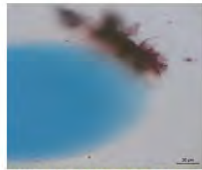
157165_ChemOx_R_63x_H&E_BF_01-image
Export-78



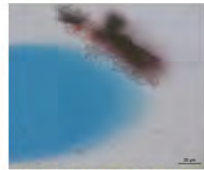
157165_ChemOx_R_63x_H&E_BF_02-image
Export-79



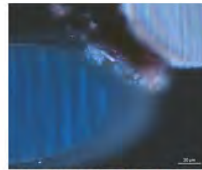
157165_ChemOx_R_63x_H&E_BF_03-image
Export-75



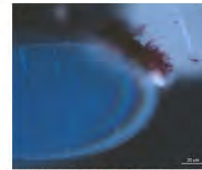
157165_ChemOx_R_63x_H&E_BF_04-image
Export-30



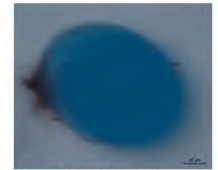
157165_ChemOx_R_63x_H&E_BF_05-image
Export-50



157165_ChemOx_R_63x_H&E_ipol_06-image
Export-74



157165_ChemOx_R_63x_H&E_ipol_07-image
Export-51



157173_ChemOx_R_63x_H&E_ana_01-image
Export-43



157173_ChemOx_R_63x_H&E_BF_01-image
Export-44



157173_ChemOx_R_63x_H&E_BF_02-image
Export-45



157173_ChemOx_R_63x_H&E_ipol_01-image
Export-48



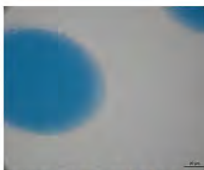
157181_ChemOx_R_63x_H&E_ana_01-image
Export-34



157181_ChemOx_R_63x_H&E_ana_03-image
Export-13



157181_ChemOx_R_63x_H&E_BF_01-image
Export-39



157181_ChemOx_R_63x_H&E_BF_02-image
Export-14



157181_ChemOx_R_63x_H&E_ipol_01-image
Export-35



157181_ChemOx_R_63x_H&E_ipol_03-image
Export-15



157181_ChemOx_R_63xzoom_H&E_BF_02-image
Export-01



157189_ChemOx_R_63x_H&E_ana_01-image
Export-17



157189_ChemOx_R_63x_H&E_ana_02-image
Export-18



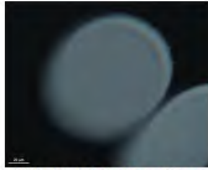
157189_ChemOx_R_63x_H&E_BF_01-image
Export-19



157189_ChemOx_R_63x_H&E_BF_02-image
Export-20



157189_ChemOx_R_63x_H&E_ipol_01-image
Export-09



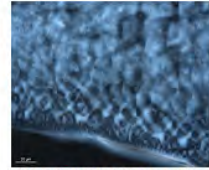
157189_ChemOx_R_63x_H&E_xpol_02-image
Export-22



157233_Pellet_ChemOx_R_63x_H&E_ana_01-image
Export-45



157233_Pellet_ChemOx_R_63x_H&E_BF_01-image
Export-35



157233_Pellet_ChemOx_R_63x_H&E_xpol_01-image
Export-47



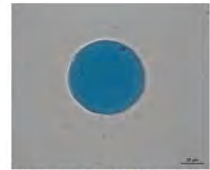
159704_ChemOx_R_10x_H&E_BF_01-Draw Scale
Bar Annotation-01-image Export-07



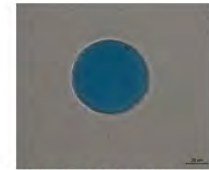
159704_ChemOx_R_10x_H&E_BF_01-image
Export-56



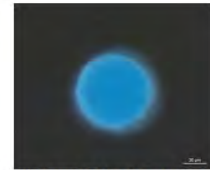
159704_ChemOx_R_20x_H&E_ana_01-image
Export-58



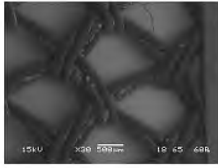
159704_ChemOx_R_63x_H&E_ana_01-image
Export-59



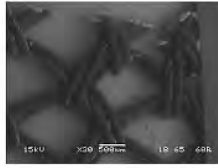
159704_ChemOx_R_63x_H&E_ana_02-image
Export-60



159704_ChemOx_R_63x_H&E_xpol_01-image
Export-61



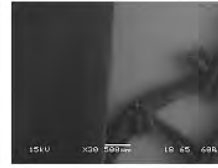
157164-TVT1-Chem Ox-P_01



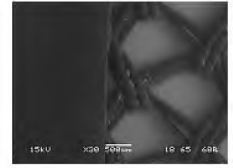
157164-TVT1-Chem Ox-P_02



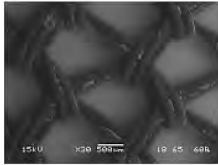
157164-TVT1-Chem Ox-P_03



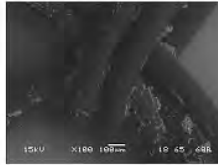
157164-TVT1-Chem Ox-P_04



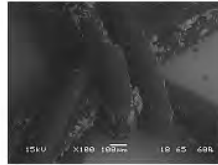
157164-TVT1-Chem Ox-P_05



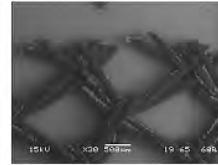
157164-TVT1-Chem Ox-P_06



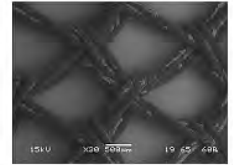
157164-TVT1-Chem Ox-P_07



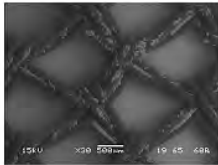
157164-TVT1-Chem Ox-P_08



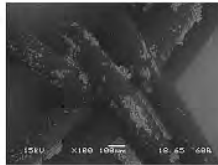
157165-TVT1-Chem Ox-R_01



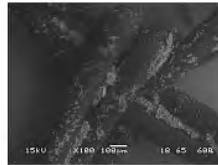
157165-TVT1-Chem Ox-R_02



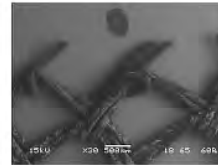
157165-TVT1-Chem Ox-R_03



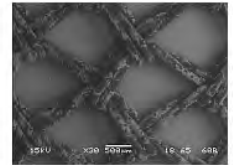
157165-TVT1-Chem Ox-R_04



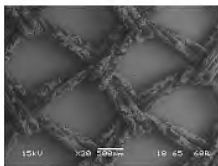
157165-TVT1-Chem Ox-R_05



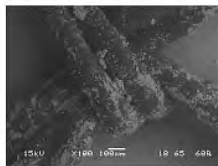
157172-TVT2-Chem Ox P_01



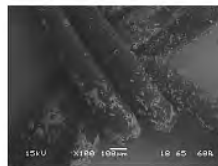
157172-TVT2-Chem Ox P_02



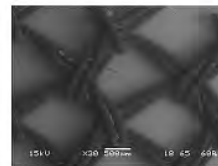
157172-TVT2-Chem Ox P_03



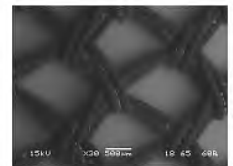
157172-TVT2-Chem Ox P_04



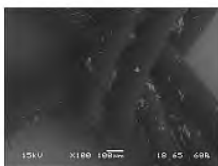
157172-TVT2-Chem Ox P_05



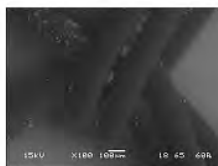
157173-TVT2-Chem Ox R_01



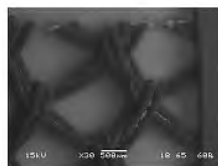
157173-TVT2-Chem Ox R_02



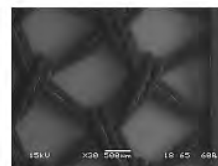
157173-TVT2-Chem Ox R_03



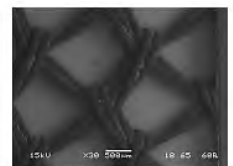
157173-TVT2-Chem Ox R_04



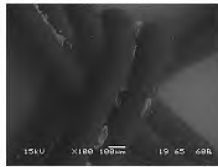
157180-TVT3-Chem Ox-P_01



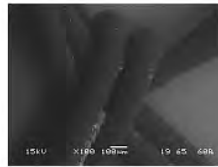
157180-TVT3-Chem Ox-P_02



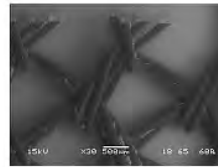
157180-TVT3-Chem Ox-P_03



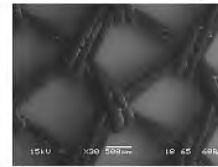
157180-TVT3-Chem Ox-P_04



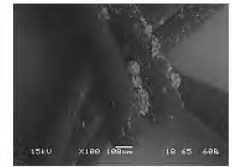
157180-TVT3-Chem Ox-P_05



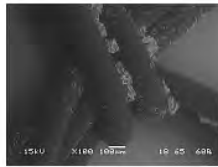
157181-TVT3-Chem Ox-R_01



157181-TVT3-Chem Ox-R_02



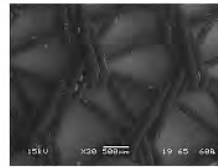
157181-TVT3-Chem Ox-R_03



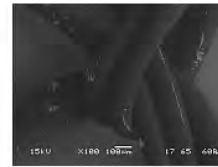
157181-TVT3-Chem Ox-R_04



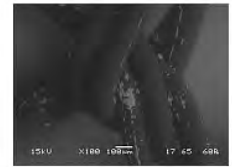
157188-Hernia Chem Ox-P_01



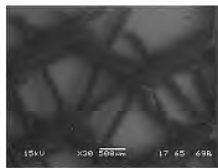
157188-Hernia Chem Ox-P_02



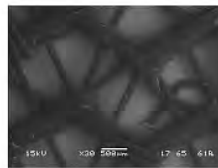
157188-Hernia Chem Ox-P_03



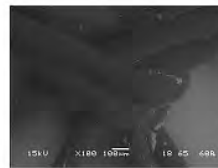
157188-Hernia Chem Ox-P_04



157189-Hernia Chem Ox-R_01



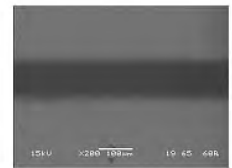
157189-Hernia Chem Ox-R_02



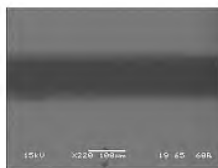
157189-Hernia Chem Ox-R_03



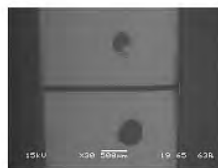
157189-Hernia Chem Ox-R_04



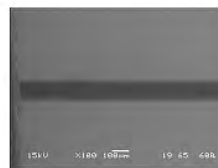
159703-Suture-Chem Ox-P_01



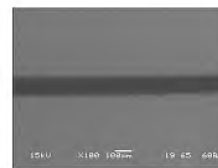
159703-Suture-Chem Ox-P02



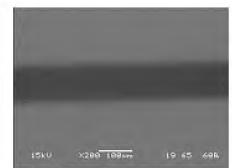
159704-Suture-Chem Ox-R_01



159704-Suture-Chem Ox-R_02



159704-Suture-Chem Ox-R_03



159704-Suture-Chem Ox-R_04



157185_Pristine_R_63x_H&E_BF_01-image Export-36



157187_QUV_R_63x_H&E_ana_01-image Export-21



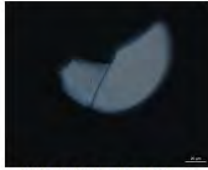
157187_QUV_R_63x_H&E_ana_04-image Export-22



157187_QUV_R_63x_H&E_BF_02-image Export-23



157187_QUV_R_63x_H&E_BF_05-image Export-12



157187_QUV_R_63x_H&E_ipol_02-image Export-24



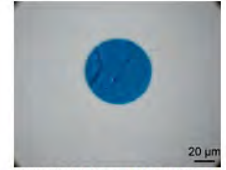
157189_ChemOx_R_63x_H&E_BF_01-image Export-25



157189_ChemOx_R_63x_H&E_ipol_01-image Export-21



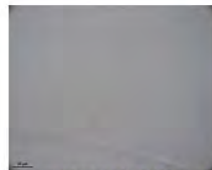
157193_Pristine_R_63x_H&E_BF_01-image Export-32



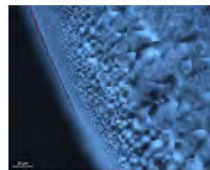
157195_QUV_R_63x-zoom_H&E_ana_01-image Export-37



157199_Serum_R_63x_H&E_BF_01-image Export-39



157233_Pellet_ChemOx_R_63x_H&E_BF_01-image Export-46



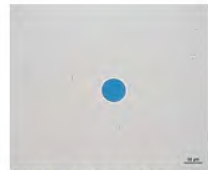
157235_Pellet_Serum_R_63x_H&E_ipol_01-image Export-62



157237_Pellet_Pristine_R_63x_H&E_BF_01-image Export-54



159704_ChemOx_R_10x_H&E_BF_01-Draw Scale Bar Annotation-01-image Export-57



159704_ChemOx_R_10x_H&E_BF_01-image Export-55



159704_ChemOx_R_20x_H&E_ana_01-image Export-56



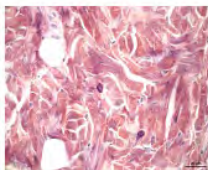
159704_ChemOx_R_63x_H&E_ana_01-image Export-57



159704_ChemOx_R_63x_H&E_ana_02-image Export-58



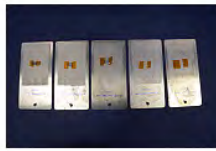
159704_ChemOx_R_63x_H&E_ipol_01-image Export-59



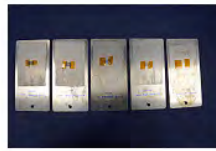
Rabbitskin_R_63x_H&E_BF_02-image Export-63



DSC_9609



DSC_9610



DSC_9611



DSC_9612



DSC_9613



DSC_9614



DSC_9615



DSC_9616



DSC_9617



DSC_9618



DSC_9619



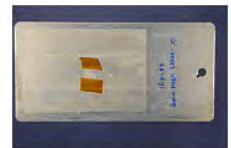
DSC_9620



DSC_9621



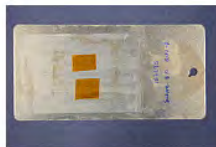
DSC_9622



DSC_9623



DSC_9624



DSC_9625



DSC_9626



DSC_9627



DSC_9628



DSC_9629



DSC_9630



DSC_9631



DSC_9632



DSC_9633



DSC_9634



DSC_9635



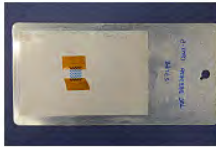
DSC_9636



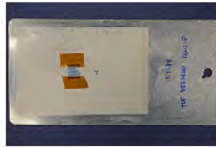
DSC_9637



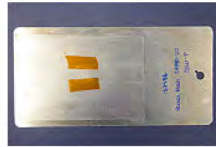
DSC_9638



DSC_9639



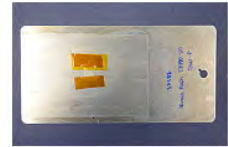
DSC_9640



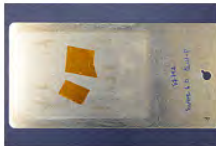
DSC_9641



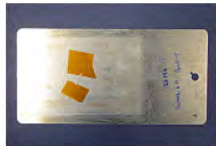
DSC_9642



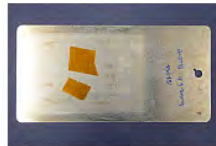
DSC_9643



DSC_9644



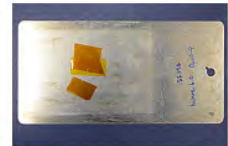
DSC_9645



DSC_9646



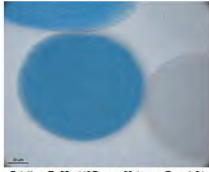
DSC_9647



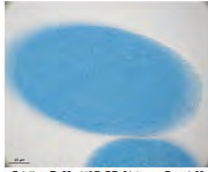
DSC_9648



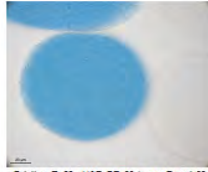
DSC_9649



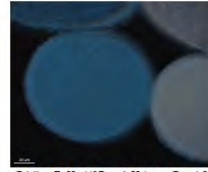
Pristine_R_63i_H&E_ana_02-image Export-01



Pristine_R_63i_H&E_BF_01-image Export-02



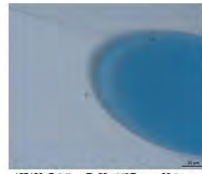
Pristine_R_63i_H&E_BF_02-image Export-03



Pristine_R_63i_H&E_ipol_02-image Export-04



157169_Pristine_R_63x_H&E_ana_01-image
Export-59



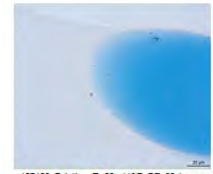
157169_Pristine_R_63x_H&E_ana_02-image
Export-60



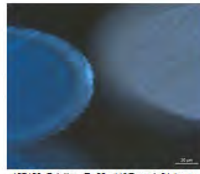
157169_Pristine_R_63x_H&E_BF_01-image
Export-61



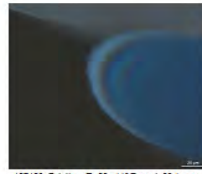
157169_Pristine_R_63x_H&E_BF_02-image
Export-62



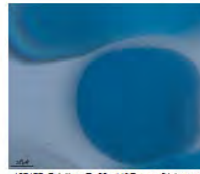
157169_Pristine_R_63x_H&E_BF_03-image
Export-63



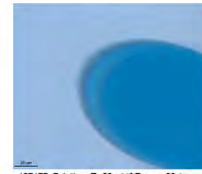
157169_Pristine_R_63x_H&E_ipol_01-image
Export-64



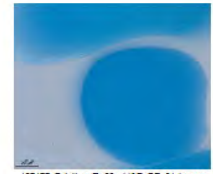
157169_Pristine_R_63x_H&E_ipol_02-image
Export-65



157177_Pristine_R_63x_H&E_ana_01-image
Export-37



157177_Pristine_R_63x_H&E_ana_02-image
Export-33



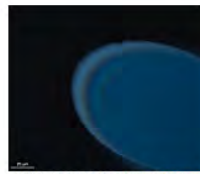
157177_Pristine_R_63x_H&E_BF_01-image
Export-46



157177_Pristine_R_63x_H&E_BF_02-image
Export-38



157177_Pristine_R_63x_H&E_ipol_01-image
Export-47



157177_Pristine_R_63x_H&E_ipol_02-image
Export-31



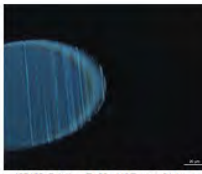
157185_Pristine_R_63x_H&E_ana_01-image
Export-01



157185_Pristine_R_63x_H&E_BF_01-image
Export-02



157185_Pristine_R_63x_H&E_BF_02-image
Export-03



157185_Pristine_R_63x_H&E_ipol_01-image
Export-04



157193_Pristine_R_63x_H&E_BF_01-image
Export-30



157193_Pristine_R_63x_H&E_ipol_01-image
Export-33



157201_Pristine_R_63x_H&E_ana_01-image
Export-41



157201_Pristine_R_63x_H&E_BF_01-image
Export-42



157201_Pristine_R_63x_H&E_ana_01-image
Export-43



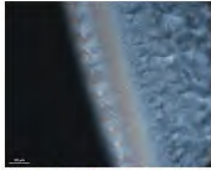
157201_Pristine_R_63x_H&E_ipol_01-image
Export-44



157237_Pellet_Pristine_R_63x_H&E_ana_01-image
Export-53



157237_Pellet_Pristine_R_63x_H&E_BF_01-image
Export-26



157237_Pellet_Pristine_Rt_63x_H&E_ysoL01-image
Export-66



157162_QUV_P_63i_H&E_ana_01-image
Export-01



157162_QUV_P_63i_H&E_ana_02-image
Export-02



157162_QUV_P_63i_H&E_ana_03-image
Export-03



157162_QUV_P_63i_H&E_ana_04-image
Export-04



157162_QUV_P_63i_H&E_BF_01-image Export-05



157162_QUV_P_63i_H&E_BF_02-image Export-06



157162_QUV_P_63i_H&E_BF_03-image Export-07



157162_QUV_P_63i_H&E_BF_04-image Export-08



157162_QUV_P_63i_H&E_BF_05-image Export-09



157162_QUV_P_63i_H&E_xpol_01-image
Export-10



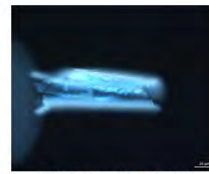
157162_QUV_P_63i_H&E_xpol_02-image
Export-11



157162_QUV_P_63i_H&E_xpol_03-image
Export-12



157162_QUV_P_63i_H&E_xpol_04-image
Export-13



157162_QUV_xpol_1-image Export-14



157170_QUV_P_63i_H&E_ana_01-image
Export-23



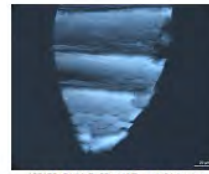
157170_QUV_P_63i_H&E_ana_02-image
Export-24



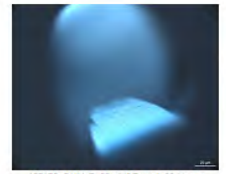
157170_QUV_P_63i_H&E_BF_01-image Export-25



157170_QUV_P_63i_H&E_BF_02-image Export-26



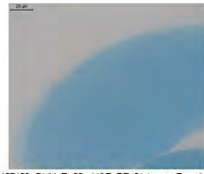
157170_QUV_P_63i_H&E_xpol_01-image
Export-27



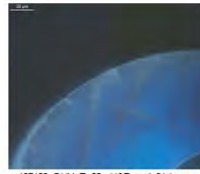
157170_QUV_P_63i_H&E_xpol_02-image
Export-28



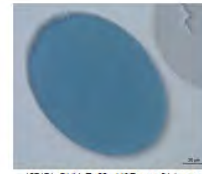
157163_QUV_R_63x_H&E_ana_01-image
Export-63



157163_QUV_R_63x_H&E_BF_01-image Export-64



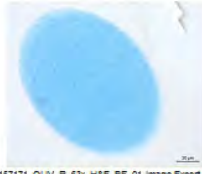
157163_QUV_R_63x_H&E_xpol_01-image
Export-61



157171_QUV_R_63x_H&E_ana_01-image
Export-66



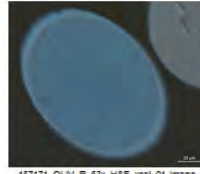
157171_QUV_R_63x_H&E_ana_02-image
Export-67



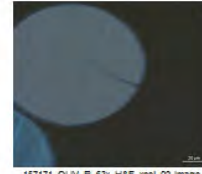
157171_QUV_R_63x_H&E_BF_01-image Export-68



157171_QUV_R_63x_H&E_BF_02-image Export-69



157171_QUV_R_63x_H&E_xpol_01-image
Export-70



157171_QUV_R_63x_H&E_xpol_02-image
Export-42



157179_QUV_R_63x_H&E_ana_01-image
Export-32



157179_QUV_R_63x_H&E_BF_01-image Export-11



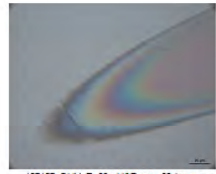
157179_QUV_R_63x_H&E_xpol_01-image
Export-12



157187_QUV_R_63x_H&E_ana_01-image
Export-05



157187_QUV_R_63x_H&E_ana_02-image
Export-06



157187_QUV_R_63x_H&E_ana_03-image
Export-07



157187_QUV_R_63x_H&E_ana_04-image
Export-08



157187_QUV_R_63x_H&E_BF_01-image Export-09



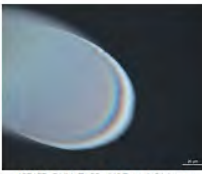
157187_QUV_R_63x_H&E_BF_02-image Export-10



157187_QUV_R_63x_H&E_BF_04-image Export-11



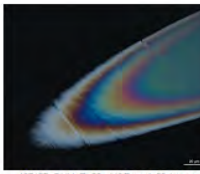
157187_QUV_R_63x_H&E_BF_05-image Export-08



157187_QUV_R_63x_H&E_xpol_01-image
Export-13



157187_QUV_R_63x_H&E_xpol_02-image
Export-14



157187_QUV_R_63x_H&E_xpol_03-image
Export-15



157187_QUV_R_63x_H&E_xpol_04-image
Export-16



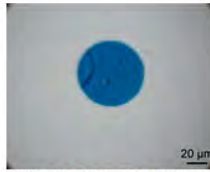
157186_QUV_R_63x_H&E_ana_01-image
Export-34



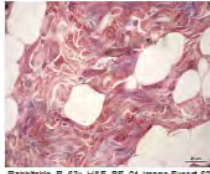
157195_QUV_R_63i_H&E_BP_01-image Export-35



157195_QUV_R_63i_H&E_ipol_01-image Export-36



157195_QUV_R_63i-zoom_H&E_ana_01-image Export-36



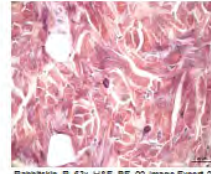
Razotskin_R_63i_H&E_BP_01-image Export-62



Razotskin_R_63i_H&E_BP_02-Draw Scale Bar
Annotation-02-image Export-64



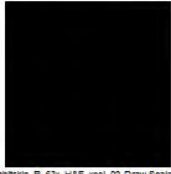
Razotskin_R_63i_H&E_BP_02-Draw Scale Bar
Annotation-03-image Export-65



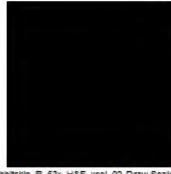
Razotskin_R_63i_H&E_BP_02-image Export-29



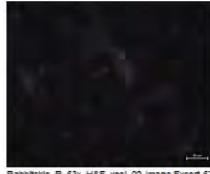
Razotskin_R_63i_H&E_BP_01-image Export-66



Razotskin_R_63i_H&E_BP_02-Draw Scale Bar
Annotation-01-image Export-68



Razotskin_R_63i_H&E_BP_02-Draw Scale Bar
Annotation-02-image Export-69



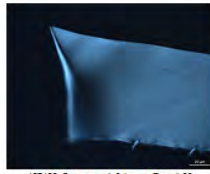
Razotskin_R_63i_H&E_BP_02-image Export-67



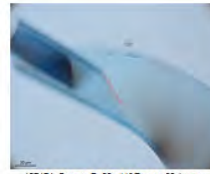
157166_Serum_BF_1-image Export-20



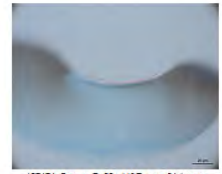
157166_Serum_BF_2-image Export-21



157166_Serum_xpol_2-image Export-22



157174_Serum_P_63x_H&E_ana_03-image Export-36



157174_Serum_P_63x_H&E_ana_04-image Export-37



157174_Serum_P_63x_H&E_BF_01-image Export-38



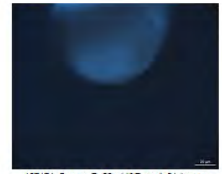
157174_Serum_P_63x_H&E_BF_02-image Export-39



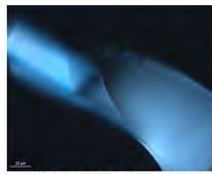
157174_Serum_P_63x_H&E_BF_03-image Export-40



157174_Serum_P_63x_H&E_BF_04-image Export-41



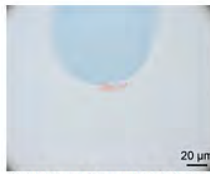
157174_Serum_P_63x_H&E_xpol_01-image Export-42



157174_Serum_P_63x_H&E_xpol_03-image Export-43



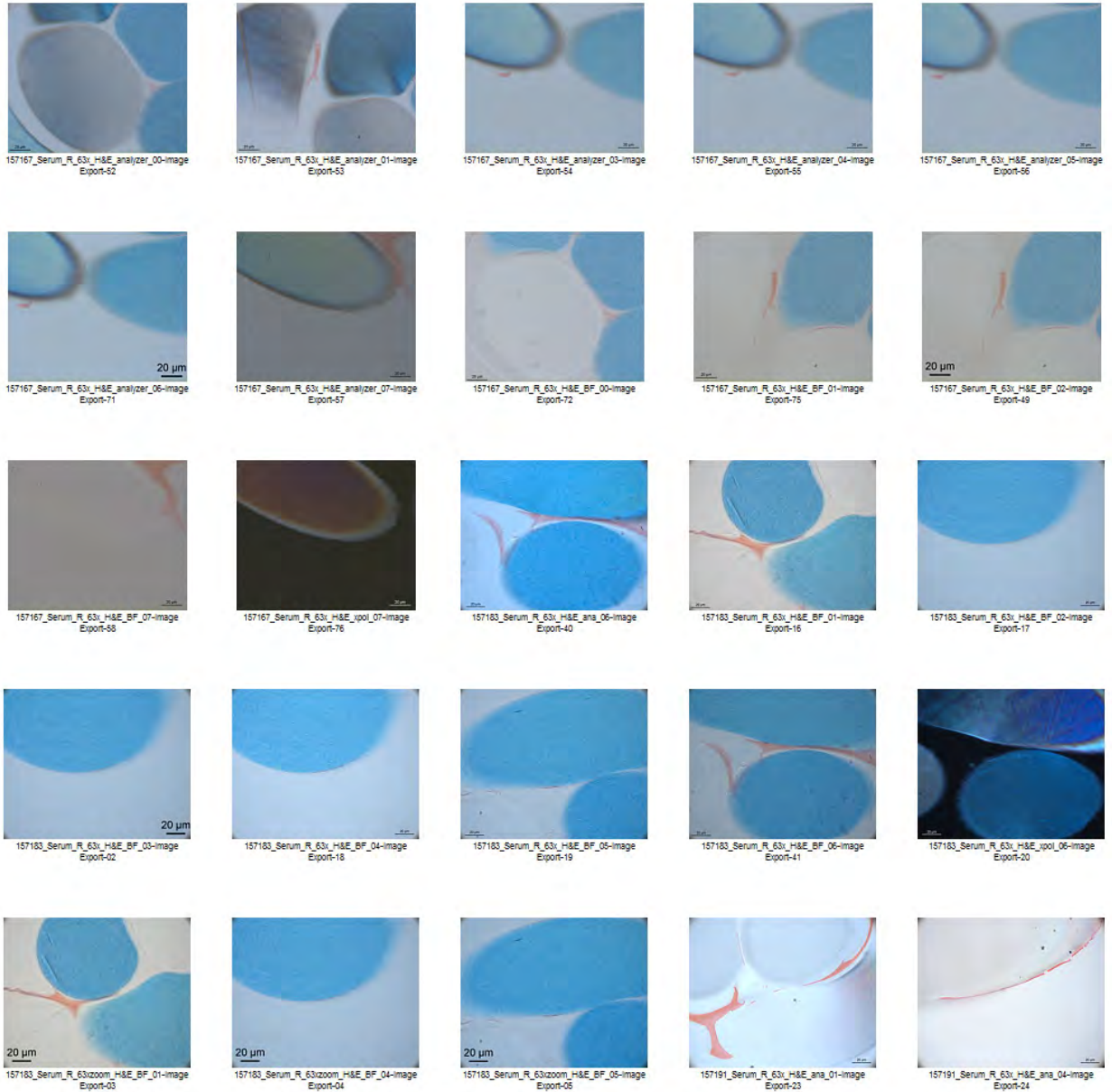
157174_Serum_P_63x_H&E_xpol_04-image Export-44

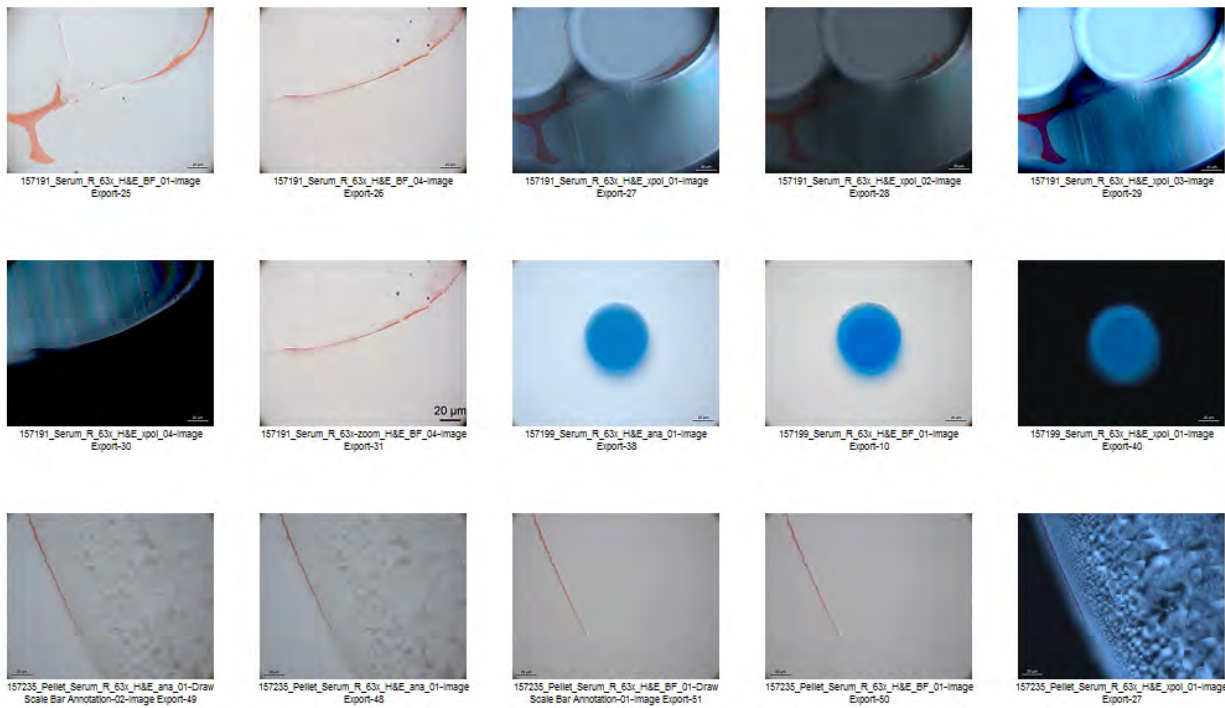


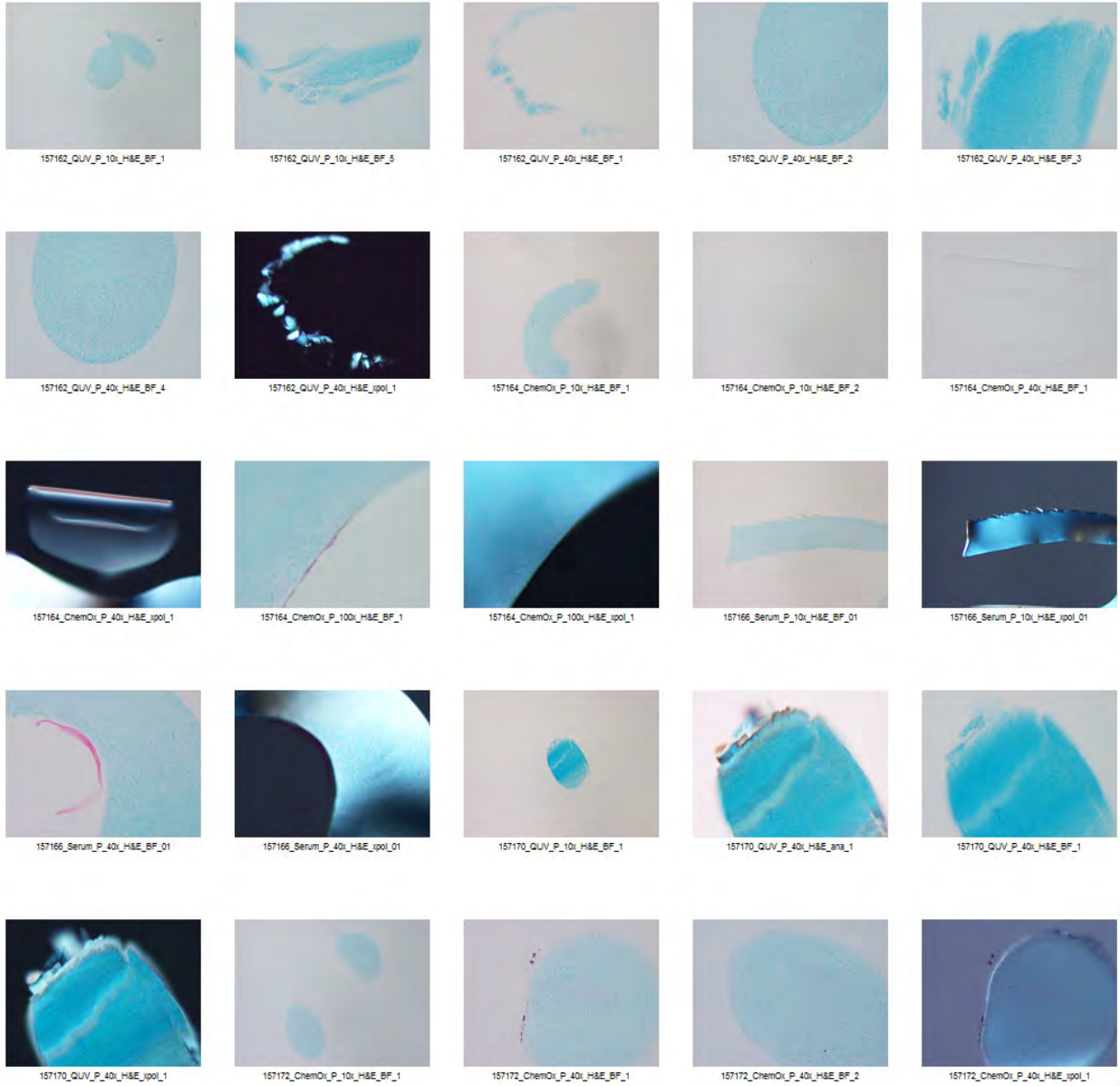
157174_Serum_P_63xzoom_H&E_BF_02-image Export-45



157235_Pellet_Serum_R_63x_H&E_ana_01-image Export-46









157174_Serum_P_10i_H&E_BF_1



157174_Serum_P_40i_H&E_BF_1



157174_Serum_P_40i_H&E_BF_2



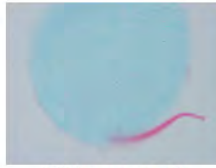
157174_Serum_P_40i_H&E_BF_3



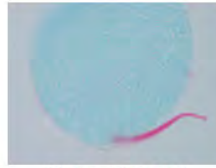
157174_Serum_P_40i_H&E_xpol_1



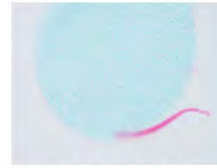
157174_Serum_P_100i_H&E_BF_1



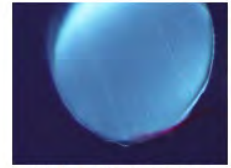
157182_Serum_P_40i_H&E_BF_01



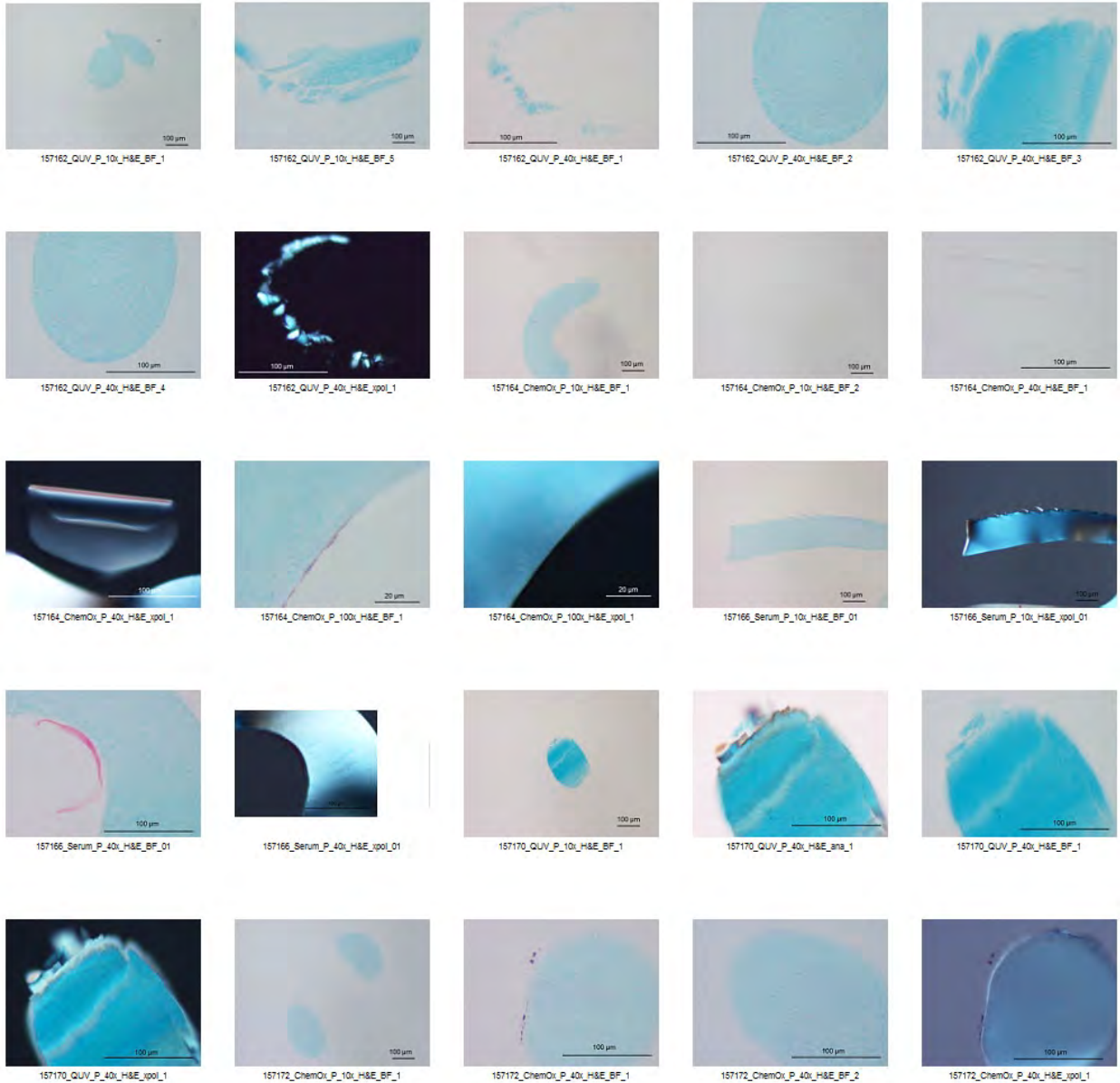
157182_Serum_P_40i_H&E_BF_02

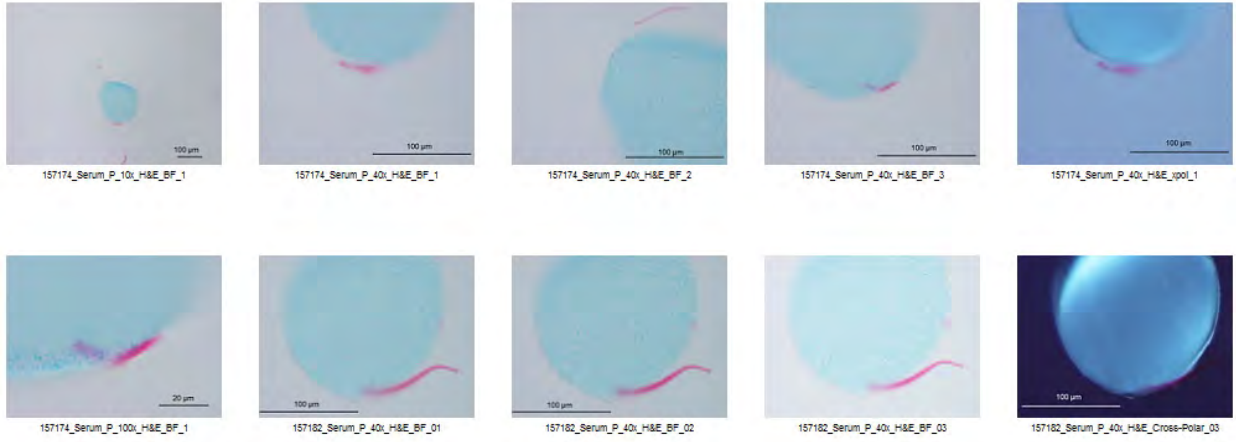


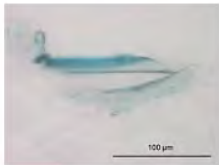
157182_Serum_P_40i_H&E_BF_03



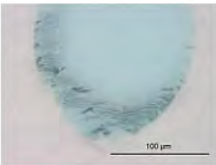
157182_Serum_P_40i_H&E_Cross-Polar_03



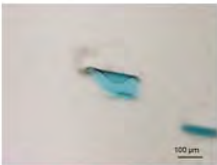




162_QUV-P_40x_Unstained_BF



162_QUV-P_40x_Unstained_BF



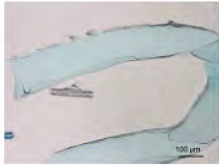
4_ChemOx-P_10x_Unstained_I



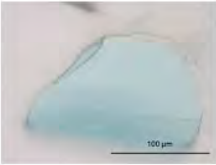
4_ChemOx-P_10x_Unstained_I



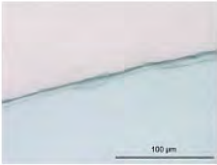
4_ChemOx-P_10x_Unstained_I



66_Serum-P_10x_Unstained_B



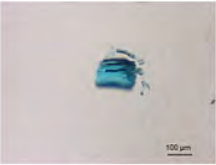
66_Serum-P_40x_Unstained_B



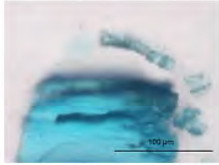
66_Serum-P_40x_Unstained_B



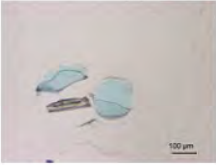
170_QUV-P_10x_Unstained_BF



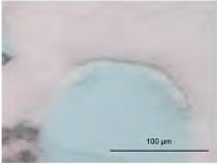
170_QUV-P_10x_Unstained_BF



170_QUV-P_40x_Unstained_BF



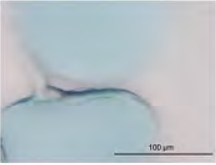
2_ChemOx-P_10x_Unstained_I



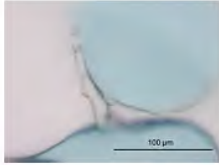
2_ChemOx-P_40x_Unstained_I



2_ChemOx-P_40x_Unstained_I



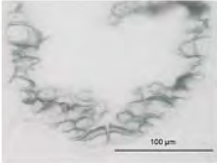
74_Serum-P_40x_Unstained_B



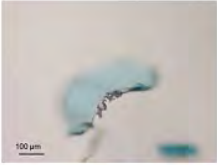
74_Serum-P_40x_Unstained_B



178_QUV-P_10x_Unstained_BF



178_QUV-P_40x_Unstained_BF



0_ChemOx-P_10x_Unstained_I



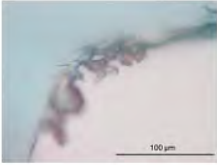
0_ChemOx-P_10x_Unstained_I



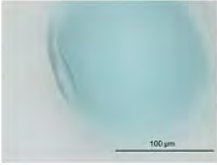
0_ChemOx-P_10x_Unstained_I



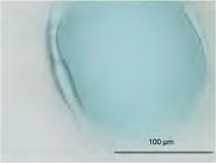
0_ChemOx-P_10x_Unstained_I



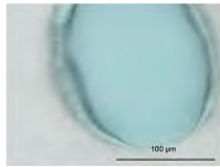
0_ChemOx-P_40x_Unstained_I



0_ChemOx-P_40x_Unstained_I



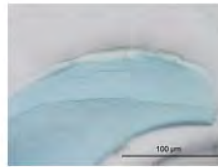
0_ChemOx-P_40x_Unstained_I



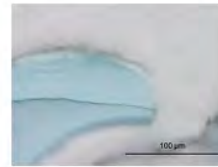
0_ChemOx-P_40x_Unstained_I



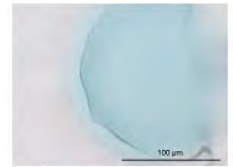
82_Serum-P_10x_Unstained_B



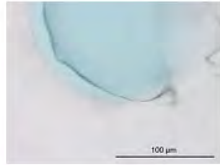
82_Serum-P_10x_Unstained_B



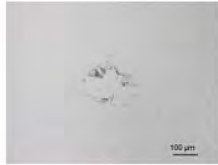
82_Serum-P_10x_Unstained_B



82_Serum-P_40x_Unstained_B



82_Serum-P_40x_Unstained_B



8_ChemOx-P_10x_Unstained_I



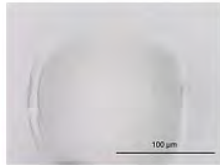
ChemOx-Pellet-P_10x_Unstain



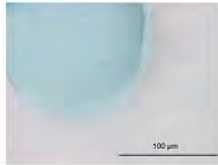
ntreatedControl_P_10x_Unstain



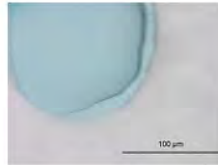
ntreatedControl_P_10x_Unstain



ntreatedControl_P_40x_Unstain



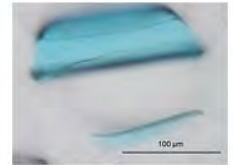
ntreatedControl_P_40x_Unstain



ntreatedControl_P_40x_Unstain



ntreatedControl_P_40x_Unstain



ntreatedControl_P_40x_Unstain



ntreatedControl_P_10x_Unstain



ntreatedControl_P_10x_Unstain



ntreatedControl_P_10x_Unstain



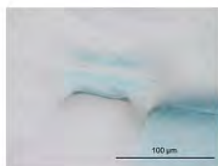
ntreatedControl_P_10x_Unstain



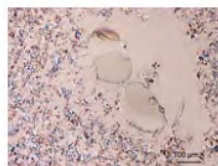
ntreatedControl_P_10x_Unstain



ntreatedControl_P_10x_Unstain



ntreatedControl_P_40x_Unstain



ntreatedControl_P_10x_Unstain



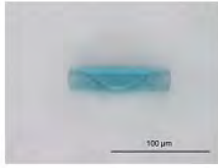
ntreatedControl_P_10x_Unstain



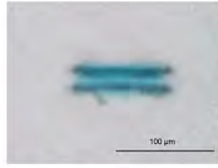
ntreatedControl_P_10x_Unstain



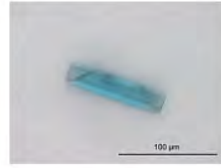
ntreatedControl_P_10x_Unstain



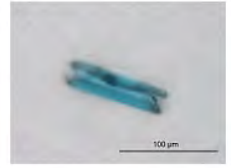
ntreatedControl_P_10x_Unstain



ntreatedControl_P_10x_Unstain



3_ChemOx_P_40x_Unstained_



3_ChemOx_P_40x_Unstained_

